The changing function of nitric oxide in the ventral cochlear nucleus during tinnitus



Adam Hockley

MRC Institute of Hearing Research
School of Life Sciences
University of Nottingham

A thesis submitted for the degree of
Doctor of Philosophy

2018

Thesis Abstract

Tinnitus chronically affects an estimated 10-15% of adults and is characterised by the perception of sound independent of external stimuli. Tinnitus is thought to occur due to an increased central gain through the auditory brainstem, a maladaptive process resulting in tinnitus perception. The neural mechanisms underlying this gain increase are poorly understood; however, an increase in nitric oxide (NO) production has recently been suggested. Nitric oxide synthase (NOS) expression has been studied in guinea pig ventral cochlear nucleus (VCN) where it is located in a sub-population of each cell type. Following unilateral acoustic over-exposure, a within-animal asymmetry of NOS expression was found exclusively in animals that developed tinnitus (Coomber et al., 2015). This provided evidence for a role of nitric oxide (NO) in tinnitus, and not simply as a biomarker for hearing loss.

The first study uses iontophoresis to determine the role of nitric oxide in the VCN of the healthy guinea pig. This provides the first data on the functional role of NO in the auditory brainstem. Iontophoresis was used to apply drugs to, and simultaneously record from, single neurons in the VCN. Drugs used in this study were two NO donors, a NOS inhibitor and a NMDA-R agonists. These data showed that the firing rates of VCN neurons are NO-sensitive, with the effect being dependent on the activity state of the cell. During high activity states, endogenous NO reduces excitability in the VCN, possibly through a homeostatic plasticity mechanism to maintain stability.

Iontophoretic application of NO-related drugs was then tested in noise exposed animals, some of which showed behavioural evidence of tinnitus. Noise exposure resulted in a greater proportion of units responding to exogenously applied NO, demonstrating an increase in sensitivity to NO. Experiments using a NOS inhibitor showed that, in tinnitus animals, endogenous NO increases excitability in a larger proportion of neurons, producing an increase in transmission through the auditory system with

potential to contribute to the 'increased central gain' thought to be present in tinnitus. This NO-mediated excitation also correlated with the strength of behavioural evidence tinnitus. Repeating this experiment with NMDA-evoked excitation as opposed to auditory input showed again an increase in excitability, but this increase occurred in all noise exposed animals, with no specific effect of tinnitus. This suggests noise exposure produces changes postsynaptically, with a presynaptic effect of NO in tinnitus increasing transmission.

My final study assessed the possibility of using NOS inhibitors to modulate endogenous NOS in the VCN, with application either by systemic injection or local perfusion using microdialysis. This was an attempt to demonstrate that NO-modulating drugs could be used to affect auditory processing in a clinical setting, possibly as future treatment for tinnitus. NOS inhibitors were applied indirectly to the cochlear nucleus, either via reverse microdialysis or systemic application, and the effect of these drugs on either VCN activity or behavioural measures of tinnitus was measured. Both routes of delivery altered activity in a small proportion of VCN neurons. Systemic NOS inhibitor application also modulated the reflex used as our behavioural measure of tinnitus, returning gap prepulse inhibition of the acoustic startle (GPIAS) to normal levels in 20% of animals with impaired GPIAS.

In summary, this thesis demonstrates a functional role of NO in the VCN, which is altered in tinnitus to produce an increased excitability capable of contributing to tinnitus generation. Targeting of the NO pathway may have clinical relevance in tinnitus, with potential to provide a target for pharmacological treatment of the disorder.

Declaration

I declare that this thesis was composed by myself, that the work contained herein is my own except where explicitly stated otherwise in the text, and that this work has not been submitted for any other degree or professional qualification.

Adam Hockley *Date*

Acknowledgements

First, I would like to extend my greatest thanks to my supervisors, Mark Wallace and Paul Smith. Mark, you have been a great mentor to me, and I appreciate every moment of it. You've made my time at IHR truly enjoyable and it's been a pleasure working with you. Your dedication to the science and to helping your students is overwhelming, and you deserve all the best in the future. Paul, your insight has been highly valuable and I have thoroughly enjoyed your probing questions at our meetings. My thanks also go out to Alan Palmer and Chris Sumner, as you both have been there on the periphery of my project with open doors, quality advice and a good laugh at all times. Also, as project leaders you must be praised for the research environment you created within the group, which has helped to keep us all going through thick and thin. Next up, it's Joel Berger. You've been a great influence on me, and I couldn't have asked for a better person to spend 3 years working with. We've had so many good times and I'm sure there still plenty more to come in America! To my friends who have been there from the start, the Ollie's, Jess, Beano and all the others: I couldn't have done this without you load of reprobates either! There are also many friends I have made throughout my PhD and all who worked at IHR old and new have made it the great place it has been. Sammy and Sam Smith you've been such fun to work with, I'll miss the times spent in the lab together. I wish you both the best for the future, and I'm sure our paths will cross again soon. Thanks to my parents, all four of you! You have all been there supporting me throughout, and I would never have got this far without you. Finally:

"Thank you for reading this thesis, you're experiencing something no one else ever will" - *Wole Burger, 2013*

Publications

Selected Conference Abstracts

Hockley, A., Berger, J. I., Hill, S. M. D., Smith, P. A., Palmer, A. R. and Wallace, M. N. (2018) NO-mediated homeostatic plasticity in the guinea pig ventral cochlear nucleus: a potential tinnitus generation mechanism *NO2018, Oxford 2018*

Hockley, A., Berger, J. I., Smith, P. A., Palmer, A. R. and Wallace, M. N. (2018) Nitric oxide as a modulator in the ventral cochlear nucleus: a potential tinnitus generation mechanism. *ARO Midwinter Meeting, San Diego 2018*

Hockley, A., Berger, J. I., Smith, P. A., Palmer, A. R. and Wallace, M. N. (2017) The role of nitric oxide in modulating neuronal activity in the ventral cochlear nucleus, a possible mechanism of tinnitus generation. *BNA Festival of Neuroscience, Birmingham 2017*

Hockley, A., Berger, J. I., Smith, P. A., Palmer, A. R. and Wallace, M. N. (2016) The role of nitric oxide in modulating neuronal activity in the ventral cochlear nucleus. *SFN Neuroscience, San Diego 2016*

List of Abbreviations

7-NI	7-Nitroindazole
ABR	Auditory Brainstem Response
AC	Auditory Cortex
aCSF	Artificial Cerebrospinal Fluid
AN	Auditory Nerve
ANOVA	Analysis of Variance
AOE	Acoustic Over-exposure
AVCN	Anteroventral Cochlear Nucleus
BBN	Broadband Noise
Ca^{2+}	Calcium Ion
CF	Characteristic Frequency
Ch	Chopper
cGMP	Cyclic Guanosine Monophosphate
CN	Cochlear Nucleus
D-NAME	Nitro-D-arginine Methyl Ester Hydrochloride
dB	Decibel
DCN	Dorsal Cochlear Nucleus

DFR	Driven Firing Rate
GLU	Glutamate
GP	Guinea Pig
GPIAS	Gap Prepulse Inhibition of the Acoustic Startle
IC	Inferior Colliculus
i.p.	Intraperitoneal
i.m.	Intramuscular
K^+	Potassium ion
kHz	Kilohertz
L-NAME	Nitro-L-arginine Methyl Ester Hydrochloride
MU	Multi-unit
Na^+	Sodium Ion
NMDA	N-methyl-D-aspartate
NMDA-R	NMDA Receptor
NT	Non-tinnitus
NO	Nitric Oxide
NOS	Nitric Oxide Synthase
eNOS	Endothelial NOS
iNOS	Inducible NOS
nNOS	Neuronal NOS
On	Onset
PDE	Phosphodiesterase
PhLo	Phase-locked
PrLi	Primary-like
PSTH	Peri-stimulus Time Histogram

PVCN	Posteroventral Cochlear Nucleus
s.c.	Subcutaneous
SFR	Spontaneous Firing Rate
sGC	Soluble Guanylyl Cyclase
SIN-1	3-Morpholinosydnonimine Hydrochloride
SNOG	S-Nitrosoglutathione
SOC	Superior Olivary Complex
SPL	Sound Pressure Level
SU	Single-unit
SLDT	Sound Level-Dependency Test
T	Tinnitus
TDT	Tucker Davis Technologies
VCN	Ventral Cochlear Nucleus

Table of Contents

List of Figures xii

List of Tables xv

1 General Introduction 1
- 1.1 Thesis introduction and structure . . . 1
- 1.2 General introduction . . . 2
- 1.3 Auditory system organisation . . . 4
  - 1.3.1 The peripheral auditory system . . . 4
  - 1.3.2 Central auditory system . . . 6
  - 1.3.3 Cell types of the ventral cochlear nucleus . . . 9
- 1.4 Animal models of tinnitus . . . 13
  - 1.4.1 Inducing tinnitus . . . 13
  - 1.4.2 Behavioural confirmation of animal tinnitus . . . 14
- 1.5 Neural correlates of tinnitus . . . 19
- 1.6 Mechanisms of tinnitus generation . . . 22
  - 1.6.1 Central gain . . . 22
  - 1.6.2 Plasticity of neural connections . . . 25
  - 1.6.3 Alternative aspects of tinnitus . . . 27
- 1.7 Nitric oxide . . . 29
  - 1.7.1 Molecular basis of production . . . 29
  - 1.7.2 Mechanism of action and regulation . . . 30
  - 1.7.3 Effect on neuronal activity . . . 32
- 1.8 The presence and action of nitric oxide in the auditory nervous system . . . 35
  - 1.8.1 Potential role in tinnitus . . . 36
- 1.9 Aims and objectives . . . 38

2 Materials and methods 39
- 2.1 Animals . . . 39
- 2.2 Behavioural tinnitus confirmation . . . 39
- 2.3 Noise exposure and ABRs . . . 42

2.4 Non-recovery surgery electrodes and recordings 44
2.4.1 Sound presentation 45
2.4.2 Recording overview 46
2.4.3 Iontophoresis 46
2.4.4 Multi-electrode recording 52
2.4.5 Reverse microdialysis 54
2.5 Neural identification 59

3 NO-mediated synaptic plasticity in the guinea pig ventral cochlear nucleus and its role in central gain control 64
3.1 Introduction 64
3.2 Iontophoresis protocol and statistical analysis 66
3.3 Nitric oxide donors 70
3.4 Nitric oxide synthase inhibition 76
3.4.1 PSTH comparisons 79
3.4.2 D-NAME 82
3.5 NOS inhibition on NMDA evoked excitation 83
3.6 No NO modulation of phase locking 87
3.7 NO modulation of spike shapes 89
3.8 A nonspecific effect of NO in the VCN 92

4 Changes in VCN nitric oxide function related to noise exposure and tinnitus 93
4.1 Introduction 93
4.2 Methods 95
4.3 ABR changes following acoustic over exposure and behavioural confirmation of tinnitus 96
4.4 The effect of noise-exposure and tinnitus on VCN unit activity 98
4.5 Iontophoresis of NO donor in noise-exposed animals. 103
4.6 Iontophoresis of NOS inhibitor in noise-exposed animals. . . 108
4.7 NOS inhibition during NMDA-evoked excitation in noise-exposed animals. 112

5 Preliminary testing of peripheral NOS inhibitor application 115
5.1 Introduction 115
5.2 Global nNOS inhibition decreases VCN activity 117
5.3 NOS inhibition in the cochlear nucleus increases VCN activity 120
5.4 Global nNOS inhibition improves GPIAS of some animals with impaired GPIAS 124

6 General discussion 127
6.1 Nitric oxide function in the cochlear nucleus 127
6.1.1 Exogenous NO application 127
6.1.2 NOS inhibition overview 128
6.1.3 NOS inhibition during low-activity states 128
6.1.4 NOS inhibition during high-activity states 129
6.1.5 Potential mechanisms of NO action 130

6.1.6 Implications 131
6.2 Nitric oxide changes following noise exposure and the development of tinnitus 132
6.2.1 Noise exposure induced changes in the VCN 132
6.2.2 The changing nitric oxide function with AOE and tinnitus 133
6.2.3 A maladaptive hearing loss compensation 134
6.2.4 NO mechanisms in the tinnitus VCN 137
6.3 Could nitric oxide-modulating drugs be used therapeutically? 138
6.4 Are changes to firing rate in the VCN following noise exposure and tinnitus frequency specific? 140
6.5 Asymmetries in NOS function after noise exposure 142
6.6 Is tinnitus the result of enhanced excitation or reduced inhibition? 143
6.7 Methodology overview 145
6.7.1 Behavioural tinnitus confirmation 145
6.7.2 Iontophoresis 146
6.7.3 Reverse microdialysis 147
6.8 Conclusions 150
6.9 Future directions 151

References **153**

List of Figures

1.1 Diagram of the human ear 4
1.2 Diagram of the cochlea 5
1.3 The ascending auditory system 7
1.4 The cochlea nucleus 8
1.5 Chopper and primary-like PSTH examples 11
1.6 Onset and phase-locked PSTH examples 12
1.7 The GPIAS test 16
1.8 Pinna reflex recording technique 17
1.9 Central gain through auditory structures 23
1.10 Synaptic plasticity 27
1.11 The NO/cGMP pathway 31

2.1 GPIAS of the pinna reflex 41
2.2 AOE stimuli used 43
2.3 Speaker maximum level output 45
2.4 Diagram of iontophoresis 47
2.5 Images of iontophoresis electrode used 48
2.6 Iontophoresis electrode superimposed on an image of a neuron 49
2.7 Glutamate iontophoresis proof of concept 52
2.8 Image of a multi-electrode 54
2.9 A diagram of the microdialysis probe 55
2.10 A microscope image of the microdialysis probe and electrode assembly 56
2.11 Reverse microdialysis proof of concept histogram 58
2.12 Reverse microdialysis proof of concept rate level function . . 58
2.13 Example of live spike analysis of a single unit 60
2.14 Spike shapes of a VCN unit 61
2.15 PSTHs and ISIHs of VCN units 62
2.16 Phase-locking analysis 63

3.1 Timings of iontophoretic drug application and analysis periods 66

3.2 Example analysis of a unit following iontophoretic NO donor application . . . 67
3.3 Example analysis of a unit following iontophoretic L-NAME application . . . 68
3.4 Example analysis of a unit following iontophoretic L-NAME and NMDA application . . . 69
3.5 Spike rate histogram of VCN units with SIN-1 application . . 71
3.6 SIN-1 induced changes to firing rates of 25 VCN units 72
3.7 Spike rate histogram of VCN units with SNOG application . 73
3.8 SNOG induced changes to firing rates of 23 VCN units . . . 75
3.9 Spike rate histogram of VCN units with L-NAME application 77
3.10 L-NAME induced changes to firing rates of 22 VCN units . . 79
3.11 Changes to PSTHs during L-NAME application 81
3.12 Spike rate histogram of VCN units with L-NAME and D-NAME application . . . 82
3.13 Spike rate histogram of VCN units with L-NAME and NMDA application . . . 84
3.14 L-NAME induced changes to NMDA-evoked excitation of 15 VCN units . . . 85
3.15 Phase locking analysis of a VCN unit before, during and after L-NAME application . . . 88
3.16 Changes to spike shapes evoked by SIN-1 application 90
3.17 ISIH changes following SIN-1 application 91

4.1 ABR amplitudes before, immediately after, and 8 weeks following acoustic over exposure . . . 96
4.2 Behavioural evidence of tinnitus 97
4.3 Changes to firing rates and frequencies following noise exposure . . . 99
4.4 Two example PSTHs from a control and tinnitus animal . . 100
4.5 The effect of noise exposure and tinnitus on mean firing rates in the VCN . . . 101
4.6 The effect of noise exposure and tinnitus on first spike latency 102
4.7 PSTH shape changes during SIN-1 application in tinnitus animals . . . 104
4.8 A rate-specific effect of NO in the VCN 105
4.9 Changes evoked by SIN-1 application and the relationship with tinnitus . . . 106
4.10 Proportion of units changing firing rates in response to SIN-1 107
4.11 Changes evoked by L-NAME application and the relationship with tinnitus . . . 109
4.12 Proportion of units changing firing rates in response to L-NAME . . . 110
4.13 Correlations between GPIAS and effect of L-NAME 111
4.14 Effect of L-NAME on NMDA-evoked excitation and the relationship with tinnitus . . . 113

4.15 Proportion of L-NAME effect on NMDA-evoked excitation . . 114

5.1 Comparison of a PSTH and LFP recorded from the same electrode 118
5.2 Effect of 7-NI on VCN activity 119
5.3 PSTH of a VCN in unit in response to BBN 121
5.4 Effect of microdialysis of L-NAME on a single unit in the VCN 122
5.5 Microdialysis of L-NAME on a RLF in the VCN 123
5.6 Data from two animals that show improved GPIAS following systemic 7-NI application 125
5.7 Effect of 7-NI on guinea pigs with impaired GPIAS 126

6.1 NO-mediated tinnitus generation following noise exposure . 136

List of Tables

1.1 Classification of NOS isoforms 30
1.2 Auditory localisation of NOS 35

2.1 Drugs used for iontophoresis experiments 51
2.2 Composition of the aCSF used 57
2.3 Drugs used for reverse microdialysis experiments 57

3.1 Composition of the aCSF used 92

4.1 Dependence of L-NAME effect on GPIAS 111

CHAPTER 1

General Introduction

1.1 Thesis introduction and structure

The purpose of this thesis is to examine the functional role of nitric oxide (NO) within the ventral cochlear nucleus (VCN) and how this may change following noise exposure and the induction of tinnitus. To address these questions, a series of experiments were carried out involving modulation of NO in the guinea pig VCN while recording from the local neural population.

This thesis will begin with a general introduction, which will give an overview of tinnitus and the auditory system, before a more detailed summary of current knowledge of tinnitus' underlying mechanisms and how NO may contribute. Following that, my methods section will describe comprehensively the techniques used in my experiments, including behavioural confirmation of animal tinnitus, noise exposure and measure of auditory brainstem responses, single unit recordings within the auditory brainstem and drug delivery by micro-iontophoresis and reverse microdialysis. *Chapter 3* is my first of three results chapters, focussing on the functional role of NO in the healthy guinea pig VCN. The following chapter assesses how this function may be altered following noise exposure and tinnitus. The final results chapter contains my data obtained using peripherally applied NO-related drugs to alter both VCN neuron function and behavioural evidence of tinnitus in our animals. Finally, my general discussion will evaluate the results shown, in the context of current knowledge within the field.

1.2 General introduction

Tinnitus is characterised by the perception of sound independent, and in the absence of, external stimuli. Despite the word tinnitus being derived from the Latin verb for ring, *tinnire*, it can present in many other forms such as buzzing, hissing or clicking. Two major classifications of tinnitus exist, objective tinnitus and subjective tinnitus. Objective tinnitus accounts for around 5% of cases and involves the perception of an internally generated sound, such as a pulsating blood vessel or muscle spasms within the middle ear. This can often be treated by pharmacologically or surgically removing the sound source (Ward et al., 1975). In comparison, subjective tinnitus is the perception of a phantom sound, with no true source. The neural basis is still debated (Roberts et al., 2010) and treatment options are very limited; this report will focus upon the study of subjective tinnitus.

The prevalence of tinnitus is higher in industrialised countries, affecting around 10-15% of adults (Baguley et al., 2013). It is therefore a common condition and, although being more prevalent in older individuals, can occur at any age (Shargorodsky et al., 2010). Some risk factors for tinnitus have been identified, namely increased age, hearing loss and frequent loud noise exposure (often due to firearm use or occupational exposure) (Shargorodsky et al., 2010).

Severe disruptions to the health and lifestyle of patients has been observed (Tyler & Baker, 1983), and tinnitus has been linked to an increased risk of depression and insomnia (Folmer et al., 1999; Folmer & Griest, 2000). Treatment currently relies primarily on procedures such as the use of hearing aids to counter the effects of hearing loss, or cognitive behavioural therapy to combat increased levels of stress. No effective drugs to treat tinnitus have yet been approved by the FDA or EMA regulatory bodies (Langguth & Elgoyhen, 2012).

One obstacle that the search for treatments needs to overcome is that the characteristics of the tinnitus perceived are often heterogeneous among patients (Baguley et al., 2013). Also, the type or severity of tinnitus does not correlate with any noise-induced hearing loss experienced (Luxon, 1993).

A major limitation in the development of pharmacological tinnitus treatments has been the lack of a widely accepted animal models with

which to test potential compounds (Langguth & Elgoyhen, 2012). Previous work on potential drugs has been labour-intensive due to the behavioural methods used, requiring the use of many animals over long periods of time for each drug tested. The variety of methodologies used in clinical trials has also limited scientific understanding in this field (Landgrebe et al., 2012).

Identifying a physiological signature for tinnitus and being able to record it in awake animals would provide more rapid and accurate tinnitus diagnosis. This would also allow faster and more accurate testing of novel drugs, requiring fewer animals over shorter periods of time. This could accelerate the identification of potentially useful drugs.

Physiological testing is also conducted to understand the neural mechanisms of tinnitus generation, as this could potentially lead to the development of pharmacological treatments. Studies have so far struggled to elucidate the mechanism and location of the source of tinnitus, however once these are found, testing of potential treatments could be conducted more rapidly. The pathophysiology of tinnitus is therefore a highly important area of basic research to further understand the underlying mechanisms providing the basis for future medical management.

The ventral cochlear nucleus (VCN) is one of a number of structures early in the auditory pathway that may have a role in generating tinnitus, based on auditory brainstem (ABR) responses in humans (Gu et al., 2012). Changes in nitric oxide synthase (NOS) expression have been shown in the VCN in tinnitus guinea pigs (Coomber et al., 2014; Coomber et al., 2015).

Therefore, in this thesis I have used electrophysiological recordings combined with drug application with the aim of determining the functional role of nitric oxide (NO) in the VCN, and resolve whether changes in NO contribute to tinnitus generation.

1.3 Auditory system organisation

In order to study tinnitus, it is first important to understand the structure and normal function of the auditory system, which will be explained briefly here, with a particular emphasis on the ventral cochlear nucleus (VCN).

The auditory system is a system that allows sensation of the vibration of air around us. These vibrations are channelled into our ear canal by the pinna, before impedance matching in the middle ear, and mechanotransduction from movement to neural signals in the inner ear. This neural information is then processed through the central auditory system before perception in the cortex.

1.3.1 The peripheral auditory system

The structure of the human ear is shown in Fig 1.1. The outer ear is formed of the pinna and ear canal. The pinna is a cartilaginous structure designed to funnel sound waves into the ear canal. Many mammals, including guinea pigs and some humans, are capable of moving their pinna using the auricular muscles. At the end of the ear canal is the tympanic membrane, often known as the ear drum. This vibrates in response to sound and transduces the changes in air pressure to movement within the middle ear.

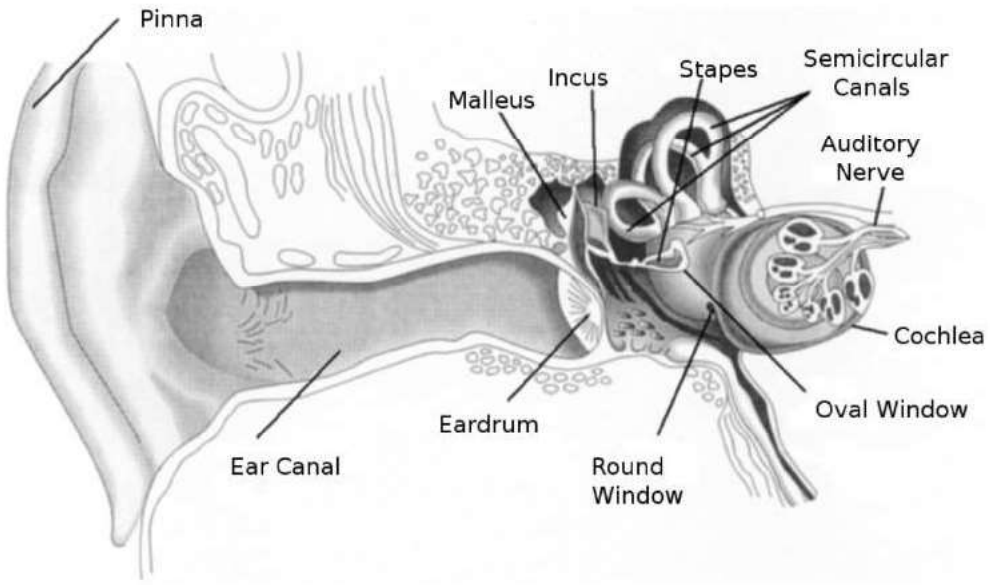


Fig. 1.1: Diagram of the human ear (Araújo et al., 2005).

The middle ear contains three bones, the malleus, stapes and incus, which are responsible for transfer of the tympanic membrane vibrations to the inner ear. Theses ossicles displace the oval window, which transfers the movements to the inelastic fluid of the inner ear (perilymph). Impedance matching occurs in the middle ear, matching the low resistance to movement of the air to the high resistance to movement of the perilymph. Pressure gain occurs in the middle ear, due to the smaller size of the oval window compared to the tympanic membrane, and the arrangement of the ossicles working as a lever. Very loud sounds can also be dampened down in the middle ear, due to a reflex contraction of the two middle ear muscles, the tensor tympani and stapedius (Misurya, 1976).

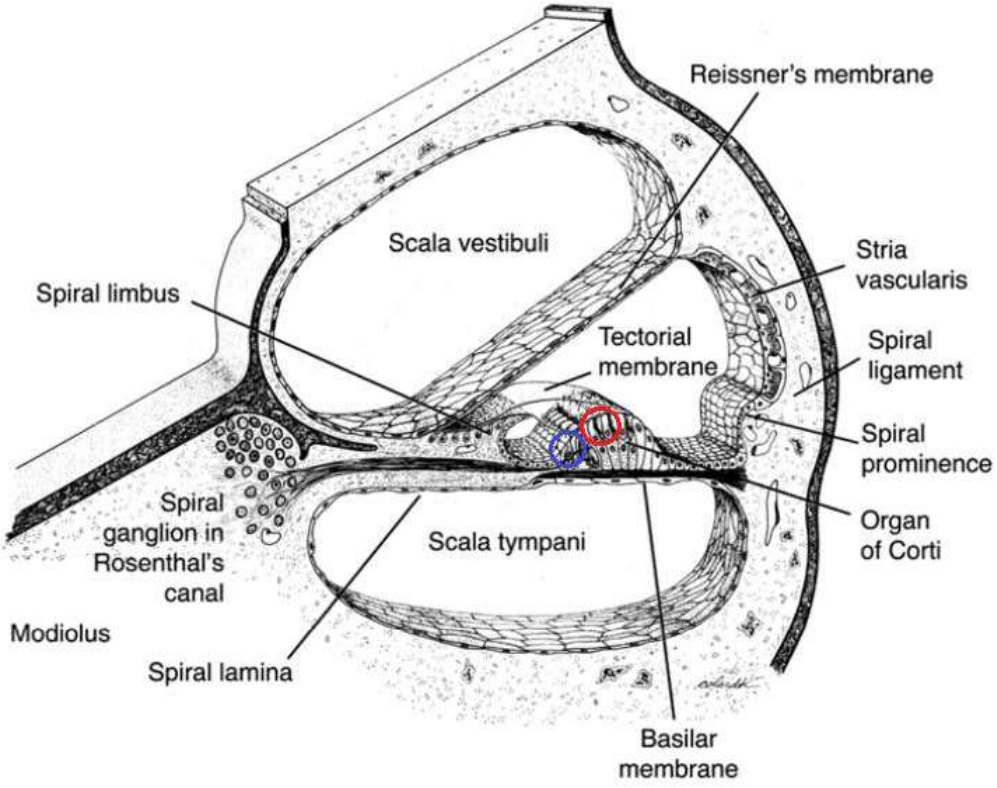


Fig. 1.2: A cross-section of the mammalian cochlea, with the location of inner and outer hair cells highlighted by blue and red circles, respectively. (Pickles, 2012)

The inner ear consists of the cochlea, a snail shaped organ formed of three compartments, the scala vestibuli, scala media and scala tympani. The cross section of the cochlea, shown in Fig 1.2, shows the three fluid filled chambers, and the separating membranes. The scala vestibuli and scala tympani are filled with perilymph, a fluid similar in composition to CSF.

When vibrations of the ossicles move the oval window, a travelling wave is produced within the cochlea. Within the organ of Corti on the basilar membrane of the cochlea are sensory hair cells. The cochlea is arranged tonotopically, with the inner hair cells at the basal end responding to high frequencies and the inner hair cells at the apical end responding to low frequency vibrations (Pickles, 2012).

Inner hair cells project into the scala media, which is filled with endolymph, a fluid with high K^+ concentration, due to K^+ transport from the stria vascularis. These hair cells allow mechanotransduction, as movement of the cochlear fluid moves the stereocilia of the hair cells, opening transduction channels which have recently been shown to be TMC1 pores (Pan et al., 2018). These transduction channels on the hair cells allow K^+ influx, inducing depolarisation of the hair cell (Konishi et al., 1978).

Upon depolarisation, neurotransmitter is released from inner hair cells onto the peripheral processes of spiral ganglion cells, which form the cochlear nerve, completing the signal transduction pathway. These myelinated neurons (named type I neurons), form 95% of the auditory nerve, and are the source of the majority of afferent input to the auditory system (Spoendlin, 1967). These afferent neurons can be classified into high threshold low spontaneous rate or low threshold high spontaneous rate fibres (Liberman 1978). RNA sequencing has recently demonstrated the diversity of type I spiral ganglion neurons, showing 3 distinct subclasses (Petitpré et al., 2018). Conversely, outer hair cells receive the majority of the efferent input to the cochlea from the unmyelinated type II neurons. Outer hair cells can expand or contract, to push or pull on the basilar membrane, amplifying or attenuating the travelling wave to modulate the output from the organ of Corti.

1.3.2 Central auditory system

Afferent input to the central auditory system is processed by many brainstem and midbrain nuclei before transmission to the auditory cortex, where processing of sounds can occur. Fig 1.3 shows a simplified view of the nuclei and ascending pathways of the auditory system.

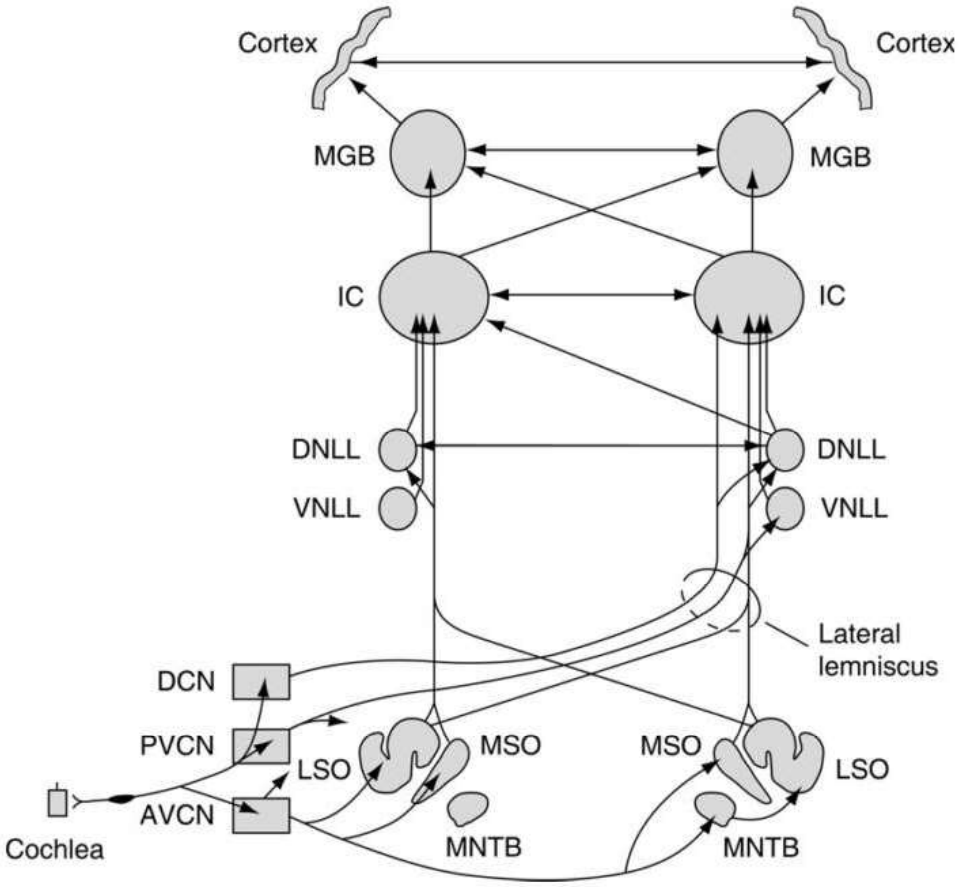


Fig. 1.3: An overview of the ascending auditory system, from unilateral input (Pickles, 2012). AVCN, anteroventral cochlear nucleus; PVCN, posteroventral cochlear nucleus; DCN, dorsal cochlear nucleus; LSO, lateral superior olive; MNTB, medial nucleus of the trapezoid body; MSO, medial superior olive; VNLL, ventral nucleus of the lateral lemniscus; DNLL, dorsal nucleus of the lateral lemniscus; IC, inferior colliculus; MGB, medial geniculate body.

The cochlear nerve forms one half of the eighth cranial nerve, the vestibulocochlear nerve. Here, each nerve fibre transmits the information from a single inner hair cell, which responds preferentially to a small part of the auditory spectrum. This specification of fibres is known as labelled-line coding, which is the basis for tonotopicity through the auditory system.

The cochlear nerve connects to the cochlear nucleus (CN), where it bifurcates into the ascending and descending branches, innervating the dorsal cochlear nucleus (DCN), posteroventral cochlear nucleus (PVCN) and the anteroventral cochlear nucleus (AVCN). The tonotopy of the cochlea is maintained throughout the cochlear nucleus, with separate

organisation in each of the three subdivision, based on the branching of the auditory nerve (Fig 1.4A) (Rose et al. 1965).

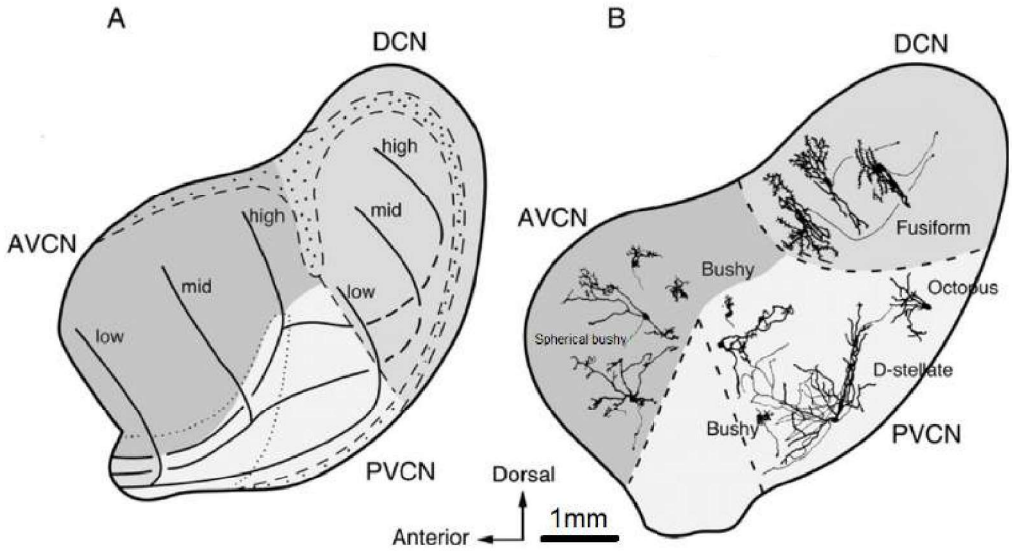


Fig. 1.4: Diagrams of sagittal cross-sections of the cat cochlear nucleus (Pickles, 2012). A: The paths of auditory nerve fibres through. B: Locations and dendritic layouts of the principal cell types of the cochlear nucleus.

The cells of the CN project ipsi-laterally and contralaterally, to various central structures. Bilateral outputs to the superior olive exist, where interaural time differences and interaural level differences are used for sound localisation (Purves, et al. 2012). Fibres from the CN also project up to the inferior colliculus (IC), where further processing of complex sounds occurs (Casseday et al., 1994). From the IC, projections travel up through the thalamus to the auditory cortex, where perception of, and attention to, sound is achieved. The tonotopic map of the cochlea is maintained all the way through the pathway to the auditory cortex, demonstrating the importance of separating sounds by frequency (Clopton et al., 1974).

Descending projections also occur within the auditory system, allowing modulation of the auditory pathway. For example, the olivocochlear system involves afferent control of the outer hair cells of the cochlea by neurons originating in the superior olivary complex (SOC). This descending control is, itself, controlled by descending input from the IC (Groff & Liberman, 2003). Descending pathways also exist from the cortex to subcortical areas, contributing to frequency tuning (Zhang et al., 1997).

Within the auditory pathway, there are a variety of cell types; which often have a specific function. These cell types can be identified morphologically or physiologically. When studying the physiology of auditory neurons, response areas and peri-stimulus time histograms (PSTHs) are often used for identification. Response areas show the spike rate of a neuron to a range of pure tones at a range of sound levels, producing a view of which tonal auditory stimuli at which levels the neuron is responsive to. From this, a characteristic frequency (CF) can be found; this is the frequency which the neuron responds to at the lowest sound intensity. By repeatedly applying a pure tone at this CF, a PSTH can be formed by recording of the frequency of neuronal firing plotted against time.

1.3.3 Cell types of the ventral cochlear nucleus

Each of the cell types of the cochlear nucleus are more prevalent in a certain subsection. The approximate locations of these principal cell types of the cochlear nucleus are shown in Fig 1.4B. The VCN is primarily composed of stellate (T- and D-stellate) cells, bushy cells (globular and spherical) and octopus cells, each named due to their morphology (Oertel et al., 1990; Wu & Oertel, 1984). Electrophysiology and intracellular labelling experiments have identified specific response patterns of these VCN neurons to tonal stimuli (Fig 1.5 & Fig 1.6) (Blackburn & Sachs, 1989; Palmer, 1987; Rhode & Smith, 1986).

Primary-like and primary-like with notch patterns have been associated with spherical and globular bushy cells in the AVCN, respectively (Fig 1.5) (Smith & Rhode, 1987). Auditory nerve synapses onto bushy cells consist of large synapses with high release probability, the ”endbulbs of Held” (Ryugo et al., 2006). Precise timing is required in spherical bushy cells, as they project to the MSO and LSO where interaural time differences (ITDs) and interaural level differences (ILDs) are detected (Purves et al., 2012) . Globular bushy cells project to principal cells of the contralateral MNTB, where they form the calyx of Held synapse, thought to be the largest synapse in the mammalian brain (Morest, 1968). The glycinergic principal cells of the MNTB which provide inhibition to the MSO and LSO are necessary for correct ITD and ILD detection (Cant & Hyson, 1992; Spangler et al., 1985).

A chopping pattern PSTH, consisting of a fluctuating spike rate for the initial period, is shown in Fig 1.5. These responses can be separated into transient and sustained chopping patterns, which are determined by the length of the chopping period, and linked with the T-stellate (multipolar) cells of the AVCN and PVCN. These are excitatory cells and form the major ascending pathway, projecting to the contralateral inferior colliculus (Oertel et al., 2011).

Onset responses in the VCN are produced by octopus and D-stellate cells of the PVCN (Arnott et al., 2004; Godfrey et al., 1975). The glycinergic D-stellate cells show onset-chopper (an onset response with two or three peaks) responses and project to the ipsilateral DCN and the contralateral cochlear nucleus (Arnott et al., 2004; Palmer et al., 2003). Octopus cells are located in a subdivision of the PVCN and produce other onset responses (On-I and On-L) (Godfrey et al., 1975).

There are also phase-locked cells in the low frequency areas (Fig 1.6), in which the firing pattern is related to the waveform of the auditory input. During a high frequency sine wave stimuli auditory nerve fibres fire randomly. However, at lower frequencies ($<$5 kHz) auditory nerve activity can be correlated with the phase of the stimulus. This is due to the waveform creating sinusoidal movement of the basilar membrane, which produces rhythmic depolarisation and hyperpolarisation of the inner hair cells. This phase-locked firing pattern is maintained in the cochlear nucleus. All cell types can phase lock at frequencies $<$1 kHz, and some up to $\approx$5 kHz (Rhode & Smith, 1986).

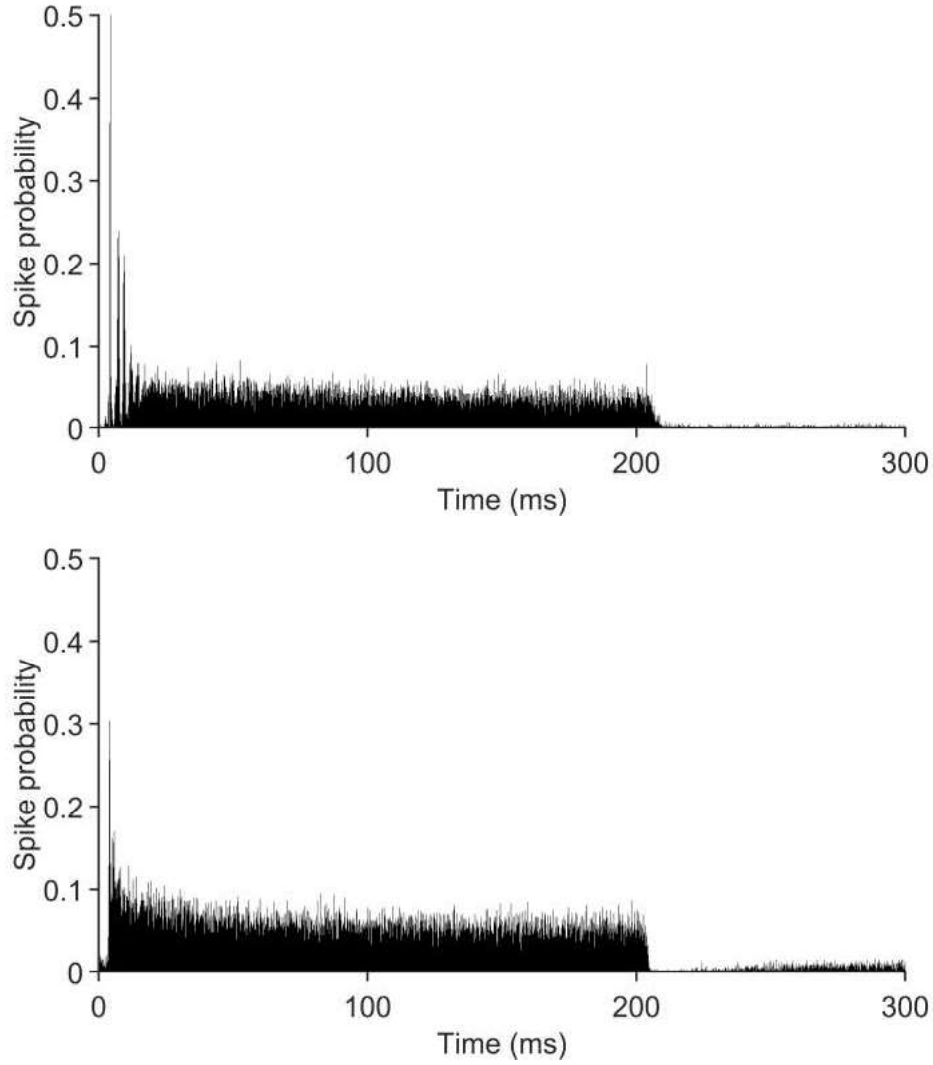


Fig. 1.5: Examples of peri-stimulus time histograms recorded from auditory neurons in the guinea pig ventral cochlear nucleus. These show classic chopper (top; T-stellate cell; CF 12 kHz) and primary-like (bottom; bushy cell; CF 25 kHz) responses. Bin sizes = 0.5ms.

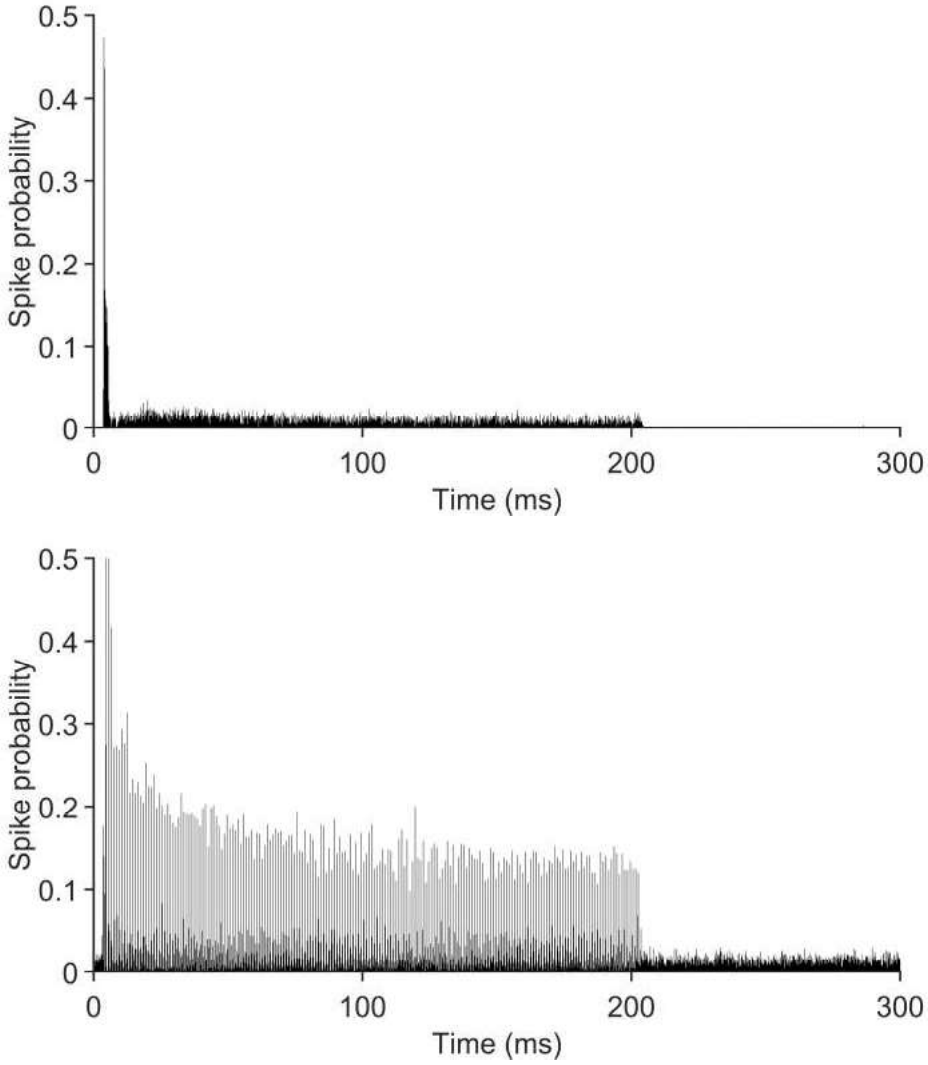


Fig. 1.6: Examples of peri-stimulus time histograms recorded from auditory neurons in the guinea pig ventral cochlear nucleus. These show classic onset (top; D-stellate or octopus; CF 13 kHz) and phase-locked (bottom; CF 1 kHz) responses.

1.4 Animal models of tinnitus

Potential treatments for tinnitus are often tested on animal models, in which tinnitus must be induced followed by behavioural testing in order to determine differences from the norm in tinnitus animals. Following this, physiological tests are conducted to study changes to the auditory system in tinnitus. This is essential for understanding of the mechanisms underlying tinnitus, which in the future may aid the development of clinical treatments in the form of medical devices or pharmaceutical products for the prevention or relief of tinnitus.

1.4.1 Inducing tinnitus

As tinnitus in man is most often thought to be caused by damage within the cochlea resulting from frequent loud noise exposure (Shargorodsky et al., 2010), the most physiologically accurate way of inducing tinnitus in animals is acoustic over exposure (AOE). AOE producing cochlear synaptopathy, a disconnection between hair cells and spiral ganglion cells, is thought to be the cause of hearing loss, and therefore tinnitus. One model of tinnitus attempts to also produce cochlear synaptopathy, in order to mirror the cause of tinnitus. This model often uses unilateral AOE to induce tinnitus, which is shown behaviourally 8+ weeks post-AOE (Turner et al., 2006).

AOE induced tinnitus is often achieved by presenting sounds of 110-124 dB SPL for 1-2 hours (Coomber et al., 2014; Dong et al., 2010; Gourévitch et al., 2009; Tziridis et al., 2015), with tinnitus developing in 50-75% of animals 8 weeks post-exposure. Variations exist in the frequency, duration and intensity of sounds presented, and number of sessions of noise exposure used to produce acoustic trauma. It may be important to standardise the AOE stimuli to ensure compatibility of results between labs, as induction of tinnitus using unequal stimuli may create difficulties comparing studies.

It has been shown that the duration and number of exposures to trauma stimuli affect the threshold and latency of auditory brainstem responses (ABRs) (Gourévitch et al., 2009). Tinnitus in humans is often caused by frequent exposure to loud sounds, as opposed to a single exposure to a traumatising sound. Therefore, mimicking this by daily exposure to sounds

greater than 85 dB SPL for many months or years could be a more accurate model for inducing tinnitus. However, this would be difficult to implement in a laboratory setting due to the time required.

One alternative tinnitus generation model is systemic salicylate administration. Salicylate is the active metabolite of the non-steroidal anti-inflammatory drug aspirin (Wu, 2000). It acts as an anti-inflammatory agent and analgesic at therapeutic doses and can be used to treat headaches and other minor conditions. At higher doses, salicylate administration produces a reversible tinnitus in humans (Mongan et al., 1973). The benefits of this model are that tinnitus is induced reliably, rapidly and reversibly, allowing recordings to be made before, during and after the perception of tinnitus.

Salicylate is taken up simultaneously by the cerebrospinal fluid and the perilymph (Jastreboff et al., 1986), and exerts its effects centrally and peripherally (See Stolzberg et al., 2012 for review). However, due to the direct central effects, the mechanisms behind this tinnitus are likely different to those that occur following AOE in humans, so this is likely not a physiologically accurate model for noise-induced tinnitus in humans. This makes it a useful methodology for studying tinnitus characteristics and behavioural testing, but less so for molecular mechanistic studies.

1.4.2 Behavioural confirmation of animal tinnitus

Animal models of tinnitus began to be developed in the late 1980's. Experiments using early behavioural models allowed assessment of the psychophysical properties of tinnitus induced in animals (Jastreboff et al., 1988). These experiments however gave no insight to the changes to neural mechanisms that underlie tinnitus, and therefore offered limited understanding of the condition. Physiological recording was then used to measure neuronal activity, in an attempt to observe abnormal changes correlating with tinnitus. Behavioural and physiological methods are now often combined in studies to complement each other by eliminating the limitations of both (Von Der Behrens, 2014).

The majority of behavioural tests are based upon measuring of conditioned motor responses to sounds and silence. Motor actions that are easily learned by animals, such as licking or button pressing, are often used in order to make conditioning more efficient and reduce training time

required. Positive or negative reinforcement, such as the presentation of food or an electric shock, can be used to train the test animals to perform an action in response to sounds. If trained to respond to sound, absence of this action therefore shows lack of sound perception, or alternatively a different behaviour can be conditioned to show the perception of silence. Behavioural tests of this sort can be used to study tinnitus as they provide a way of assessing the sound perception of the test animal (Hayes et al., 2014).

For example, in 1988 Jastreboff et al. used footshocks to train rats to fear the offset of sound. This was achieved by exposure to constant low level sounds, and footshock stimuli upon cessation of the sound. The rats were partially water deprived and trained to lick a water spout during the presence of a sound. Water consumption was measured via a lickometer. After 4-10 footshocks, the rats would show fear behaviour during silence, even without the presentation of a footshock, and this behaviour would reduce the rate of licking. This therefore provided a method for analysing the auditory perception of the rat, with the prediction being that animals perceiving tinnitus (due to treatment with ototoxic drugs or AOE) would show weaker fear behaviour during silence due to the tinnitus percept. This effect was indeed observed after salicylate administration (Jastreboff & Sasaki, 1988), supporting the model. Further control testing confirmed that this effect was not due to hearing loss, or the effect of salicylate on any other sensory modalities (Jastreboff, 1990).

This method was accepted as a way of inducing and detecting tinnitus in animals, and by changing parameters within the stimulus design it was possible to determine psychophysical properties, such as pitch and loudness, of tinnitus in animals. However, it was a lengthy process which required weeks of training before tinnitus could be induced, and there were many confounding factors such as hyperacusis (increased sensitivity to certain sounds), motivation or memory. To counteract these, an alternative behavioural model was created by Turner in 2006 based upon the acoustic startle.

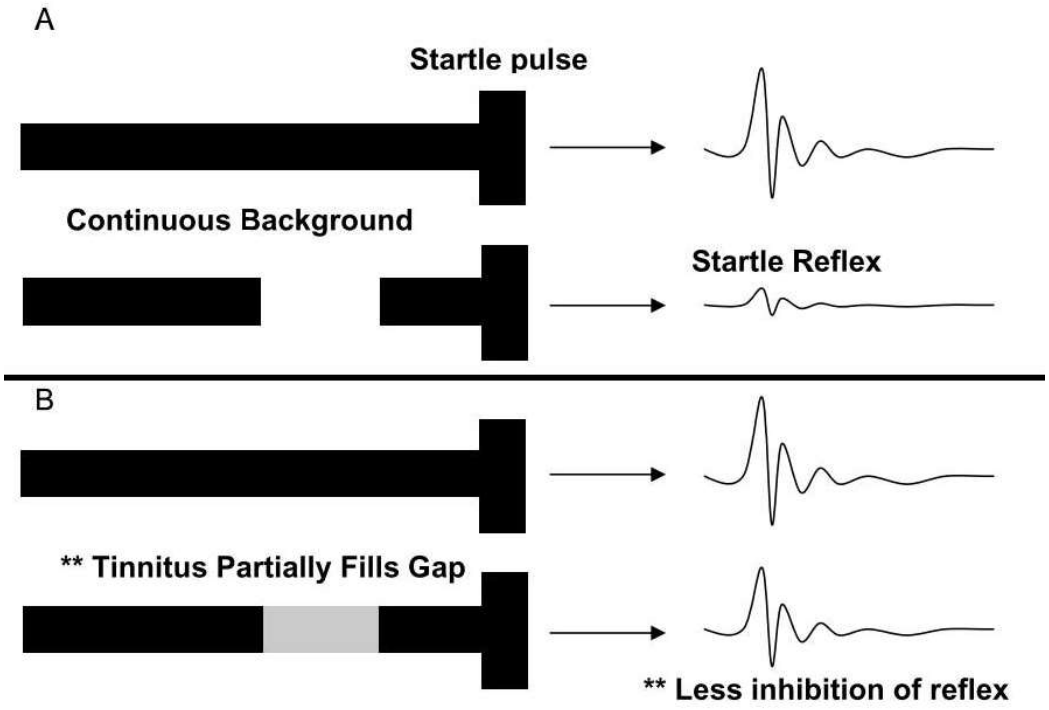


Fig. 1.7: Demonstration of the auditory stimuli and resulting reflexes in the GPIAS test. (Turner & Parrish, 2008)

The acoustic startle is a reflex response to sudden loud noise that is exhibited by mammals, and often measured using the whole-body startle using a pressure platform. If an auditory pulse is placed within background noise that is slightly preceded by a gap in the background noise, the resulting acoustic startle is reduced (Fig 1.7A). This is a form of gap-induced prepulse inhibition. It was hypothesised by Turner that if an animal is experiencing tinnitus it will at least partially fill the gap in background noise, reducing the inhibition of the startle by the gap (Fig 1.7B). This is referred to as gap prepulse inhibition of the acoustic startle (GPIAS) test, and it has several advantages over the conditioning model. Firstly, it is not dependent on learned actions by the animals so testing is more efficient and memory and motivation play no role. Also, it is a reliable reflex which can be seen in almost all animals and is predominantly a lower brainstem reflex (Davis et al., 1982) that does not require any training. It is, however, subject to emotional modulation and is potentiated by stress and fear (Andreski et al., 1998; Anisman et al., 2000). Using this method, it is also possible to assess the frequency and estimate the loudness of the tinnitus experienced by the animal.

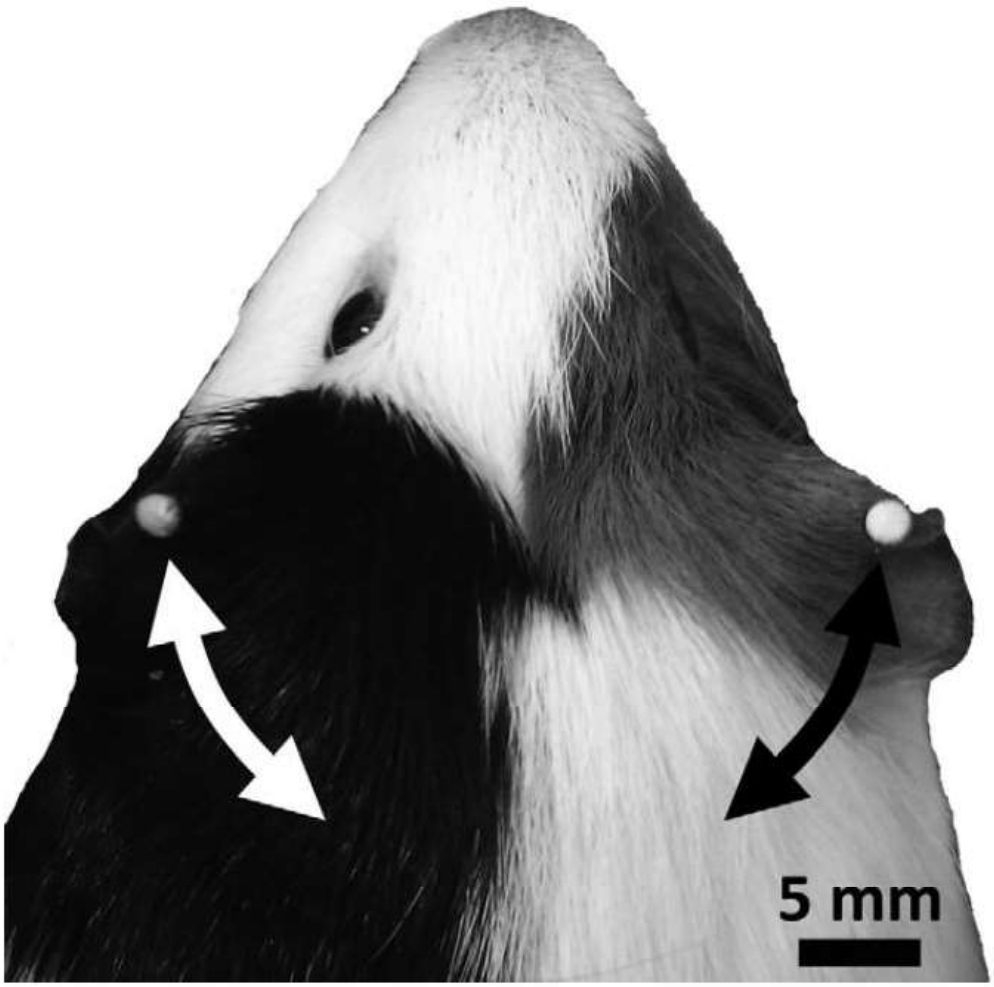


Fig. 1.8: A guinea pig with reflective markers on each ear to allow optical tracking of pinna movements. (Berger et al., 2013)

A variation of this test involving measurement of the Preyer reflex has since been developed in guinea pigs (Fig 1.8; Berger et al., 2013). This involved measurement of the pinna movement in response to a startle and was found to be a more robust measure than the whole body startle, showing less habituation through trials and a higher signal to noise ratio. Using this method, GPIAS was observed at all different frequencies in all animals tested, and the sensitivity of GPIAS to salicylate was much greater than when measuring the whole body startle. This suggested that GPIAS as a reflex can be used as a more accurate demonstration of tinnitus.

The GPIAS test does however have some caveats. First, the need to control for hearing loss, which can occur following noise exposure or administration of ototoxic drugs. Hearing loss can affect the test by

reducing the detection of the background sound or the startle. To counteract this, the background noise can be set at intensities of around 60 dB SPL, which is sufficient to be resilient to hearing loss. Using a pre-pulse before a startle stimulus within silence could also be used to determine an appropriate background sound intensity. If the pre-pulse reduces the startle response then perception of the sound at that level is determined, suggesting it is a useful background sound intensity.

Decreases in the startle intensity to a pre-pulse have been observed following noise exposure, potentially indicating hearing loss (Lobarinas et al., 2013). However, hyperacusis can also occur in animals following noise exposure, which would be expected to increase startle amplitudes. Increased acoustic startle responses following noise exposure have been observed, consistent which a hyperacusis-like augmented auditory perception (Chen et al., 2013).

This behavioural method, as with all others, has the limitation that it cannot show the pathophysiological cause of the tinnitus percept. Physiological methods must therefore be utilised, potentially in tandem with behavioural methods, to gain insight to the neural mechanisms underlying tinnitus.

1.5 Neural correlates of tinnitus

Electrophysiological recordings can be used to measure the activity of neurons in the auditory system as single-units, multi-units or as gross potentials created by their activation within brain areas. It is thought that, as tinnitus is the perception of a phantom sound, there must be mechanisms present which alter the neural activity during the absence of auditory input. The assumption is that the alterations of neural activity during silence would resemble the activity resulting from auditory input. It therefore seems the most likely neural correlate of tinnitus would be increased spontaneous activity through the auditory system, as this would create the perception of a phantom sound at higher centres. However, hearing loss also results in increases in spontaneous activity, creating a confounding variable when studying tinnitus (Eggermont, 2015). Due to this, physiological techniques have so far struggled to elucidate the neural correlates of tinnitus. The mechanism and location of the source of the spontaneous activity has so far been elusive, and its role in tinnitus is unconfirmed.

Electrophysiological recording has been used throughout the auditory system to study single-unit activity. This has allowed the categorisation of nuclei and cells, often based upon their firing pattern in response to auditory stimuli (Palmer, 1987). Changes to the firing patterns and rates of these cells following the induction of tinnitus have been studied frequently in tinnitus animals (Auerbach et al., 2014), with the changes from control potentially providing clues to the neural activity underlying tinnitus perception. One of the suggested changes is that there is an increase in the synchrony of firing among groups of neurons within an auditory structure (Eggermont & Tass, 2015).

Changes in gross activation patterns of neural structures in the whole brain have also been assessed in relation to tinnitus. This is often studied using EEG or neuroimaging techniques such as MRI, PET or mapping of metabolic activity (Adjamian et al., 2012; Middleton & Tzounopoulos, 2012). Imaging studies carry the advantage that they can be performed on humans and animals, as they are non-invasive. Again, changes are compared to control animals or humans in order to determine changes in auditory system activity that may be related to tinnitus. These studies are most widely used in the auditory cortex, where they have shown humans

with tinnitus have reduced alpha activity and increased delta and gamma activity compared to healthy controls (van der Loo et al., 2009; Weisz et al., 2005). Increased gamma activity is often suggested to be related to phantom perception, and this increased gamma activity in tinnitus has been shown to be correlated with the subjective tinnitus loudness (van der Loo et al., 2009). However not all studies have confirmed this, as one study of rock musicians with transient tinnitus who also showed increased gamma oscillations but with no clear relationship to the magnitude of perceived tinnitus (Ortmann et al., 2011). This view of gamma contributing to tinnitus has also been challenged. A study using a technique known as residual excitation to temporarily increase the perception of tinnitus has shown that this temporarily increased tinnitus correlates with a decrease in gamma oscillations (Sedley et al., 2012). It is therefore possible that gamma oscillations have a negative effect on tinnitus, they may be elevated in tinnitus patients not as a production mechanism, but as a mechanism to control tinnitus.

Electrophysiological recordings are also used in an attempt to identify molecular mechanisms responsible for increasing activity in the auditory system (Kraus et al., 2009; Tzounopoulos, 2008). Drugs affecting neuronal signalling can be applied to single cells using micro-iontophoresis, locally using glass pipettes or canulae inserted stereotaxically, or systemically. Using physiological methods to understand the molecular mechanisms of tinnitus generation could potentially lead to the development of pharmacological treatments, so this is an important area of basic scientific research.

There are some problems present in physiological studies of tinnitus. They cannot show that animals are experiencing tinnitus, only that a physiological measurement has differed from the norm. Therefore, either a reliable inducer of tinnitus such as salicylate must be used, or behavioural testing must also be used to confirm tinnitus induction.

Also, some physiological studies, such as electrophysiological recording from central auditory structures may require animals to be anaesthetised. Anaesthetics have been shown to affect activity in the auditory system in many ways; by changing the frequency tuning and tonotopic organisation in central auditory nuclei (Gaese & Ostwald, 2001; Imig & Morel, 1985); by reducing spontaneous firing in the inferior colliculus, auditory thalamus

and cortex, possibly through potentiation of the action of GABA (Kuwada et al., 1989; Zurita et al., 1994); and by differentially affecting the size of burst discharges (Zurita et al., 1994). These effects are often central and specific to the anaesthetic used, reducing the clarity of which signatures in physiological studies can be identified as tinnitus markers and which are a result of anaesthesia.

1.6 Mechanisms of tinnitus generation

Tinnitus is characterised by the perception of sound with no external origin. When tinnitus was first studied it was believed to be generated peripherally, so the auditory nerve was sectioned in an attempt to remove all auditory input and cure the tinnitus. It was known that this would cause deafness, highlighting the extent some people will go to escape their tinnitus. In about 40% of patients the tinnitus was improved, suggesting a potential peripheral origin, while also demonstrating the heterogeneity of tinnitus (House & Brackmann, 1981). The other half of patients showed increased severity of tinnitus following sectioning of the nerve. Overall the effect was small, forcing surgeons to stop using the technique. It was then clear that central mechanisms contributed to tinnitus, and it was not a purely peripheral disorder. This section will analyse the scientific literature that studied the pathophysiology of tinnitus in the central nervous system.

1.6.1 Central gain

The neural basis of tinnitus is poorly understood; in some cases, tinnitus is thought to occur in response to damage of inner or outer hair cells in the ear by loud sounds, ototoxic drugs, or other cochlear pathologies; which result in compensatory changes in the neuronal activity of the auditory pathway. Changes in electrophysiological activity associated with tinnitus have been observed at different levels of the nervous system in both humans and animals, with a decrease in activity closer to the periphery and an increase further up the system often observed (Salvi et al., 2000). This maladaptive increase through the system is known as central gain.

One way to assess central gain is to measure auditory brainstem responses (ABRs), which are auditory-evoked potentials normally recorded by surface electrodes (Pratt et al., 1981). A wave formation is seen, with each peak relating to the activation of a neural tract in the auditory system. There are generally accepted to be 5 waves in a guinea pig ABR, with wave I deriving from the auditory nerve, wave III originating from output from the cochlear nucleus and wave V generated by output from the inferior colliculus. In tinnitus patients and animals, a decrease in wave I amplitude is seen, due to cochlear damage (Dehmel et al., 2012a; Schaette & McAlpine, 2011). Following this, normal or increased waves III and V are observed, demonstrating an increase in transmission from the cochlea up to the

auditory cortex (Shargorodsky et al., 2010). The increase in amplitudes through the auditory system is often pointed to as a central gain form of tinnitus. However, distinguishing between tinnitus and hyperacusis using ABRs can be especially complicated (Auerbach et al., 2014).

Locating the origin of central gain is a complicated issue, as changes are seen in many of the auditory nuclei following noise exposure. After noise exposure, measurements of local field potentials (LFPs) show increased thresholds at the cochlear nerve, inferior colliculus and auditory cortex in guinea pigs (Popelár et al., 1987) and chinchillas (Salvi et al., 1990).

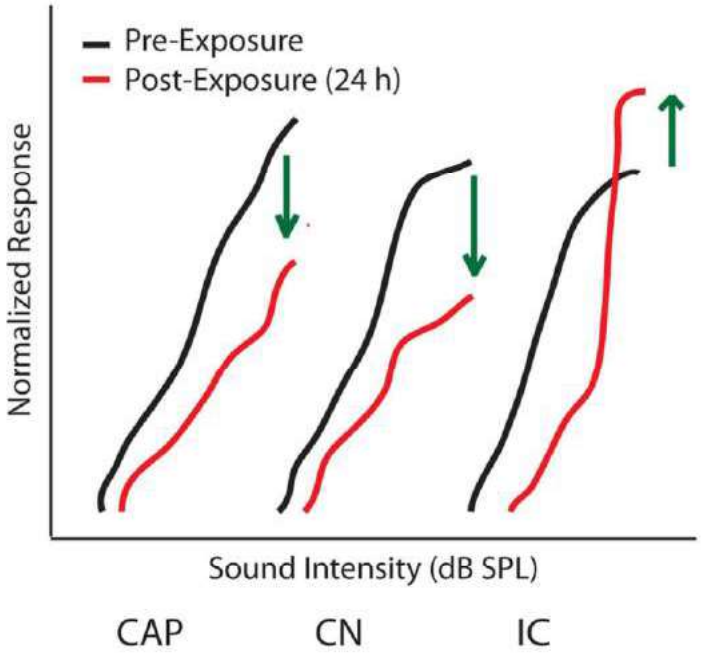


Fig. 1.9: Intensity-level functions from three stages of the auditory system, cochlea (CAP), cochlear nucleus and inferior colliculus. Gain is seen in the IC 24 hours post-noise exposure (Auerbach et al., 2014).

Despite these threshold shifts, increases of activity in response to supra-threshold noise are increased at the level of the IC (Fig 1.9) and AC of awake guinea pigs (Popelár et al., 1987). The same changes to threshold and evoked activity were observed in chinchillas following administration of an ototoxic drug that selectively damaged inner hair cells (Salvi et al., 2000), further confirming that the central changes were in response to the reduced input from the periphery. These same increases in LFP amplitude are not found in the cochlear nucleus (Gerken et al., 1984), however this

does not rule out the CN as a source of central gain for several reasons. LFPs measure a large neural population therefore if changes in CN were only in a small proportion of cells or cell type specific, they may not be detected.

When studying single unit activity, as opposed to the hundreds of neurons that LFPs record simultaneously, changes are seen at the level of the cochlear nucleus. Studies in monkeys and chinchillas demonstrate that changes in activity here appear to be cell type specific (Boettcher & Salvi, 1993; Lonsbury-Martin & Martin, 1981). More recently, work in the cat VCN has shown an enhancement of rate-level functions in chopper cells 33-121 days post-AOE (Cai et al., 2008). This suggests that a gain system is in place, increasing excitability in response to higher input from the auditory nerve. Note that in this study enough time was left that tinnitus may have developed inadvertently, so the enhancement of these chopper rate-level functions may be related to tinnitus and not simply noise exposure. The opposite was seen in primary-like cells, with reduced responses at higher sound levels in noise-exposed animals. This possibly demonstrates why there are no changes in LFPs from the VCN following acoustic trauma, as the increases in activity of choppers and decreases in primary-like units may cancel each other out. Chopper cells project directly to the IC and form a major ascending pathway, making them an interesting target for further studies into tinnitus generation.

Similarly, in the DCN, enhanced rate level functions have been shown in guinea pig fusiform cells at 16 days post-AOE (Dehmel et al., 2012b), data that suggests increases in DCN and VCN activity may play a role in the induction of central gain. It is likely, however, that the cochlear nucleus is not the sole origin of central gain, as only a 25% gain can be observed within the VCN (Boettcher & Salvi, 1993), which is lower than is seen at higher nuclei such as the IC (Salvi et al., 1990).

Human studies using EEG indicate that people with chronic tinnitus may show a reduction in alpha activity and increases in delta or gamma activity (Müller et al., 2013; Weisz et al., 2005), and this may be due to an increase in input from the brainstem resulting from central gain. The mechanisms involved in central gain enhancement are still debated; with evidence for both decreased inhibition and increased excitation (Kaltenbach, 2011). A role has also been suggested for synaptic plasticity strengthening transmission between neurons (Auerbach et al., 2014; Noreña, 2011).

1.6.2 Plasticity of neural connections

One mechanism thought to contribute to the development of tinnitus is synaptic plasticity. Synaptic plasticity allows the strengthening and weakening of synapses over time, in response to changes in neuronal activity. Often changes in synaptic strength are due to changes in neurotransmitter release, receptor density or synaptic structure, and there are multiple mechanisms in place to alter these variables. There are 2 main forms of synaptic plasticity; Hebbian and homeostatic plasticity (Vitureira & Goda, 2013).

Hebbian plasticity includes short-term plasticity, long term potentiation (LTP) and long term depression (LTD). Short-term plasticity involves changes in activity over a period of up to one minute, and can produce either an enhancement or depression of transmission (Zucker & Regehr, 2002). The overall effect differs between synapses, and it is thought this is due to a summation of enhancement and depression effects at synapses.

Long-term potentiation produces an enhancement of synaptic transmission, which lasts longer than a minute, up to one year (Abraham et al., 2002). Long-term depression reduces synaptic strength for prolonged time course. Both of these changes are a form of positive feedback, as high frequency synaptic activity often results in LTP, with lower frequency activity resulting in LTD. The mechanisms underlying long-term synaptic plasticity can vary between individual neurons, and there is evidence for pre- and post-synaptic contributions to LTP (Granger & Nicoll, 2013). When combined, these two types of plasticity allow the synapse to produce the changes in strength that underlie learning and memory (Abraham et al., 2002), and may contribute to tinnitus.

Hebbian synaptic plasticity could underlie the central gain seen within auditory structures during tinnitus, as it allows amplification of inputs over long time frames. Some studies have focussed on synaptic plasticity in the DCN (Tzounopoulos, 2008), finding that the strength of synaptic transmission can be altered by the history of activation (Tzounopoulos et al., 2004). They found evidence for LTP and LTD in fusiform and cartwheel cells respectively, which combined to increase activity in fusiform cells, the direct projection cells from the DCN to the inferior colliculus.

Studies into plasticity in the VCN have often analysed the expression of growth associated protein 43 (Chen et al., 2004; Kraus et al., 2009; Kraus et al., 2013; Kraus & Illing, 2004;). GAP-43 is highly expressed in neuronal growth cones, with increased expression observed following LTP induction; suggesting it aids growth of new synapses, therefore strengthening transmission between neurons (Benowitz & Routtenberg, 1987).

Two other potential biomarkers for synaptic plasticity are mitogen-activated protein kinase (MAPK) and cAMP response element binding protein (CREB). These form part of an intracellular signal cascade which regulates the transcription of DNA, therefore any long-term synaptic changes involving changes in protein production may show changes in these factors (Abraham et al., 2002).

One issue with Hebbian plasticity is that it destabilises circuits. This is due to the positive feedback having the capability to increase or decrease synaptic strength in a continuing manner (Fig 1.10A). It therefore needs some form of control mechanism to prevent this run-away change of synaptic strength. This control is called homeostatic plasticity, and it acts very differently to Hebbian plasticity, counteracting it. Hebbian plasticity destabilises circuits and homeostatic plasticity using negative feedback, works to maintain mean firing rates (Fig 1.10B; Turrigiano, 1999). Homeostatic plasticity is thought to act through two mechanisms; synaptic scaling and metaplasticity. Synaptic scaling involves the up or down-regulation of all synapses of a neuron in response to a decreased or increased firing rate respectively (Turrigiano, 1999). In contrast, metaplasticity is often defined as the ”plasticity of synaptic plasticity” and controls the balance between LTP and LDP (Abraham, 2008). A maladaptive homeostatic plasticity mechanism may be more likely to produce central gain, as this could allow an increased gain following reduced input from the periphery, producing an increased firing rate in higher auditory nuclei. Homeostatic plasticity has been suggested as a tinnitus generation mechanism (Schaette and Kempter, 2006), however, no studies have yet focussed on the mechanisms of this homeostatic plasticity in tinnitus.

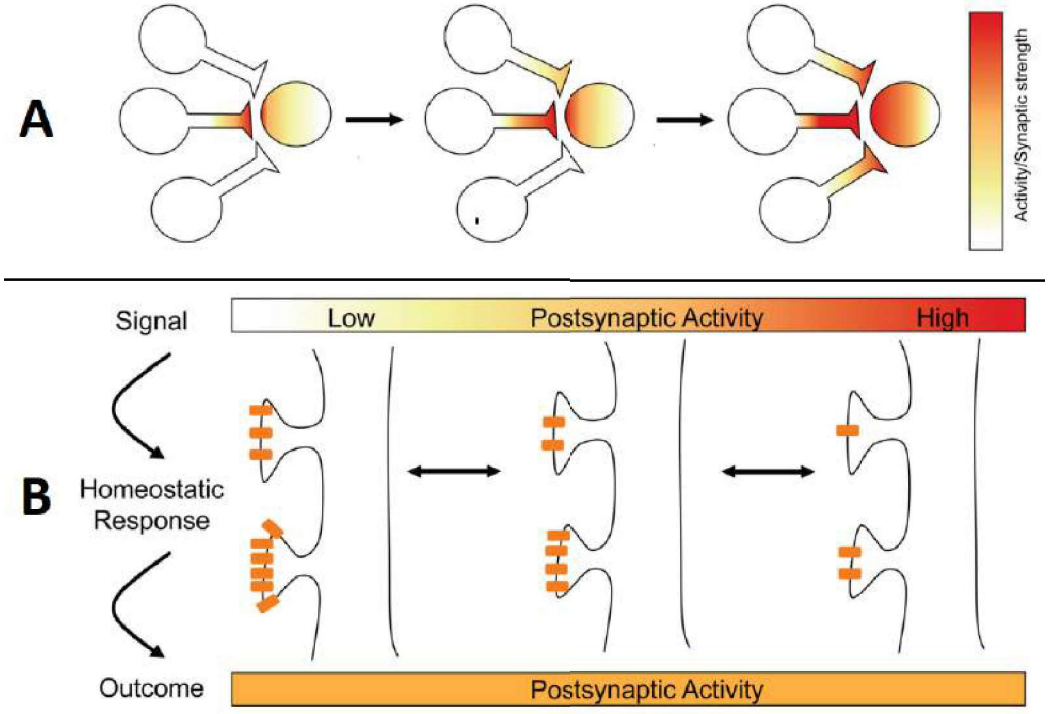


Fig. 1.10: (A) The diagrams from left to right show the effect of uncontrolled LTP, with increased activity further increasing activity. (B) A homeostatic plasticity mechanism, in this case receptor density is increased or decreased to maintain mean firing rate. (Watt & Desai, 2010)

1.6.3 Alternative aspects of tinnitus

In some types of tinnitus it has been observed that by providing somatosensory input, often by rubbing the jaw or neck, tinnitus can be temporarily relieved (Levine et al., 2003). This is thought to involve the DCN, which combines multimodal information in order to reduce the perception of self-induced sounds such as movements of the head and neck. Electrophysiological studies in this nucleus have shown spike-dependent timing plasticity (SDTP) (Wu et al., 2015), which alters post synaptic excitability based on the relative timing of two different inputs to a single neuron.

The limbic system may also have a role in determining the severity of tinnitus and its pathological correlates (Leaver et al., 2011), as the degree of annoyance of the tinnitus is not correlated with its intensity, but is correlated with comorbidities such as anxiety, depression and sleeplessness (Cianfrone et al., 2015). Therefore, it is proposed that activation of the limbic system in tinnitus patients may vary, and by reducing this we may be

able to relieve some of the stress involved with chronic tinnitus (Leaver et al., 2011).

1.7 Nitric oxide

Nitric oxide (NO) is a gaseous free radical that acts as an important cell signalling molecule in almost all organisms. It was first discovered by Robert F. Furchgott in 1978, who named it endothelium-derived-relaxing factor (EDRF), as he had established that it was released from endothelial cells to promote blood vessel relaxation. At first the chemical structure was unknown, but by 1986 his studies revealed that EDRF was NO, and he received the 1998 Nobel Prize in Physiology or Medicine for his work, along with Louis J. Ignarro and Ferid Murad (SoRelle, 1998). NO has been identified in many forms of synaptic plasticity and has been shown to be present in the cochlear nucleus, therefore it is a likely to be implicated in tinnitus. This chapter will give an overview of nitric oxide, before the following chapter explains the known roles of NO in the auditory system.

Most work into NO has focused on its effect on blood vessels and blood pressure. Study of the NO pathway has resulted in drugs being developed which can alter blood pressure. One common example of this is sildenafil citrate, a phosphodiesterase inhibitor often known by the trade name Viagra. This promotes vasodilation of the penis, stimulating erections (Michelakis et al., 2000).

1.7.1 Molecular basis of production

The most common route of NO production is cleavage from the amino acid L-arginine by the enzyme nitric oxide synthase (NOS). This requires arginine, NADPH + H^+ and O_2, and produces citrulline, $NADP^+$ and NO. Three types of NOS are present in mammals; endothelial NOS, neuronal NOS and inducible NOS (See Table 1.1 for more information).

NAME	GENE	LOCATION	FUNCTION
NEURONAL NOS (NNOS)	NOS1	Nervous system Skeletal muscle	Cell communication
INDUCIBLE NOS (INOS)	NOS2	Immune system Glial cells	Immune defence
ENDOTHELIAL NOS (NOS)	NOS3	Endothelium	Vasodilation

Table 1.1: Classification of NOS isoforms.

An alternative method of NO production, the nitrate-nitrite-nitric oxide pathway, involves the production of NO from nitrate, an ion previously thought to be biologically inert (Lundberg et al., 2008). This has been shown to occur during hypoxia or acidosis (Shiva, 2013), which should not occur to a great extent in healthy animals. It is assumed in this report that the entirety of NO production occurs via cleavage from L-arginine by NOS.

1.7.2 Mechanism of action and regulation

The activity of eNOS and nNOS is regulated by an increase in intracellular Ca^{2+} levels, via the calcium sensing protein calmodulin (Weissman et al., 2002). Binding of Ca^{2+} to calmodulin forms the Ca^{2+}/Calmodulin complex which binds to NOS, activating it (Purves et al., 2012). Increases in Ca^{2+} intracellularly may be due to extracellular influx through NMDA receptors or release from intracellular stores such as the endoplasmic reticulum.

As shown in Fig 1.11, NOS enzymes act intracellularly to catalyse the reaction which cleaves NO from L-arginine. This free NO can then act to increase the action of soluble guanylyl cyclase (sGC), which catalyses the conversion of guanosine triphosphate (GTP) to cyclic guanosine monophosphate (cGMP). cGMP has 2 main intracellular targets; protein kinase G (PKG) and cyclic nucleotide gated ion channels (CNGCs). Its levels are regulated by cyclic nucleotide phosphodiesterase (PDE) mediated breakdown (Rang et al., 2012). There are 11 isoforms of PDE, some of which are spatially specific through the mouse brain (Maurice et al., 2014).

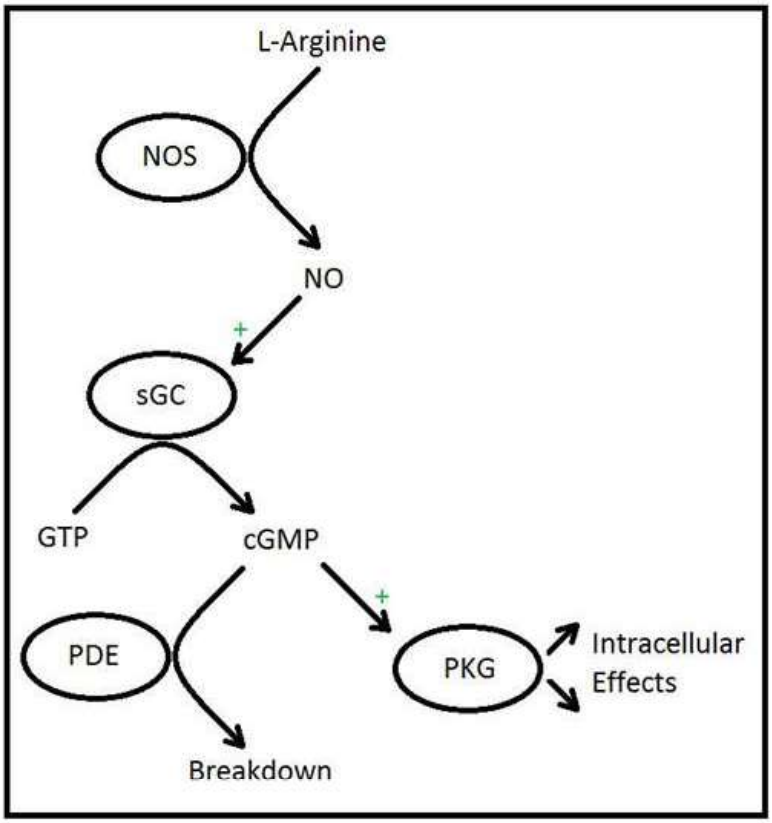


Fig. 1.11: A simplified view of the intracellular nitric oxide/cGMP pathway. NOS, nitric oxide synthase; NO, nitric oxide; sGC, soluble guanylyl cyclase; GTP, guanosine triphosphate; cGMP, guanosine monophosphate; PDE, phosphodiesterase; PKG, protein kinase G.

The action of cGMP on protein kinase G (PKG) increases its enzyme activity. PKG phosphorylates proteins at serine and threonine residues, allowing it to exert a functional control on proteins (Ahern et al., 2002). PKG can regulate many ion channels, producing a variety of intracellular effects dependent on the state of the cell (Jonas & Kaczmarek, 1996; Light et al., 1990).

cGMP also binds to cyclic nucleotide gated channels (CNGCs), allowing Na^+ and Ca^{2+} influx (Ahern et al., 2002). This action can increase excitability by depolarising resting membrane potentials and calcium influx may also provide a positive feedback loop for NO production.

Since intracellular cGMP competes with cAMP for binding at phosphodiesterases (PDEs); an increase in cGMP can lead to a reduction in cAMP breakdown, raising the intracellular concentration of cAMP and

potentiating processes mediated by this cyclic nucleotide (Rang et al., 2012).

It is important to note that NO does not act solely via sGC. At higher concentrations it can also produce a direct post-translational modification effect on proteins (Jaffrey et al., 2001). Known as S-nitrosylation, this is a mechanism by which NO can bind to and modulate ion channels, increasing excitability independent of cGMP (Ahern et al., 2002).

Alteration of the nitric oxide/cGMP signalling pathway can be achieved at many different stages. In order to increase activity of PKG, the concentration of L-arginine or NO can be increased by direct application onto cells. Inhibition of PDEs can also increase the activity of PKG indirectly, by reducing the breakdown of cGMP. PDE inhibitors have clinical significance in heart disease and erectile dysfunction due to the role of the nitric oxide/cGMP cascade in regulating vasodilation (Rang et al., 2012).

Reduction of PKG activity through inhibition of NOS or sGC is possible. Comparison of the effects of NOS inhibitors and sGC inhibitors can help elucidate whether the NO effect is mediated solely or partially by sGC (Sammut et al., 2010).

1.7.3 Effect on neuronal activity

More recently the role of NO as a neuromodulator has been identified (Postorino et al., 1998; Sha et al., 1995). NOS is found in the cell soma and at the post-synaptic density, bound by PSD-95 (Brenman et al., 1996). Neuronally generated NO can freely permeate membranes and diffuse through extracellular media, allowing it to act presynaptically and intracellularly on neurons up to 100 μm from the site of production (Steinert et al., 2008), altering synaptic plasticity between multiple adjacent cells.

As previously discussed, there are 2 main forms of synaptic plasticity; Hebbian and homeostatic. Three main types of Hebbian synaptic plasticity exist; short-term plasticity, long term potentiation (LTP) and long term depression (LTD), and 2 forms of homeostatic plasticity; synaptic scaling and metaplasticity. These mechanisms allow for changes in strength of synaptic transmission over time, in response to changes in recent input activity.

NO is a neuromodulator that contributes to synaptic plasticity in a number of ways. First, it has been implicated in playing a role in the production of short-term plasticity (Sammut et al., 2010); however, as long-term synaptic changes are a more likely mechanism to contribute to tinnitus, they will be the focus of this section.

Long-term potentiation has been shown to be reliant on a rise in intracellular Ca^{2+}, caused by influx through NMDA receptors during prolonged stimulation (Malenka, 1991). This Ca^{2+} also increases NO production (Alderton et al., 2001), suggesting that it may contribute to LTP. As NO can freely diffuse across cell membranes and through extracellular space, presynaptic effects of NO on LTP are possible. Mechanisms of NO-dependent LTP had long been predicted (Huang, 1997), and more recently these mechanisms have been discovered. It has been shown that PKG can upregulate the mitogen-activated protein kinase (MAPK) pre- and postsynaptically (Ping & Schafe, 2010), which is required for LTP and LTD (Rosenblum et al., 2002; Thiels et al., 2002). Therefore, this may be a mechanism by which NO contributes to the genetic changes required for LTP.

The idea that NO may also act presynaptically to increase glutamate release has been around for decades (Huang, 1997), though mechanisms to allow this have only recently been elucidated. It has been shown that sGC, once activated by NO, can act at presynaptic hyperpolarisation-activated cyclic nucleotide gated channels (HCNs), leading to enhanced pre-synaptic depolarisation and glutamate release, creating a feed-forward loop (Neitz et al., 2011). The same group have also shown a post-synaptic effect of NO, with cGMP altering NMDA receptor currents (Neitz et al., 2014).

The mechanisms underlying NO and LTP are still debated; however the application of the NOS inhibitor nitro-L-arginine methyl ester hydrochloride (L-NAME) removes evidence of LTP both behaviourally (Li et al., 2012) and electrophysiologically (Lange et al., 2012), indicating a strong relationship between NO signalling and LTP.

Homeostatic plasticity is also mediated by NO (Le Roux et al., 2009), where it maintains firing rates by increasing the availability of synaptic vesicles, and release probability (Hardingham et al., 2013). It is not known how this may relate to the auditory system, and in particular tinnitus; however

it must be considered as a possible mechanism for tinnitus induction as central gain could involve homeostatic plasticity mechanisms.

Due to the variety of intracellular processes affected by NO, it cannot be viewed as either a typical excitatory or inhibitory neurotransmitter, and its action on individual neurons can be difficult to predict. Often the effect of NO is dependent on a number of factors such as baseline activity, receptor densities, previous activity and enzyme expressions.

1.8 The presence and action of nitric oxide in the auditory nervous system

NOS has been identified in many stages of the auditory system, from the cochlea up through the cochlear nuclei, SOC, IC and to the auditory cortex (Table 1.2). The presence of nitric oxide throughout the auditory system strongly suggests that it contributes to auditory processing; however what role it plays at different stages is still unclear.

AUDITORY STRUCTURE	ANIMALS IN WHICH IT IS EXPRESSED	REFERENCES
COCHLEA	Guinea pig	Fessenden et al., 1994
	Rat	Rodrigo et al., 1994
		Fessenden et al., 1999
VCN	Guinea pig	Coomber et al., 2014
	Rat	Rodrigo et al., 1994
		Fessenden et al., 1999
		Burette et al., 2001
	Mouse	Eliasson et al., 1997
DCN	Human, mammals, guinea pig	Baizer et al., 2014
	Rat	Rodrigo et al., 1994
IC	Guinea pig	Coote & Rees, 2008
	Rat	Rodrigo et al., 1994
	Rat	Wu et al., 2008
SOC	Rat	Rodrigo et al., 1994
		Fessenden et al., 1999
CORTEX	Rat	Lee et al., 2008

Table 1.2: Localisation of NOS through the auditory system.

In order to establish the functional role of NO in the auditory system, most studies have focussed on changes following pathological simulation. Methods that have been used to alter the function of the NO pathway in order to elucidate its function include cochleotomy, noise and blast induced hearing loss, and drug treatments. Drug treatments can be intended to simulate tinnitus, such as salicylate, or alter the NO pathway at various stages.

Some *in vitro* studies have utilised intracellular recordings at the calyx of Held in MNTB slices to determine the function of NO in this part of the auditory system. The calyx of Held, as the largest synapse in the mammalian brain, is easier to record from than other synapses.

Activity-dependent release of NO has been demonstrated in the MNTB, where it acts postsynaptically to alter excitability and synaptic strength (Steinert et al., 2008). The following paper showed that postsynaptic excitability was modulated by glutamatergic synaptic activity, via a NO-dependent mechanism which switches action potential repolarisation from predominantly Kv3, to Kv2 potassium channels (Steinert et al., 2011).

1.8.1 Potential role in tinnitus

A role of nitric oxide in tinnitus is a relatively recent idea. However, since NO contributes to synaptic plasticity and gain changes in neural systems, it is certainly an interesting avenue of research. Nitric oxide has previously been established as a potential therapeutic target in neuropathic pain; a condition often likened to tinnitus due to the similarities of increased gain following peripheral damage (Cury et al., 2011). However, due to the complicated, versatile effects of NO and the difficulty targeting it, very few NO-targeting analgesic drugs have made it to clinical trials.

Changes in the nitric oxide function in the auditory system have been studied in a variety of ways that suggest it may contribute to tinnitus generation.

Following cochleotomy, nNOS expression increases in the AVCN, in correlation with increased GAP-43 in the surrounding synaptic boutons (Chen et al., 2004). As previously discussed, GAP-43 contributes to synaptogenesis, therefore suggesting that cochleotomy results in synaptogenesis in the AVCN, possibly mediated by NO.

In the first work relating NO to tinnitus, the expression of nNOS was studied in the coclear nucleus (CN) using immunohistochemistry. With a salicylate model of tinnitus in rats, it was shown that there is an increase in the number of NOS-containing neurons in the ventral cochlear nucleus (VCN) following treatment, but no increase in NOS-containing dorsal cochlear nucleus (DCN) neurons (Zheng et al., 2006). No changes in the overall level of NOS protein in the CN were found using western blotting, however, an inability to separate the VCN and DCN may have resulted in a lack of increase in the DCN masking a significant increase in the VCN.

NOS expression has also been studied in guinea pigs following tinnitus induction by unilateral acoustic over-exposure. A within-animal asymmetry

of NOS expression was found exclusively in the ≈75% animals that developed tinnitus. However, it could not be determined whether this was due to an increase within the noise exposed VCN or a decrease in expression on the unexposed side (Coomber et al., 2014).

Further research has showed that NOS is not localised to any specific cell type within the VCN, with a sub-population of each cell type displaying NOS expression (Coomber et al., 2015). The unilateral NOS expression changes were observed as soon as 1 day after acoustic over exposure, and the changes in NOS expression did not correlate with the time course of hearing loss changes. This provided further evidence to the role of NO in tinnitus, and not just as a biomarker for hearing loss.

Limited research targeting the NO/cGMP cascade relating to tinnitus has been conducted. Two studies have used inhibitors of the phosphodiesterase PDE5 in order to increase cGMP action. The first used sildenafil (Viagra) treatment on blast-exposed rats and showed a reduction in high frequency tinnitus, suggesting that PDE inhibition may aid tinnitus treatment (Mahmood et al., 2014). However, a clinical study in humans using another PDE5 inhibitor, vardenafil, failed to show any efficacy in reducing chronic tinnitus (Mazurek et al., 2009).

To further aid clinical trials of NO-related pharmacological tinnitus treatments, the underlying pathophysiology must be better understood. This has been the focus of my work, as I have attempted to identify the physiological role of NO in the cochlear nucleus, its changing role in tinnitus.

1.9 Aims and objectives

Previous work on NO in the auditory system and more specifically the VCN, has demonstrated that NOS is present in the VCN, and is altered in tinnitus animals. However, the physiological function of NO in the VCN has not been studied, hence that is the the basis of my research.

My initial aim was to identify the functional role of NO in the control guinea pig VCN. To do this, the following questions had to be addressed:

1) Can nitric oxide modulate excitability and plasticity in the VCN?

2) Are the changes cell-type specific, potentially differing between inhibitory cells and excitatory cells?

Building upon this information, the role of nitric oxide in tinnitus generation would be assessed by studying the following questions:

3) Are there changes in the role of NO following AOE and does this relate to behavioural measures of tinnitus?

4) Does altered NO in the VCN following AOE contribute to hyperexcitability and does this relate to behavioural measures of tinnitus?

A subsidiary aim was to determine whether altering NO production throughout the brain would have any effect on tinnitus by answering the following questions:

5) Do systemically administered NO-related drugs affect neuronal processing in the cochlear nucleus?

6) Does systemically administering NO-related drugs to noise-exposed animals affect behavioural measures of tinnitus?

CHAPTER 2

Materials and methods

2.1 Animals

All procedures were carried out under licences P93F656FD and 40/3616 issued by the UK Home Office under the Animals (Scientific Procedures) Act 1986 to Mark Wallace and Alan Palmer respectively. Experiments were run in accordance with the European Communities Council Directive of 24 November 1986 (86/609/EEC) and the approval of the Animal Welfare and Ethical Review Body at the University of Nottingham, UK. Male and female pigmented guinea pigs weighing 400-1200 g were used. Guinea pigs were bred in-house and group-housed on a 12/12 h light-dark cycle, with food and water readily available.

2.2 Behavioural tinnitus confirmation

Motion tracking of the pinna reflex was used to measure gap prepulse inhibition of the acoustic startle (GPIAS), and therefore confirm tinnitus (Berger et al., 2013). A 4 mm diameter reflective marker was glued to each pinna using cyanoacrylate adhesive, and a motion-tracking camera system (Vicon Motion Systems, Oxford, UK) was used to record movement of these markers. The Vicon system used these reflective markers to triangulate the position of the ears and measure distance between the two markers, at a sampling rate of 200 Hz, during presentation of startling stimuli.

Auditory stimuli were generated using Adobe Audition from standard 16-bit digital waveform files (.wav) files, and presented through a 25 mm loudspeaker (Peerless DX25, Tymphany, Hong Kong) located outside the

end of the cage, facing inwards. Sound pressure level calibration was performed using a 1/2 inch free-field microphone (Bruel & Kjaer, Model 4165) which was calibrated with a Bruel & Kjaer Type 42 Sound Level Calibrator. The position of the guinea pig relative to the speaker would often change between and within trials, because the animals were not restrained. Therefore, sound levels perceived by the animal were not always constant.

The gap prepulse inhibition of acoustic startle (GPIAS) method developed by Turner et al. (2006) requires a continuous background noise, with a gap preceding a startling stimulus. For these experiments a background noise of either narrow-band noise at 4-6, 8-10, 12-14 or 16-18 kHz, or broadband noise was used. Startling stimuli were broadband noise bursts (20 ms; rise/fall time of 1 ms). A gap of 50 ms duration with a rise/fall time of 2 ms was used, with a delay of 100 ms between the gap onset and the startle stimulus onset. These values were previously demonstrated to be optimal for maximising gap detection ability, and have previously been used in this set-up (Berger et al., 2013; Friedman et al., 2004; Leitner et al., 1993). Each trial consisted of 10 presentations of each condition (startle stimulus with or without the preceding gap), randomly presented within a period of 2 minutes of continuous background noise. Each session was made up of 5 trials, one at each different background frequency (4-6 kHz, 8-10 kHz, 12-14 kHz, 16-18 kHz, BBN). The 5 different trial types were delivered in a pseudo-randomised order to ensure variability in when a trial was tested in each session. Sound levels were chosen optimally for each GP using a sound level-dependency test consisting of trials using BBN at 6 different background and startle sound levels (55-100, 55-105, 60-100, 60-105, 70-100, 70-105 db SPL). The sound level that elicited the greatest GPIAS was chosen for further testing.

Five sessions of behaviour were run as the baseline pre-AOE, resulting in up to 50 startle responses in each group. Pinna startle amplitudes were separated into gap and no-gap groups and outliers (greater than 2 standard deviations) were removed. The two groups were compared using the Mann-Whitney *U* test, and if the inclusion of a gap resulted in a significant decrease in startle amplitude at all 5 frequencies tested, GPIAS was confirmed and the animal was noise-exposed. Fig 2.1 shows the amplitude of gap vs no gap trials at one frequency of one animal with significant GPIAS. Occasionally, a sixth trial was required to achieve

significant GPIAS. Using this paradigm, 80% of animals were deemed to have significant GPIAS.

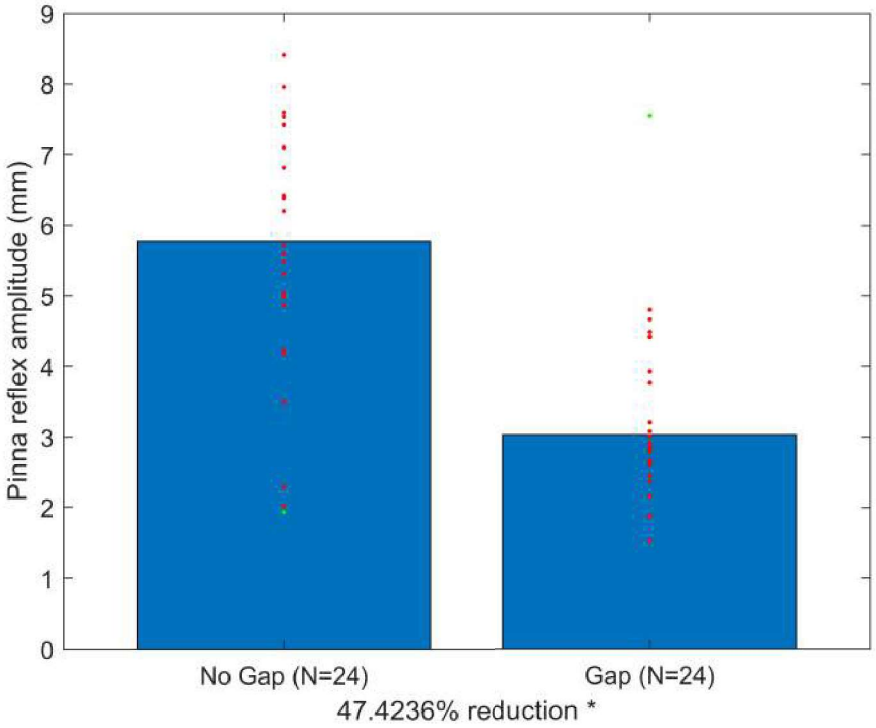


Fig. 2.1: The change in distance between guinea pig pinna during startle stimuli. Example of differences between gap and no-gap startle response amplitudes (8-10 kHz, 60-105 dB). Reds dots show individual startle responses included, while green dots show excluded outliers.

2.3 Noise exposure and ABRs

Anaesthesia was induced with ketamine (40 mg/kg, i.p.; Fort Dodge Animal Health Ltd, Southampton, UK) and xylazine (8 mg/kg, i.p.; Bayer PLC, Newbury, UK), which was further supplemented when required with administrations of a ketamine (100 mg/ml) and xylazine (20 mg/ml) mix (3:2; i.m.). The forepaw withdrawal reflex was used to determine level of anaethesia throughout the procedure. Core body temperature was monitored throughout and maintained at 38 $\pm$ 0.5 °C using a rectal probe and a homeostatic heating pad (Harvard Apparatus Ltd, Edenbridge, UK).

After anaesthetic induction, hypodermic needles were inserted through the skin over the right and left mastoids, and the vertex point, to act as recording electrodes and a reference, respectively. These electrodes were connected via a low-impedance headstage amplifier (RA4LI; TDT: Alachua, FL, USA) via a digitizing pre- amplifier (RA16PA; TDT: Alachua, FL, USA) to a TDT System 3 interface (RX7; TDT: Alachua, FL, USA).

Auditory stimuli for ABRs were presented by 25 mm loud speakers (Peerless DX25). Polyethylene tubes (diameter 20 mm) were connected to the speakers and then formed a seal around each ear in order to maintain a closed speaker system. Calibration was performed using a 40BP 0.25-inch pressure condenser microphone, 26AC pre- amplifier and 12AR power supply (all G.R.A.S, Holte, Denmark) attached to a calibrated 1 mm diameter probe positioned as close as possible to the entrance of the ear canal.

ABRs were recorded bilaterally before and after acoustic over exposure (AOE) to determine changes in hearing thresholds. After AOE, ABR's on the left side were recorded immediately, with the right side recorded after (approx 20 mins post-AOE). This was chosen as threshold shift would be expected in the left ear, with none expected in the right ear.

ABR recordings were made in a sound-proof and electrically earthed booth, where the animals remained during noise-exposure. Visual monitoring of the animal's breathing was possible through an infra-red camera within the booth. Left and right ABRs were recorded independently in response to ipsilateral sound presentation. Pure tone bursts of 5, 7, 10, 14 and 20 kHz (5 ms duration; rise/fall ramp of 1 ms) were presented at randomised sound levels (20, 25, 30, 40, 50, 60 & 70 dB SPL). This allowed determination

of the auditory-evoked response threshold based on the absence of a discernible ABR signal (sampling duration 30 ms; filtered at 300 Hz to 1 kHz).

After pre-noise exposure ABR recordings, the polyethylene tube of the right speaker was plugged with cotton wool. This was then positioned over the right pinna, which was folded over to cover the ear canal. This reduced the risk of producing hearing deficits in the right ear. The left ear was then exposed to band-passed noise (centre frequency 9 kHz; bandwidth 2 kHz), presented at 110 dB SPL for 1 hour (Fig 2.2).

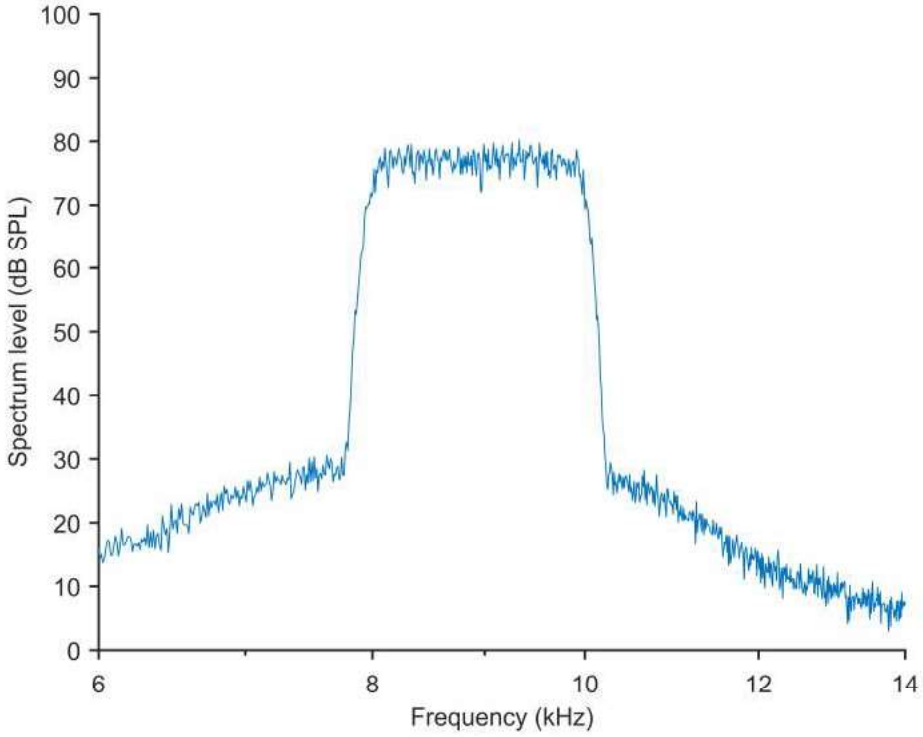


Fig. 2.2: The noise-exposure stimulus used. Narrow band noise of 8-10 kHz, total 110 dB SPL.

2.4 Non-recovery surgery electrodes and recordings

For iontophoresis experiments using solely L-NAME in healthy animals, the following surgery was carried out in incomplete aseptic conditions. Following a Home Office license change, all other non-recovery experiments were conducted aseptically. This involved; wearing full sterile clothing, assistance from a non-sterile surgical nurse, having a hot bead steriliser available to use, and sterilisation of all instruments, drapes, tissues, gauze, string and cannulas.

GP's were anaesthetised with 20% w/v urethane (4.5 ml/kg i.p.; Sigma, St Louis, MO, USA) supplemented by Hypnorm solution (fentanyl/fluanisone). Further injections of Hypnorm of up to 0.2 ml i.m. were applied when required to maintain surgical anaesthesia. These anaesthetic top-ups were scheduled to reduce interference with recordings, although one would occasionally need to be made mid-recording, this would not be expected to affect cochlear nucleus function (Samra et al., 1984). A single injection of atropine (600 μg/ml, 0.2 ml s.c.) was administered to reduce respiratory secretions. Lidocaine (20 mg/ml) was applied to incisions in order to produce topical anaesthesia. A tracheotomy was performed and the GP was artificially respired with 100% oxygen (tidal volume 3.5-6.5 ml, respiratory rate 100 breaths/min.), and exhaled CO_2 levels were monitored. ECG electrodes allowed monitoring of heart rate. A homoeothermic heating blanket (Harvard apparatus) connected to a rectal thermometer was used to maintain the physiological temperature of 38 $\pm$ 0.5 °C. GPs were then placed within a sound-attenuating and electrically earthed chamber that acted as a Faraday cage. The animal was positioned in a stereotaxic frame where the ear bars were replaced with hollow speculae that allowed a direct view of the tympanic membrane which could be clearly visualised. The skull was exposed and levelled with points positioned at 5 and 13 mm anterior to ear bar zero (Rapisarda & Bacchelli, 1977). Pressure across the tympanic membrane was equalised by a cannula sealed with Vaseline into a small hole in the ethmoid bone which allowed access to the bulla. The posterior fossa was also exposed and the covering dura cut to allow relief of CSF pressure in order to reduce brain movements. The temporalis was removed and a craniotomy was performed from 1-5 mm lateral of midline to allow access to the cochlear nucleus. Dura mater was removed and the exposed

brain surface was kept moist by regular application of warm saline or a thick layer of agar. This surgery would often take ≈ 2 hours. At the end of the experiment the animal was killed by a Schedule 1 method (3 ml i.p. pentobarbitone).

2.4.1 Sound presentation

Auditory stimuli were presented monaurally through sealed acoustic systems, formed of Radioshack 40-1377 tweeters inserted into the hollow speculae. The speakers were driven by a TDT System 3 (RZ2; TDT: Alachua, FL, USA), controlled by Brainware (software developed by J. Schnupp, University of Oxford, UK).

Calibration was performed using a Brüel & Kjær 4143 condenser microphone, 26AC preamplifier and 12AR power supply (both G.R.A.S.) attached to a calibrated 1 mm diameter probe positioned close to the tympanic membrane. The maximum power output of the system (Fig 2.3 was reduced by head attenuators of 20 dB to prevent inadvertent damage to the inner ear.

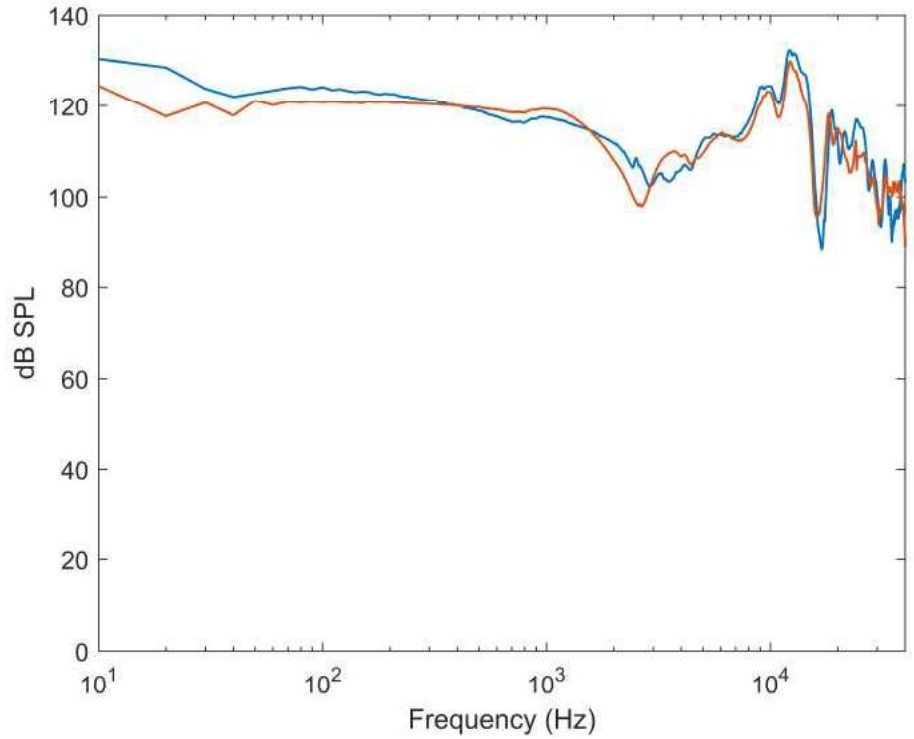


Fig. 2.3: Maximum sound level output of the speaker system used.

2.4.2 Recording overview

Electrodes were advanced through the cerebellum to the cochlear nucleus at a 45°angle from vertical using a Burleigh Inchworm, with a Burleigh 6000 Controller and 6005 handset (Burleigh Instruments, Fishers, NY). The ventral cochlear nucleus (VCN) was located stereotaxically using coordinates from a guinea pig brainstem atlas (Voitenko & Marlinsky, 1993), often 3.5-4.5 mm lateral of midline, $\pm$ 1 mm anterior/posterior of ear bar zero, and 0-2 mm dorsal of ear bar zero. Single glass-coated tungsten electrodes with tip lengths of $\approx$ 10 μm were made in-house (Bullock et al., 1988) and were used to locate the VCN before introduction of larger electrode assemblies. Spikes were collected in Brainware (software developed by J. Schnupp, University of Oxford, UK) by an arbitrarily set threshold, never less than twice the amplitude of the mean background noise.

Recordings were live-monitored using a VC-6545 digital storage oscilloscope (Hitachi, Tokyo, Japan), an AM8 audio monitor (Grass Technologies, RI, USA) and in a constantly updating peristimulus time histogram (PSTH) using the Brainware software. All data were recorded in Brainware and analysed offline with self-made MATLAB scripts.

2.4.3 Iontophoresis

Iontophoresis allows ejection of small amount of drug onto single units using electrical current, with the concentration of drug ejected being linearly proportional to the current applied. My set up combined a 5-barrelled glass pipette for drug ejection with a glass coated tungsten electrode for extracellular recording (Fig 2.4).

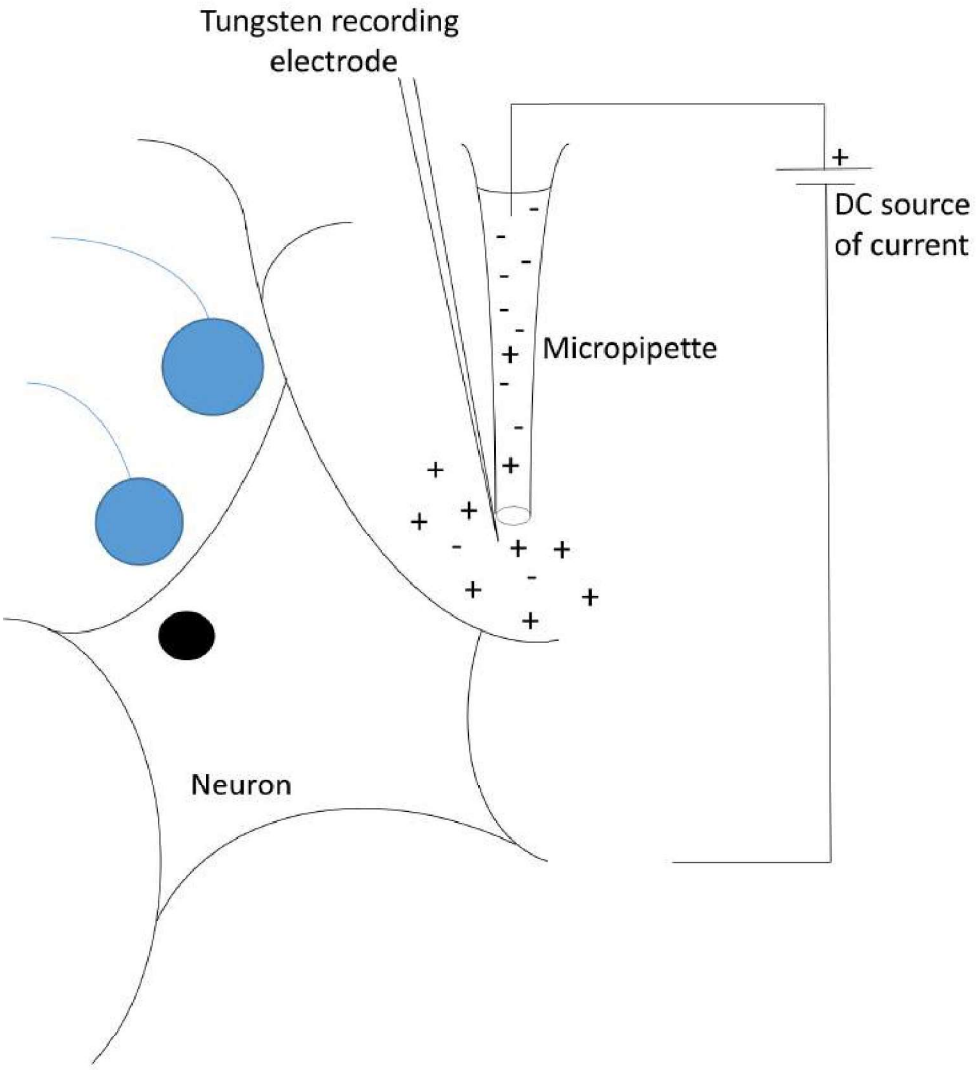


Fig. 2.4: A schematic diagram of the iontophoresis drug ejection and recording method used.

Extracellular drug application was achieved using five-barrelled glass micropipettes where each glass tube had a microfilament to aid with filling (5B120F-4; WPI, FL, USA). These electrodes were pulled with a microelectrode puller (Ealing) and the tips broken back to ≈ 20 μm across under a microscope by insertion into a molten ball of borax before cooling of the borax and removal of the electrode. A taper to tip length of 10-15 mm was found to be optimal to achieve the desired impedance and to reach the cochlear nucleus. Glass-coated tungsten recording electrodes with a tip length of ≈ 10 μm were made in house (Bullock et al., 1988). These were glued to the micropipette using 5-minute epoxy resin, with the tip

extending 20-30 μm beyond the pipette barrels (Fig 2.5) to allow recording electrode positioning at the target neuron without causing damage with the larger glass pipette (McAlpine & Palmer, 2002).

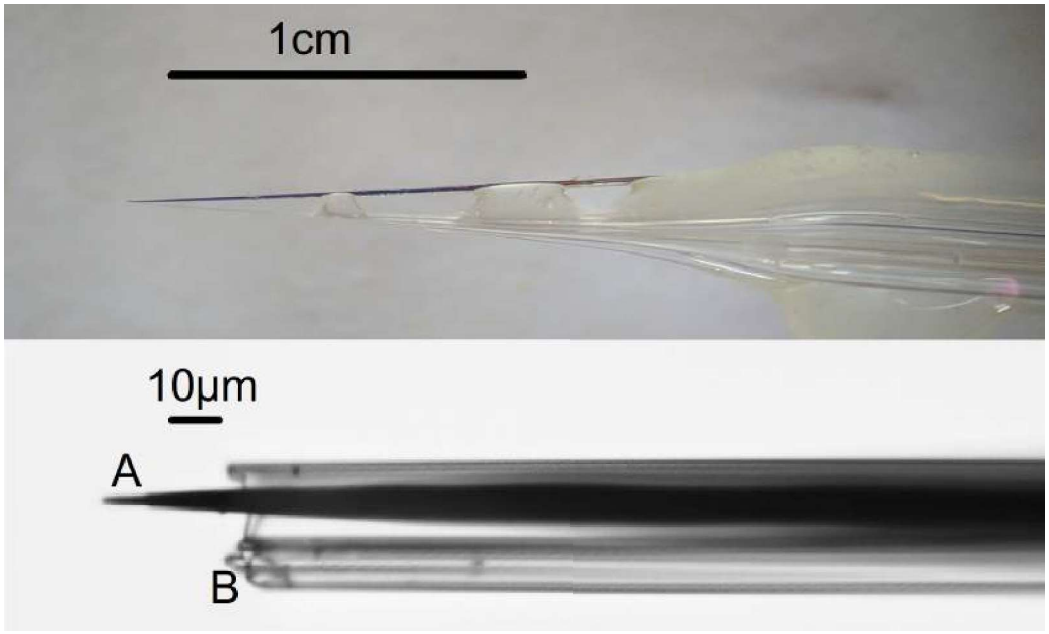


Fig. 2.5: Microintophoresis electrode assembly. Top: whole assembly showing piggy-back tungsten glued to the pulled glass pipette. Bottom: electrode tip under light microscope (20 X). A: The recording tip of the tungsten electrode, with glass coating removed. B: The 5 barelled glass pipette for iontophoresis ejection.

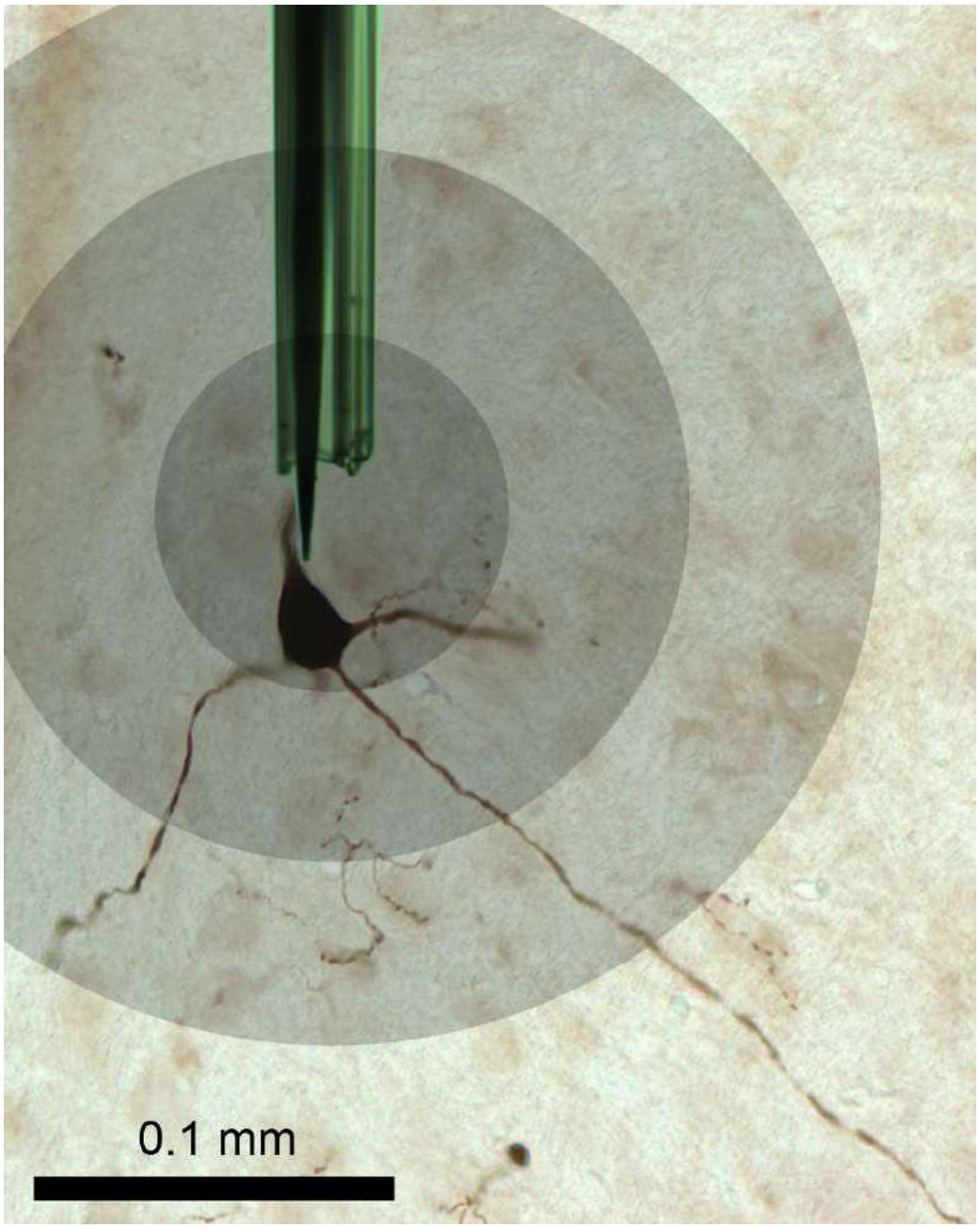


Fig. 2.6: Photomicrograph showing electrode assembly superimposed on an image of a biocytin filled large stellate cell (onset-chopper) (Arnott et al., 2004). The grey circles show a sequence of spheres with a diameter increasing by 0.1 mm representing the effective drug concentration. Concentration of the applied drugs would be highest in the area around the soma and proximal dendrites.

Iontophoresis electrodes were filled using a 1 ml syringe, filter unit (0.22 μm, Millex) and MicroFil syringe needle (34 gauge/67 mm, WPI). The central barrel was filled with 2 M NaCl solution, to allow current balancing, with the remaining barrels filled with drugs

dissolved in distilled water. Drug solutions used were as follows: N(G)-Nitro-L-arginine methyl ester hydrochloride (L-NAME, 50 mM, pH 6.5; Sigma), N(G)-Nitro-D-arginine methyl ester hydrochloride (D-NAME, 50 mM, pH 6.5; Sigma), S-Nitrosoglutathione (SNOG, 15 mM, pH 4.5; Abcam), 3-Morpholinosydnonimine hydrochloride (SIN-1, 40 mM, pH 4.5; Sigma), N-Methyl-D-aspartic acid (NMDA, 10 mM, pH 8; Sigma) or glutamate (GLU, 100 mM, pH 8; Sigma). When an 80 nA ejection current was applied to citrate-buffered saline of equal concentration and pH of drug solutions, no alterations to VCN unit activity were observed (n = 11).

Retaining currents of 10 nA were applied to drug barrels between ejections, the polarity of these opposite to the charge of the drug to be ejected, in order to prevent drugs leaking out passively. These were positive for NMDA and GLU and negative for L-NAME, D-NAME, SNOG and SIN-1. Cycling was used to maintain drug concentrations at the electrode tip, where each drug barrel would be supplied with the ejection current for 8 s every 36 s while searching for the cochlear nucleus. Ejection currents varied depending on the experiment but were between 40-120 nA. Retention and ejection currents were applied by a Neurophore (Digitimer, Hertfordshire, UK) BH-2 iontophoresis system consisting of four IP-2 iontophoretic pump modules and one BM-2 control and balance module.

Nitric oxide donors are molecules that release the free radical NO either spontaneously, via enzymatic oxidation or through another chemical reaction. The two used in these experiments, SIN-1 and SNOG, both release NO when at physiological pH. This suited my methodology as they were stable in the iontophoresis pipette at a low pH (4.5) then would release NO once ejected into the desired location.

DRUG	FUNCTION	SUPPLIER	CONCENTRATION USED	PH	CHARGE
D-NAME	Inactive isomer of L-NAME	Sigma	50 mM	6.5	+ve
GLUTAMATE	Excitatory neurotransmitter	Sigma	100 mM	8	-ve
L-NAME	NOS inhibitor	Sigma	50 mM	6.5	+ve
NMDA	NMDA-R agonist	Sigma	10 mM	8	-ve
SIN-1	NO donor	Sigma	40 mM	4.5	+ve
SNOG	NO donor	Abcam	15 mM	4.5	+ve

Table 2.1: Drugs used for iontophoresis experiments.

To test pipette function, ejection currents were applied to a glutamate barrel with the electrode tip within the cerebellum. An excitation response suggested that the iontophoresis set-up was functioning correctly. The iontophoresis assembly was then advanced into the VCN and after neuronal isolation and identification, tests involving drug applications began.

The single tungsten recording electrodes were connected through a HS-2 headstage (x1; Axon Instruments Inc.) and an axoprobe-1A multipurpose microelectrode amplifier (x100; Axon Instruments Inc.) then further amplified x100 (IHR 4 Channel Amplifier). The resulting x10000 amplified signal then passed to a TDT System 3 filter (RZ2; TDT: Alachua, FL, USA) for bandpass filtering, and online data collection was facilitated by Brainware at a sampling rate of 25 kHz.

Initially, proof of concept experiments were carried out to ensure the drug ejection and recording techniques were working effectively. To test the response of units to GLU, it was applied for up to 40 seconds during a one minute recording of the neuron's activity during silence. Application of GLU was halted prematurely if firing was increasing to rates potentially liable to cause cell death. 80 nA ejection currents were applied to a single glutamate iontophoresis barrel following isolation of a VCN unit. As seen in Fig 2.7 top & middle, glutamate ejection often caused substantial increases in cell firing. A period of 5-10 s of glutamate ejection was required before an increase in firing rate was observed. Upon cessation of glutamate ejection,

spike rate reduced rapidly (within 2 s). However, in one cell (Fig 2.7 bottom) glutamate application produced no clear effect.

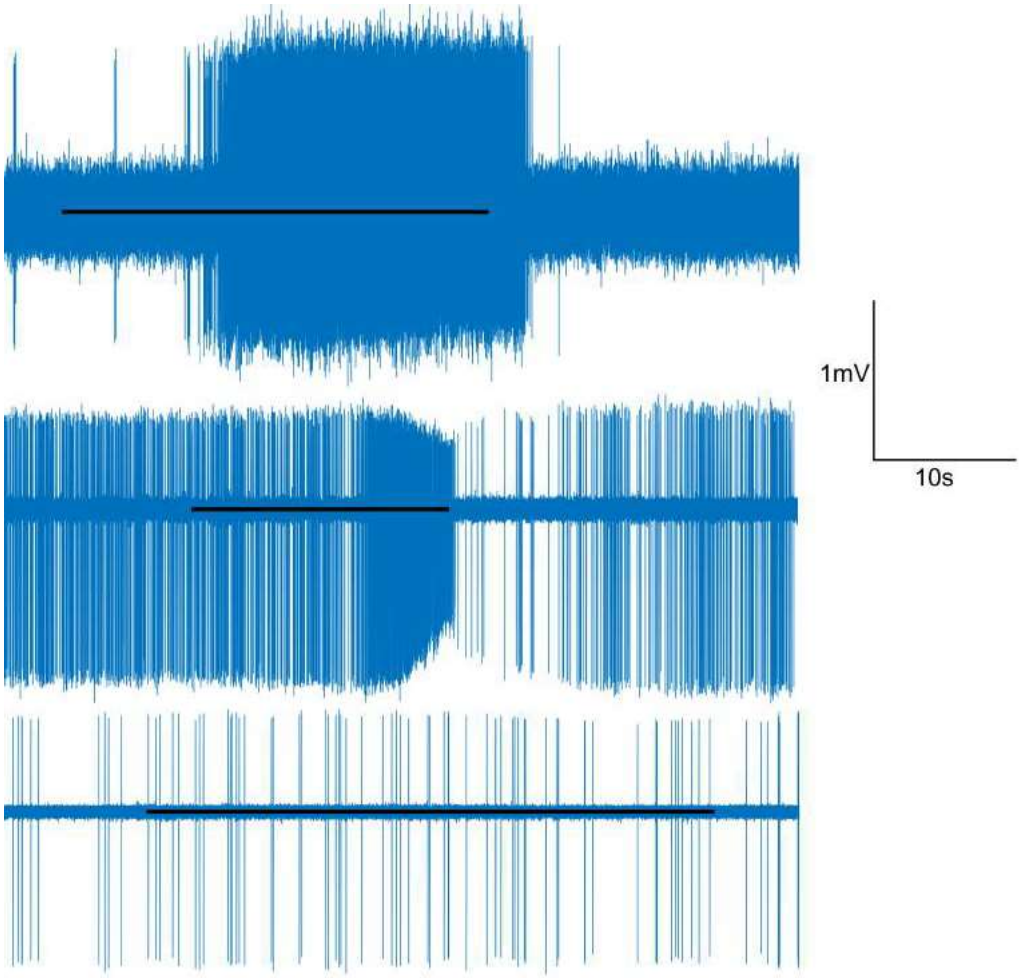


Fig. 2.7: Spike recordings from 3 different cochlear nucleus units during silence recorded over 1 minute with 80 nA iontophoretic glutamate ejection indicated by black bars. The top two units show increases in firing rate with glutamate application, with one displaying a decreased excitability following glutamate application. The bottom unit does not respond to glutamate application.

2.4.4 Multi-electrode recording

In order to make multi-electrodes for recording, glass-coated tungsten electrodes were made in-house with tip lengths of $\approx$ 10 μm (Bullock et al., 1988) and aligned on an 18 channel DIL electrode board made in-house with 200 μm between the tips. Fig 2.8 shows this electrode assembly, with the tungsten electrodes set in place with 5-minute epoxy resin and sealed to connections using silver conductive paint.

For this multi-channel recording, a PZ5 NeuroDigitizer was used for amplification and bandpass filtering was applied with TDT System 3 filter (RZ2; TDT: Alachua, FL, USA) and data collected with Brainware software at a sampling rate of 25 kHz. This system allowed recording of two channels from a single tungsten electrode, allowing separate amplification and filtering for single-unit activity and local field potentials. For single units, filters were set between 300 Hz and 3 kHz, and for LFPs filtering was between 60 Hz and 300 Hz.

Using two of these multi-electrodes allowed simultaneous recording from 4 electrodes in the VCN bilaterally while drugs were administered systemically. The stimuli used for these experiments were bilateral 90 dB broadband noise pulses, with a 50 ms pulse every 200 ms. 7-Nitroindazole (7-NI; Sigma) was administered i.p. in 1 ml of peanut oil, in doses up to 50 mg/kg to assess the effect of global nNOS inhibition on activity within the VCN.



Fig. 2.8: Example of a multi electrode used.

2.4.5 Reverse microdialysis

Single-use microdialysis probes were made in-house by threading a silica fused fibre (110 μm/170 μm, SGE analytical Science, Australia) through three cut and filed steel tubes (Goodfellow stainless steel (AISI 304 (Fe72/Cr18/Ni10) diameter 0.5 mm, wall thickness 0.06 mm), and gluing the structure in place. The silica fibres were positioned so that the end of the inlet fibre protruded 1 mm from the steel tube, with the outlet fibre approximately 1/3rd of the way inside. A semipermeable diffusion membrane (Hospal AN-69) was glued to the end and sealed with 5-minute epoxy. These microdialysis probes were glued to the electrode assembly described in *Sections 2.6*, ensuring no contact between the electrodes and

the steel of the microdialysis probe. A gap of 0.5-1 mm separated the tips of the electrodes and the dialysis membrane as shown in Fig 2.9.

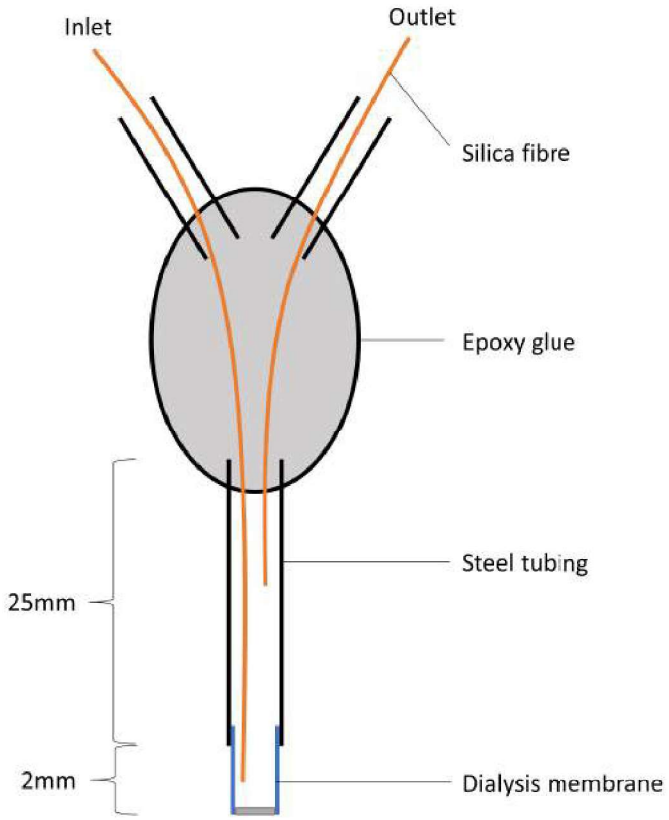


Fig. 2.9: A diagram of the microdialysis probe.

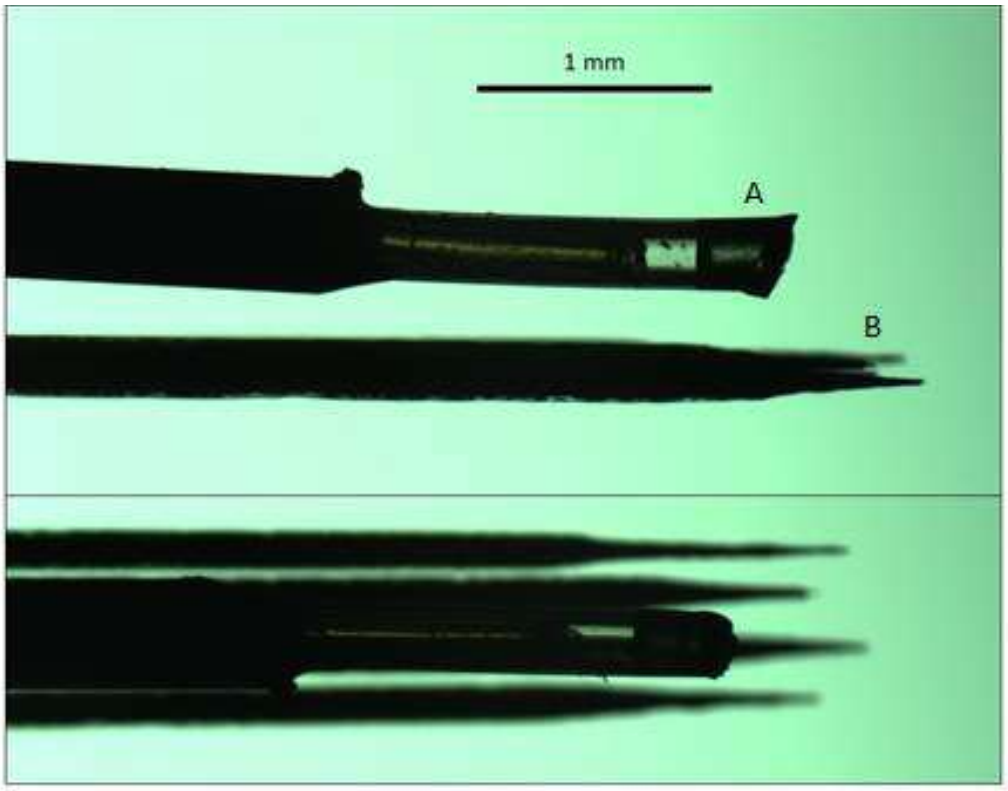


Fig. 2.10: A light microscope (2.5 X objective lens) image of the tip of the dialysis probe and electrode assembly. Top: The distance between the dialysis membrane (A) and the tips of the four tungsten electrodes (B). Bottom show the spread of tungsten electrodes, approximately 200 μm between each tip.

The semipermeable membrane used allows molecules of up to 10 kilodaltons to diffuse down their concentration gradient. This permits drugs to be delivered locally by retrodialysis. Gluing of the microdialysis probe to the electrode board allowed control of the location of retrodialysis in relation to the recording site. The microdialysis probe was positioned medial to the recording electrodes, with recording tracts starting in the medial portion of VCN and moving laterally each time. This ensured recordings were not taken from an area damaged by the large microdialysis probe.

A Pump 11 Elite syringe driver (Harvard apparatus) that held two 5 ml syringes was used to pass fluid through the dialysis probe at a rate of 2 μl/min. This consisted of aCSF (Composition explained in Table 2.3), or aCSF containing drugs (Overview in Table 2.4). aCSF was prepared from stock solutions on the morning of the experiment, with the required drugs also added to the aCSF at this time.

CHEMICAL	SIGMA CODE	CONCENTRATION
NaCl	S7653	126 mM
KCl	P9541	3 mM
NaH_2PO_4	S3139	1.25 mM
$MgSO_4.7H_2O$	63138	2 mM
$NaHCO_3$	S5761	26 mM
Glucose	G6152	10 mM
$CaCl_2.2H_2O$	C3306	2 mM

Table 2.2: Composition of the aCSF used.

DRUG	FUNCTION	COMPANY	CONCENTRATION
NMDA	NMDA-R agonist	Sigma	30, 100 mM
L-NAME	NOS inhibitor	Sigma	30, 100, 300 mM

Table 2.3: Drugs used for reverse microdialysis experiments.

Syringes were attached to the microdialysis probe by a 23 gauge needle inserted into non-sterile tubing (0.5 mm I.D./1 mm O.D., Lab Unlimited). This tubing ran for approximately 2 m into the recording booth. Inside the booth, one of the two tubes could be connected to a 10 cm piece of BOLA PTFE tubing (0.3 mm I.D./0.6 mm O.D., Sigma), which stayed connected to the inlet tubing on the microdialysis probe. This connection tube had an internal volume of approximately 28 μl, resulting in a 14 minute delay from changing tubing to the new solution reaching the dialysis probe, assuming no diffusion. With this set-up, the booth had to be entered and tubing changed manually to change drug condition.

An initial proof of concept experiment using NMDA was used to confirm correct function of the microdialysis probe. The auditory stimuli were 50 ms BBN pulses every 200 ms at 10 different levels (30-120 dB SPL, 10 dB steps) randomly presented, creating a total sweep length of 2 s. This allowed plotting of the spike rate over time for each sound level, and

production of a rate level function (RLF) before, during and after drug application. Fig 2.11 & Fig 2.12 show a spike rate histogram and RLF, both indicating an increase in firing rate following NMDA application.

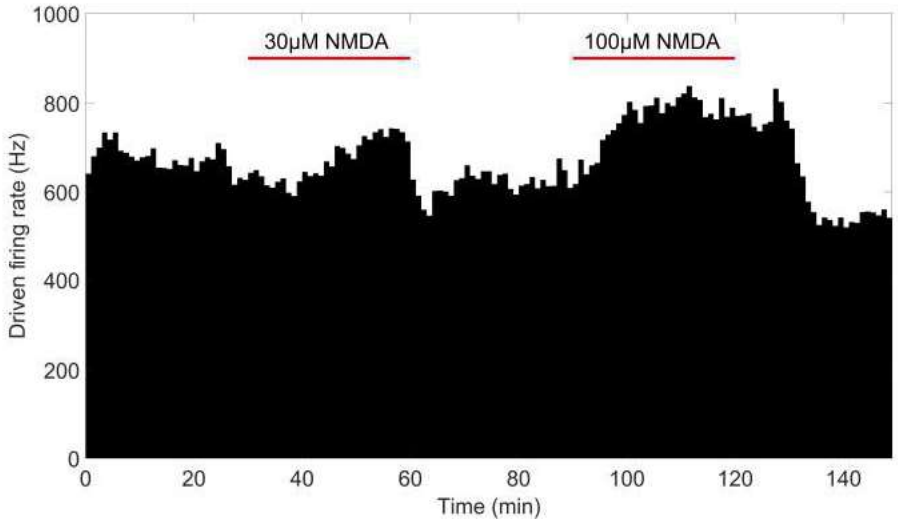


Fig. 2.11: A spike rate histogram for a VCN unclassified unit in response to a 50 ms 110 dB BBN stimulus every 2 s. Bin width 1 min.

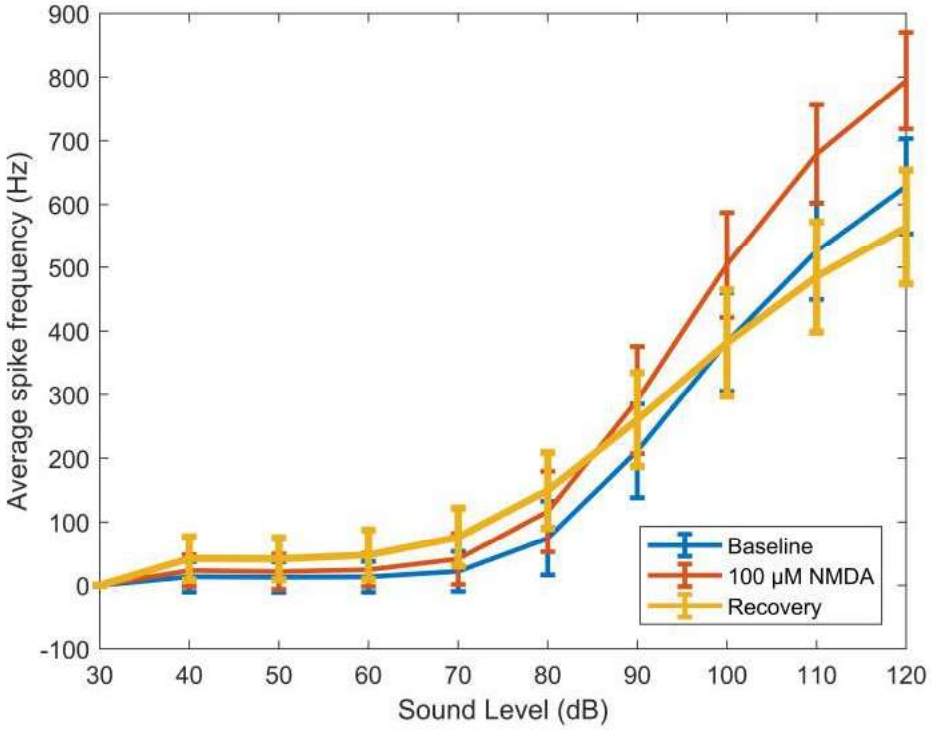


Fig. 2.12: The RLF for the same unit as Fig 2.11 at different time points (80-90 mins, Baseline; 110-120 mins, NMDA; 140-150 mins, Recovery).

2.5 Neural identification

Identification and characterisation of neurons took place in Brainware (Fig 2.13) during the recording using the following protocol. A wideband noise burst (80-120 dB SPL, 50 ms, 200 ms repeat rate) was used as a search stimulus, in order to maximise identification of auditory neurons. Once an evoked response was observed, search tones of 1-40 kHz in 1 kHz steps were used to estimate characteristic frequency (CF). Frequency response areas were plotted to determine the CF of the isolated cell. This was achieved by measuring the response to pure tone bursts (50 ms, 200 ms repeat rate) over a range of frequencies ($\pm$ 1 octave from estimated CF, 0.1 octave spacing) and sound levels (0-100 dB SPL, step size = 10 dB), giving a total of 231 conditions that were randomly interleaved. Two repeats of each condition were presented, resulting in a total test time of 92.4 s.

Following this, a rate-level function was measured by applying pure tone bursts (CF, 50 ms, 200 ms repeat rate) at varying sound levels (0-100 dB SPL, step size = 10 dB). Each sound level was repeated 10 times in a pseudo random order of sound levels, allowing the test to be completed in 22 s. From this rate-level function the threshold firing level of the isolated neuron could be estimated.

Peri-stimulus time histograms were then obtained by applying CF stimuli at 20 dB above threshold (50 / 200 ms, 200 / 1000 ms repeat rate, 150 repeats). These could be used to identify the neuronal subtypes (Palmer, 1987) and combined with the CF, estimate the location within the cochlear nucleus before experimental recordings were made. Frequently more than one cell per track was isolated and studied.

Offline, after the initial data acquisition it was possible to further analyse the properties of identified units. PSTHs, inter-spike interval histograms (ISIHs), first spike latencies and spike shapes were analysed in custom-written MATLAB scripts.

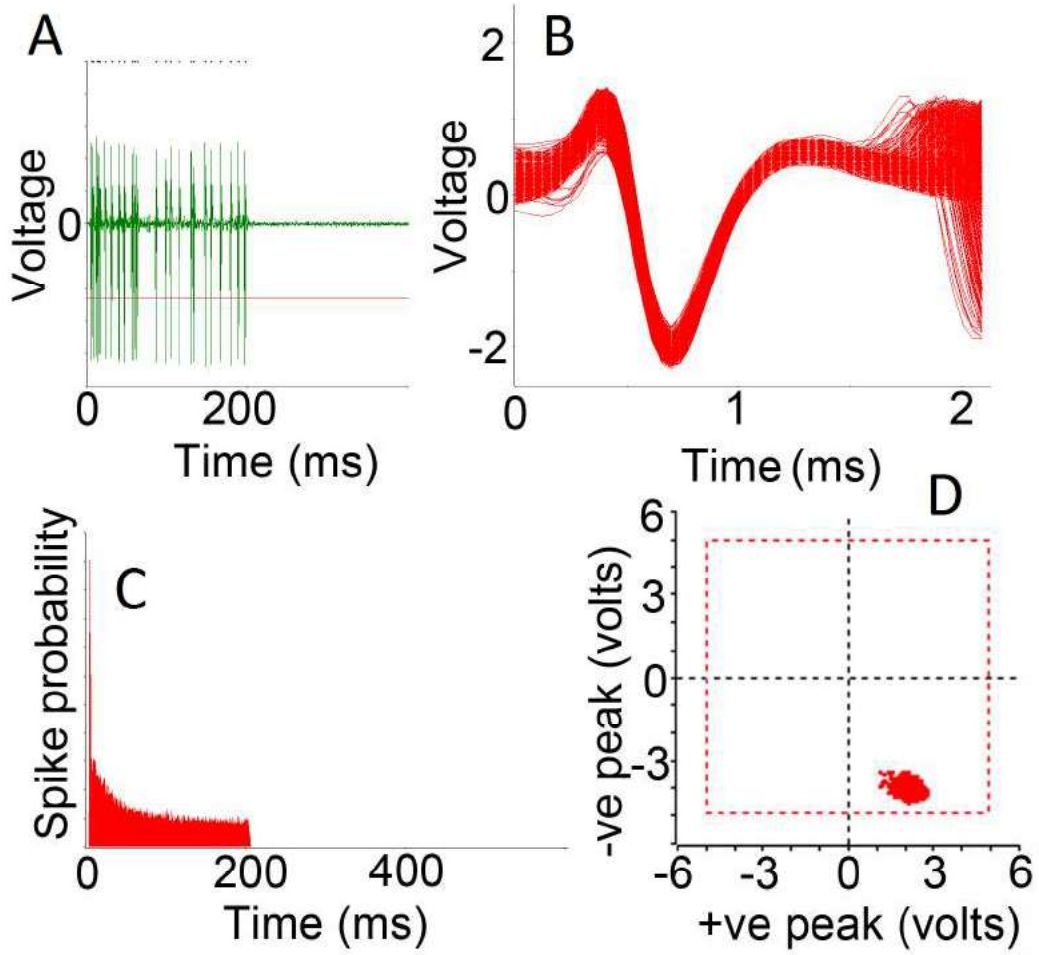


Fig. 2.13: Example of live spike analysis of a single unit (Primary-like; 6 kHz; 200 ms tone at 70 dB SPL) in the Brainware software used for these experiments. A: Live visualisation of spike timings and detection threshold (red line) over a single sweep. B: The superimposed spike waveforms confirm that a single unit was being collected. C: A rolling average PSTH across sweeps. This unit displayed a primary-like characteristic. D: Spikes could be sorted by plotting characteristics such as positive and negative peak amplitude but most units ($\approx$ 98%) were simply isolated by threshold discrimination. This is an example of a single unit with primary like properties that corresponds to a bushy cell.

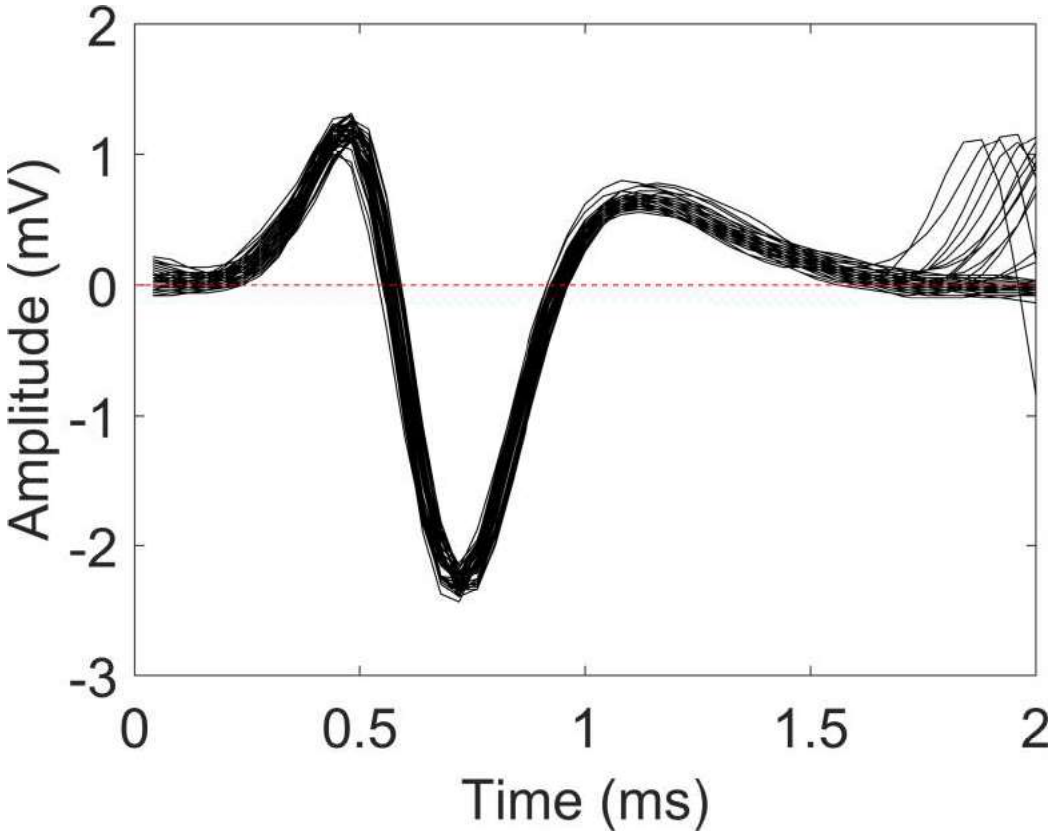


Fig. 2.14: Spike shapes (n = 46) from a single VCN unit, analysed offline in MATLAB. 25 kHz sampling rate.

Spike shapes were used to confirm single units, as multi-units would present as multiple spike shapes. Fig 2.14 shows a spike shape corresponding to a recording of a single unit.

Peri-stimulus time histograms (PSTHs) were obtained from the data using a custom written MATLAB script (bin sizes 0.2 ms). These could be used to identify the neuronal subtypes and combined with the CF, estimate their location within the cochlear nucleus.

Inter-spike interval histograms (ISIHs) were produced by calculating the time of all inter-spike intervals in the first 25 ms of the stimulus period of the 120 sweeps. The first 25 ms were chosen in order to focus on the initial period of firing where units are more clearly distinguished. The coefficient of variation was calculated for these ISIHs, which can aid in quantitatively distinguishing between unit types (Rhode et al., 2010).

Fig 2.15 shows the 4 categories that units were classified into, chopper (Ch), primary-like (PrLi), onset (On) and phase-locked (PhLo). Some other units

were not easily distinguishable, so were placed in an unclassified category (UN). A small proportion of these, roughly 1% of all units, were multi-units. Sub-populations of these unit types have been identified (Rhode et al., 2010), but it was deemed unnecessary to these experiments to divide further. As units had to be held for at least an hour each while drugs were applied, this meant that only relatively small numbers of units could be collected, and it was not considered appropriate to break them down into too many sub-groups.

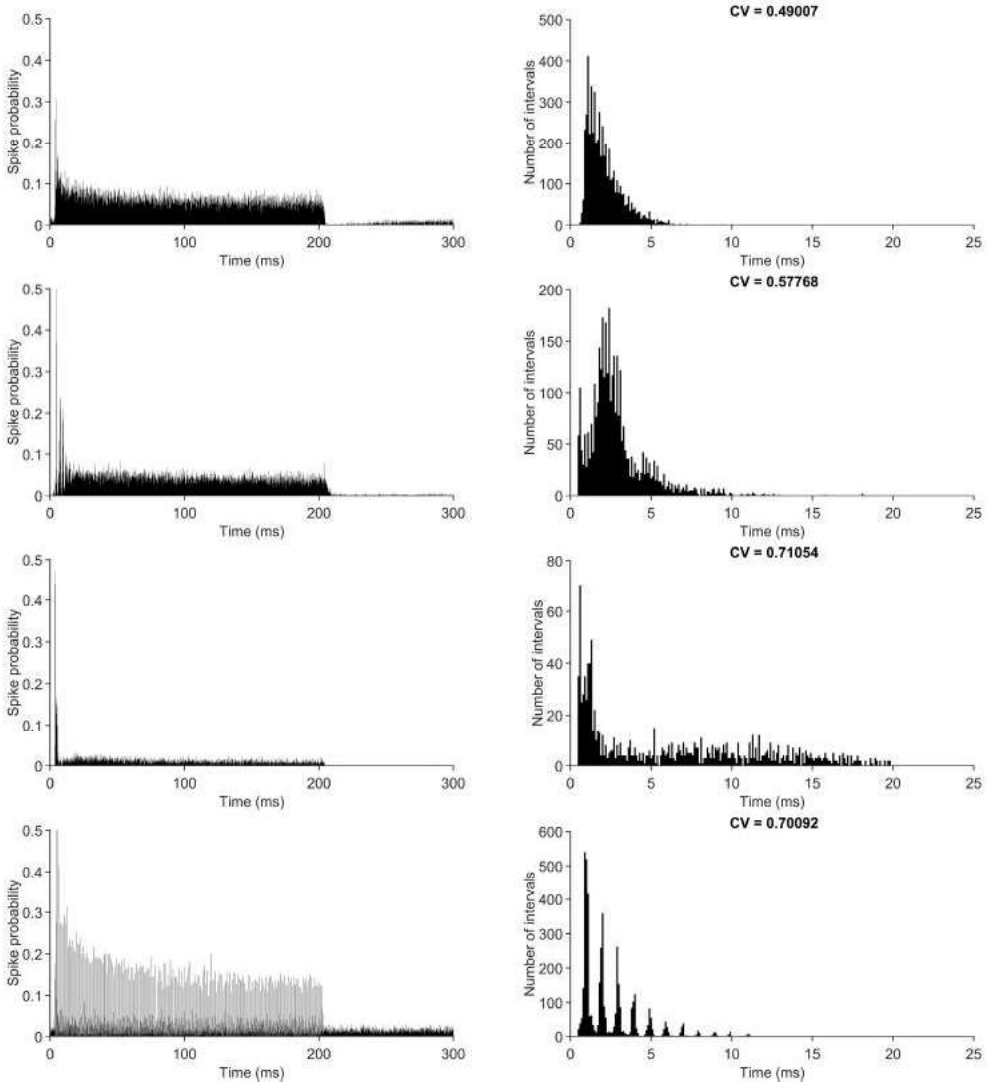


Fig. 2.15: PSTHs (left) and accompanying ISIHs (right) for the 4 types of VCN unit, from top to bottom: primary-like (PrLi), chopper (Ch), onset (On) and phase-locked (PhLo). Coefficient of variance (CV) can be used to further subdivide population classes.

Further phase-locking analysis was used to characterise phase-locked units. This followed the standard protocol for phase-locking analysis (Goldberg & Brown, 1969). This consisted of creating a vector histogram and circle plot on all units with a CF $\leq$ 5 kHz (Fig 2.16). Spike times between 20 ms and the end of the stimulus for each sweep were used. Data from the initial 20 ms of activation not used as it was often not synchronised and gave inaccurate phase-locking data overall. Fig 2.16 shows the phase-locking analysis for the phase locked unit in Fig 2.15.

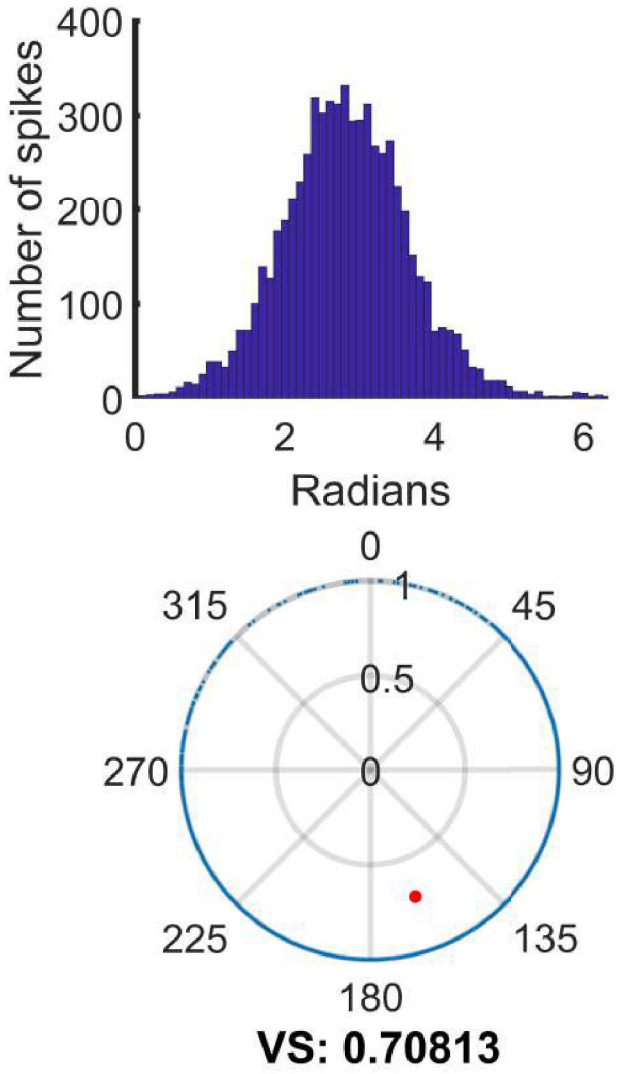


Fig. 2.16: Phase-locking analysis for the unit in Fig 2.15. Top: a vector histogram showing the number of spikes over the course of the sine shaped stimulus. Bottom: circle plot showing spikes as blue dots around the edge. Vector strength (length along radius) and characteristic phase (degrees) are indicated by the red circle.

CHAPTER 3

NO-mediated synaptic plasticity in the guinea pig ventral cochlear nucleus and its role in central gain control

3.1 Introduction

Central gain is an adaptive process by which neurons of the central auditory system alter their sensitivity in response to changes in peripheral input. Maladaptive central gain in response to peripheral damage has been proposed as a model for tinnitus, with synaptic plasticity, in particular homeostatic plasticity, suggested as a potential mechanism (Auerbach et al., 2014; Noreña, 2011; Schaette & Kempter, 2006; Zhao et al., 2016). To further understand this central gain control, the mechanisms underlying it must be established.

The NO-forming enzyme, nitric oxide synthase (NOS) has been identified in many stages of the auditory system, from the cochlea, through the cochlear nucleus, superior olivary complex, inferior colliculus and auditory cortex (Baizer et al., 2014; Burette et al., 2001; Coote & Rees, 2008; Eliasson et al., 1997; Fessenden et al., 1994; Fessenden et al., 1999; Lee et al., 2008; Rodrigo et al., 1994). The presence of NOS throughout the auditory system strongly suggests that NO contributes to auditory processing, however its physiological role at different stages is still unclear. Given its expression and function, it is possible that NO modulates gain through the auditory system.

NOS is present both in the spiral ganglion neurons that provide the main innervation to the ventral cochlear nucleus (VCN) (Zdanski et al., 1994), and the major types of neuron within the VCN, including bushy cells,

stellate cells and octopus cells. The afferent input from the auditory nerve and the majority of projection neurons in the VCN are excitatory other than the large onset cells which are glycinergic and therefore inhibitory. All three types of neuron can contain nitric oxide synthase, but within a class there are large variations in the quantity of enzyme present (Coomber et al., 2015). The effect of nitric oxide may be cell type specific, potentially acting differentially on excitatory and inhibitory cells to maintain the correct balance.

This chapter studies the role of nitric oxide in the VCN of the healthy guinea pig, to determine how it might contribute to synaptic plasticity and central gain control. If nitric oxide contributes to central gain control, then changes in this system induced by altered peripheral input may contribute to the maladaptive central gain observed in tinnitus. As nitric oxide can contribute to short term, long term and homeostatic plasticity (*Section 1.7*), it is also important to establish the time course of any effect.

Nitric oxide synthase (NOS) expression has previously been studied in guinea pig VCN where it is located in a sub-population of each cell type (Coomber et al., 2015; Zheng et al., 2006). The function of NO in the VCN has not been previously studied; that is the focus of this chapter. This chapter will explain the use of iontophoresis to apply drugs directly to single units within the VCN, which were recorded simultaneously. Drugs used in this study were NO donors (*Section 3.3*), a NOS inhibitor (*Section 3.4*) and NMDA-R agonists (*Section 3.5*).

3.2 Iontophoresis protocol and statistical analysis

This section explains the auditory stimuli used for iontophoresis experiments, and the analysis used to confirm statistical increases or decreases of firing rates.

Iontophoresis and recording methods were as detailed in *Section 2.4*. Upon isolation and characterisation of a VCN unit, a pure tone pulse-train was presented at the CF of the isolated unit (200 ms tone, 1000 ms repeat rate), 20 dB above threshold. Spike times throughout the sweep were recorded, allowing analysis of the frequency of driven spikes (initial 200 ms) and spontaneous spikes (final 700 ms). Tracking changes in the frequency of driven and spontaneous spikes over all the sweeps presented (usually 3600, totalling 1 hour) allowed analysis of the temporal effect of iontophoretically applied drugs on neural activity. For driven data, mean first spike latency (FSL) over each 5 minute period was also analysed. All data were analysed offline with custom-written MATLAB scripts, with statistical analysis carried out in Graphpad Prism 7 software.

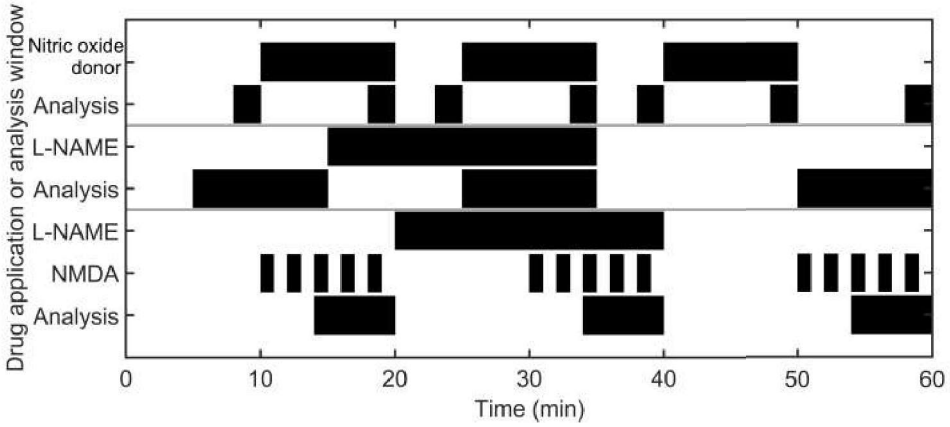


Fig. 3.1: The timings of drug application periods and the periods of recording used for statistical analysis in all iontophoresis experiments.

When testing the NO donors SNOG and SIN-1 in preliminary tests, they showed rapid effects. Therefore, they were applied for 10 minutes 3 times over an hour, in increasing concentrations of 40, 80 and 120 nA at 10-20, 25-35 and 40-50 minutes respectively (Fig 3.1).

In chronological order, the 7 analysis periods were named B, 40 nA, R1, 80 nA, R2, 120 nA and R3. With the data in 10s bins, the final 2 minutes of baseline (B), each drug ejection and each recovery (R) period were tested for statistical confirmation of changes using Kruskal-Wallis test with Dunn's multiple comparison test. Responses were deemed significant if there was a significant change in the same direction from R1-80 nA and R2-120 nA, followed by a significant return toward baseline from 120 nA-R3. The firing rate of a VCN unit during each analysis period, which showed a significant increase in response to SIN-1, is shown in Fig 3.2.

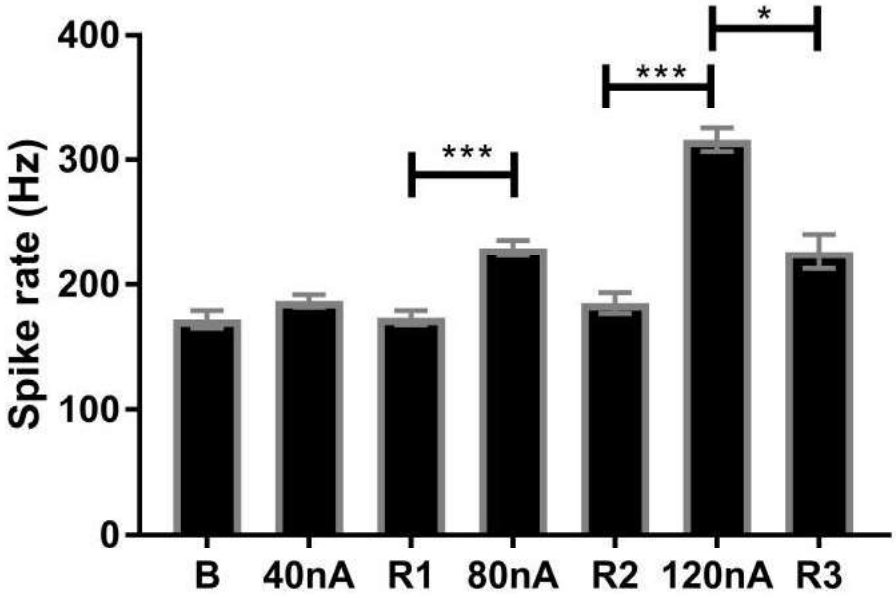


Fig. 3.2: The mean +/- s.d. firing rate of a VCN unit during the seven analysis periods for NO donor application. Comparisons using Kruskal-Wallis test with Dunn's multiple comparison test, number of bins per analysis period = 12. Using my criteria, this unit would be deemed to have a significantly increased firing rate.

To test the effect of L-NAME, it was applied at 80 nA for 20 minutes (from 15-35 min) during an hour-long recording (Fig 3.1). This longer time frame was used as preliminary experiments showed a longer time to take effect than NO donors. With spike rate in bins of 1 minute, the final 10 minutes of drug ejection was compared to the final 10 minutes of baseline and recovery using a Kruskal-Wallis test with Dunn's multiple comparison test. Changes of the spike activity were deemed significant if both comparisons

were significant at $p < 0.05$. An example of the firing rates of a unit which fitted this criteria is shown in Fig 3.3.

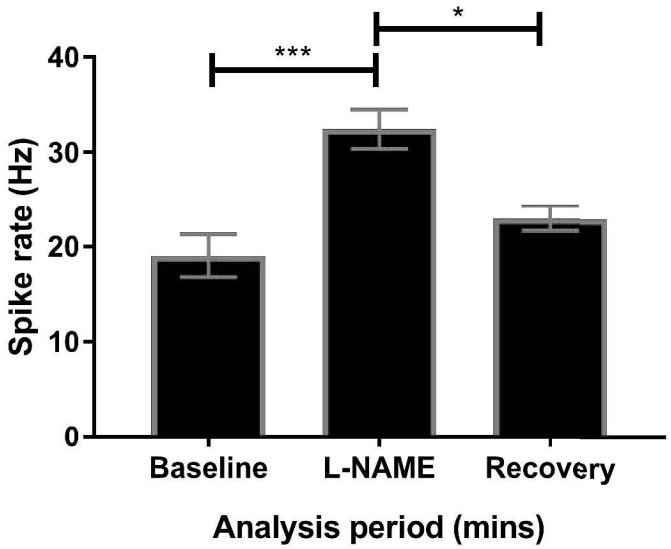


Fig. 3.3: The mean +/- s.d. firing rate of a VCN unit during the three analysis periods for L-NAME application. Comparisons using Kruskal-Wallis test with Dunn's multiple comparison test, number of bins per analysis period = 10. Using my criteria, this unit would be deemed to have a significantly increased firing rate.

When testing the effect of L-NAME on NMDA-evoked excitation, NMDA was applied at 80 nA for 1 minute bursts every 2 minutes between 10 and 20 mins, 30 and 40 mins and 50 and 60 mins. L-NAME was applied at 80 nA from 20-40 mins (Fig 3.1). This gave one baseline period of NMDA responses, one period of responses in the presence of L-NAME and one recovery period.

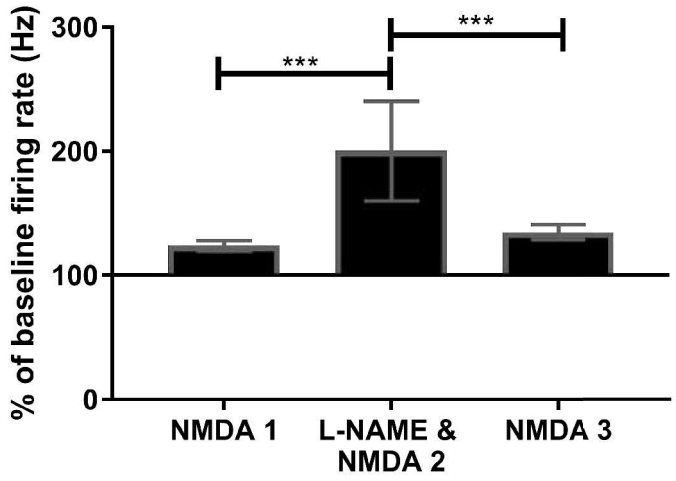


Fig. 3.4: The mean +/- s.d. of change in firing rate of a VCN unit during three periods of NMDA application. Comparisons using Kruskal-Wallis test with Dunn's multiple comparison test, number of bins per analysis period = 18. Using my criteria, this unit would be deemed to have a significantly enhanced NMDA-evoked excitation.

To analyse this data, with the data in 10 s bins, the 6 bins with the greatest firing rate from the final 3 NMDA applications of each period were used as the peak firing rate during the ejection period. These firing rates were divided by the baseline firing rate (mean of 180 s before the initial NMDA application of that period) to give the percentage increase evoked by NMDA application. These increases for each period were compared using a Kruskal-Wallis test with Dunn's multiple comparison test. An example unit is shown in Fig 3.4, which displayed an enhanced NMDA response during L-NAME application.

3.3 Nitric oxide donors

Nitric oxide donors are molecules that release the free radical NO either spontaneously, via enzymatic oxidation or through another chemical reaction. The two used in these experiments, SIN-1 and SNOG, both release NO under physiological conditions. This suited my methodology as they were stable in the iontophoresis pipette at a low pH (4.5) then would release NO once ejected into the desired location. Iontophoretic application of NO donors allowed characterisation of the effect of exogenous NO.

Fig 3.5 shows the spike rates of two VCN units over 1 hour. SIN-1 can clearly be seen to cause dose-dependent increases and decreases in firing rate of these units, with higher current ejection eliciting a greater response. The first spike latency (FSL) was not affected by SIN-1 application.

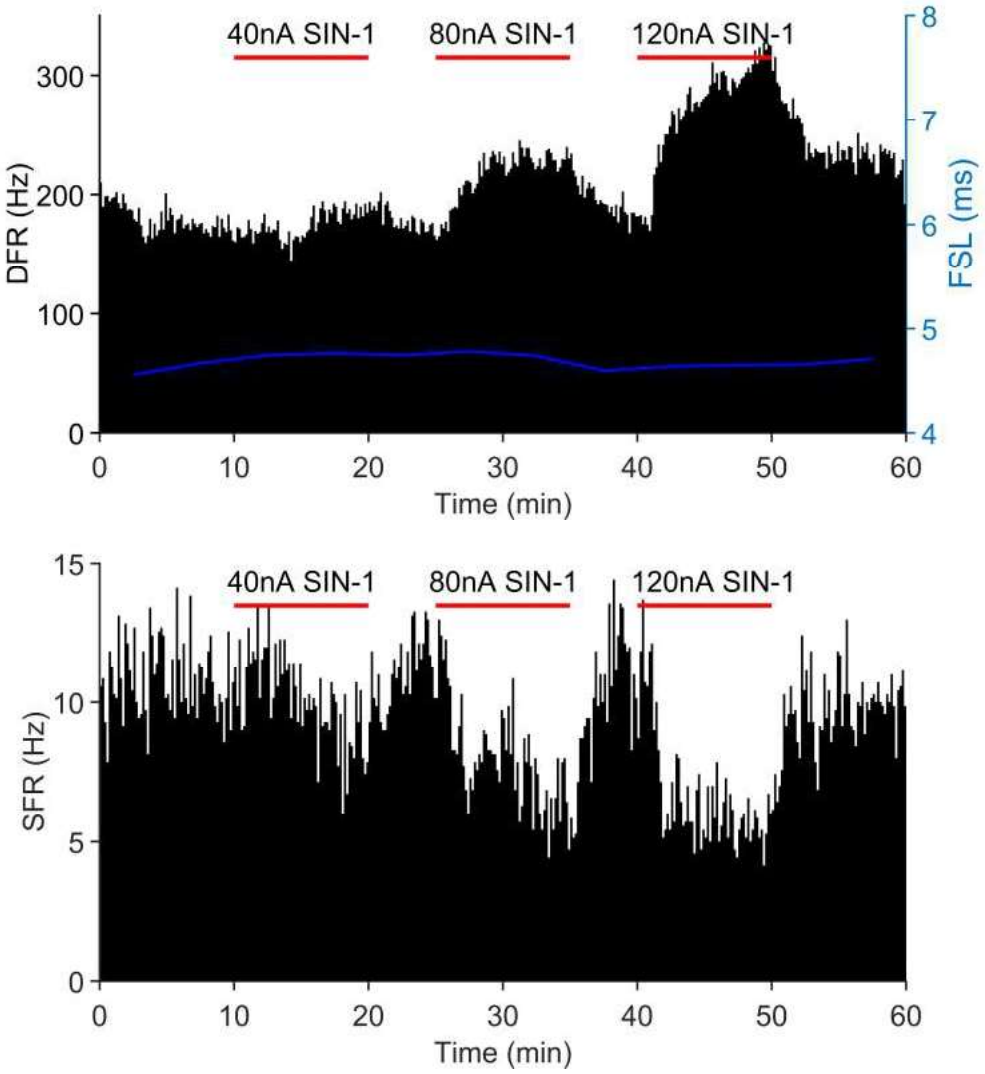


Fig. 3.5: Spike-rate histograms (bin size 10 s) of two VCN units over one hour. Three periods of SIN-1 ejection at varying strength are indicated by the red bars. Top: chopper 3 kHz driven firing rate (DFR); Bottom: Unclassified 12 kHz spontaneous firing rate (SFR). For driven firing rate, first spike latency (FSL) has also been plotted over the hour and averaged every 5 minutes (blue line).

The NO donor SIN-1 was applied to 25 units (14 Ch, 1 PrLi, 3 PhLo, 3 On and 4 Un) from 4 animals (2 male, 2 female). For the same set of recordings driven (DFR) and spontaneous (SFR) firing rates were analysed separately.

The 120 nA application caused increases from baseline (141.6%, s.d. 28.9) in the driven activity in 5/25 (20%) of units (Ch 2.5, 3, 8 and 12 kHz, PrLi 9 kHz). A decrease to 52.3% of baseline was observed in the spontaneous activity in 1/25 (4%) unit (PhLo 1600 Hz) (Fig 3.6).

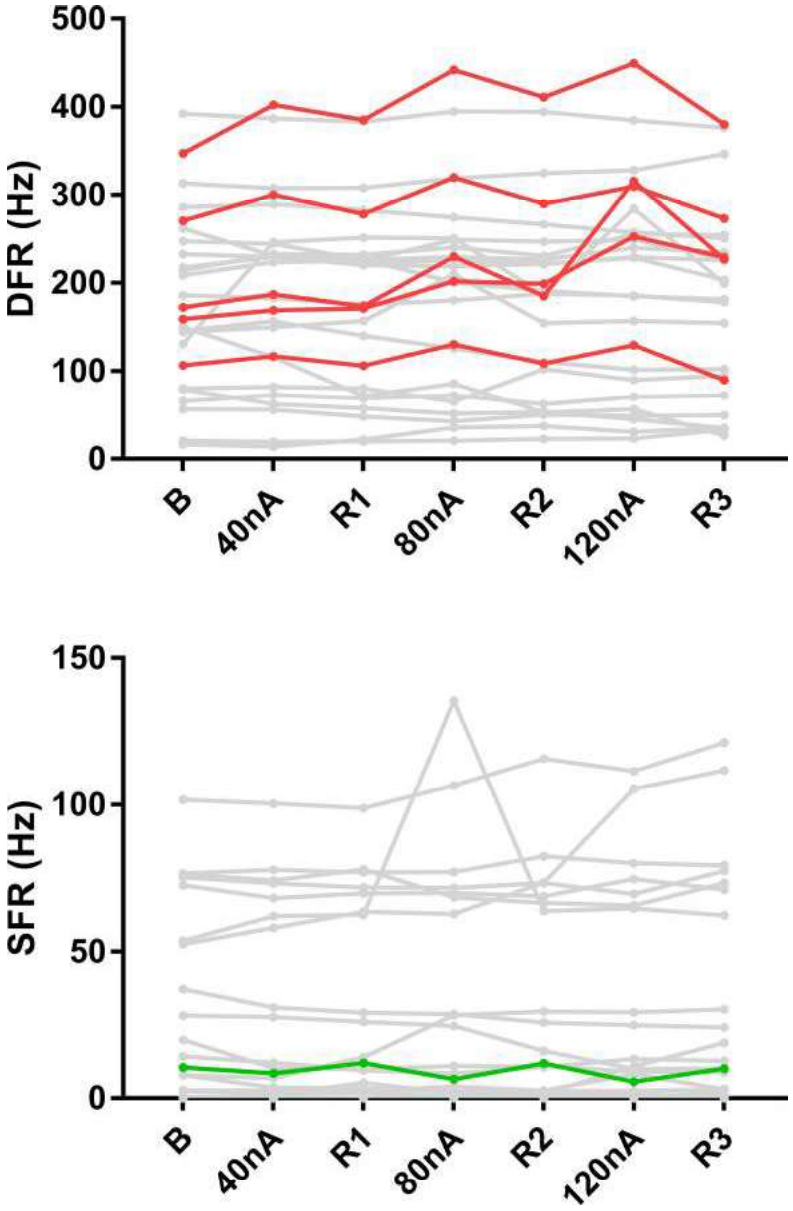


Fig. 3.6: Mean firing rates of 25 VCN units during SIN-1 application. Changes in SFRs and DFRs elicited by SIN-1 application (n = 25). Red highlights significant increases and green shows significant decreases.

As shown in Fig 3.7, iontophoretic ejection of the NO donor SNOG increased and decreased firing rates of units, without affecting FSL. SNOG was applied to 23 units (5 Ch, 5 PrLi, 0 PhLo, 8 On and 5 Un) from 4 male animals.

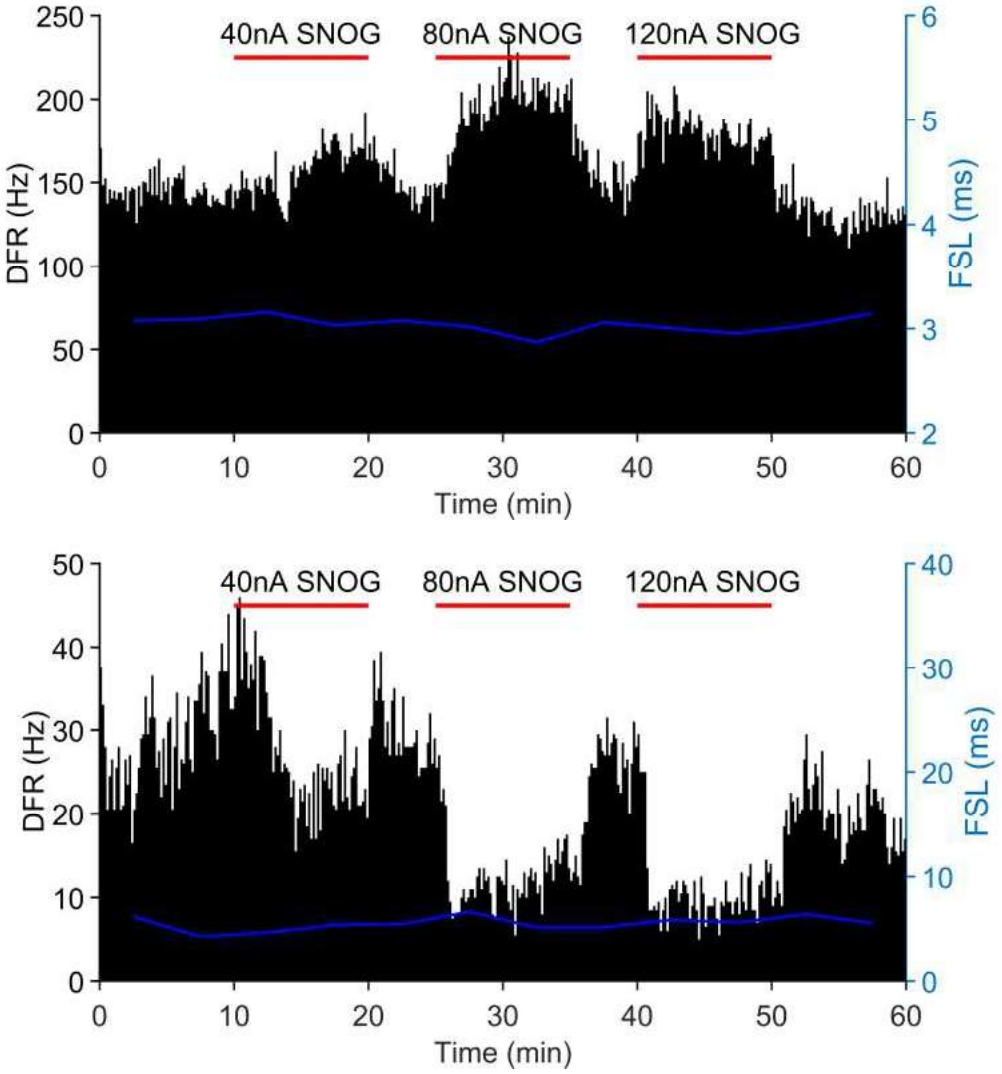


Fig. 3.7: Example of spike-rate histograms from VCN units over one hour demonstrating increases and decreases during SNOG application (Bin size 10 s). Three periods of SNOG ejection of increasing strength are indicated by the red bars. Top: chopper 17 kHz; Bottom: PrLi 12 kHz. First spike latency (FSL) was also recorded over the hour (blue lines).

When analysing the driven spike rate, 6 (26%) units responded to SNOG application, with 3 showing a significant increase (170.0%, s.d. 38.8) from baseline during SNOG ejection and 3 units significantly decreasing (56.3%, s.d. 24.7). The cell types and CF's of these responsive neurons were as follows: increases (Ch 12 kHz, Ch 17 kHz, PrLi 2 kHz) decreases (Ch 2.5 kHz, PrLi 12 kHz, On 12 kHz).

When analysing the spontaneous spike rate, 6 (26%) units responded to SNOG application, with 4 showing a significant increase (378.0%,

s.d. 202.4) from baseline during SNOG ejection and 2 units significantly decreasing (20.2%, s.d. 7.4). The cell types and CF's of these responsive neurons were as follows: increases (Ch 12 kHz, PrLi 2 kHz, UN 19 kHz, UN 500 Hz) decreases (PrLi 9.5 kHz, On 12 kHz).

Application of the NO donor SNOG resulted in units increasing and decreasing their driven and spontaneous activity in similar proportions. However, as can be seen in Fig 3.8, the set of units recorded from in experiments using SNOG had very variable spontaneous and driven firing rates in comparison to other experiments conducted.

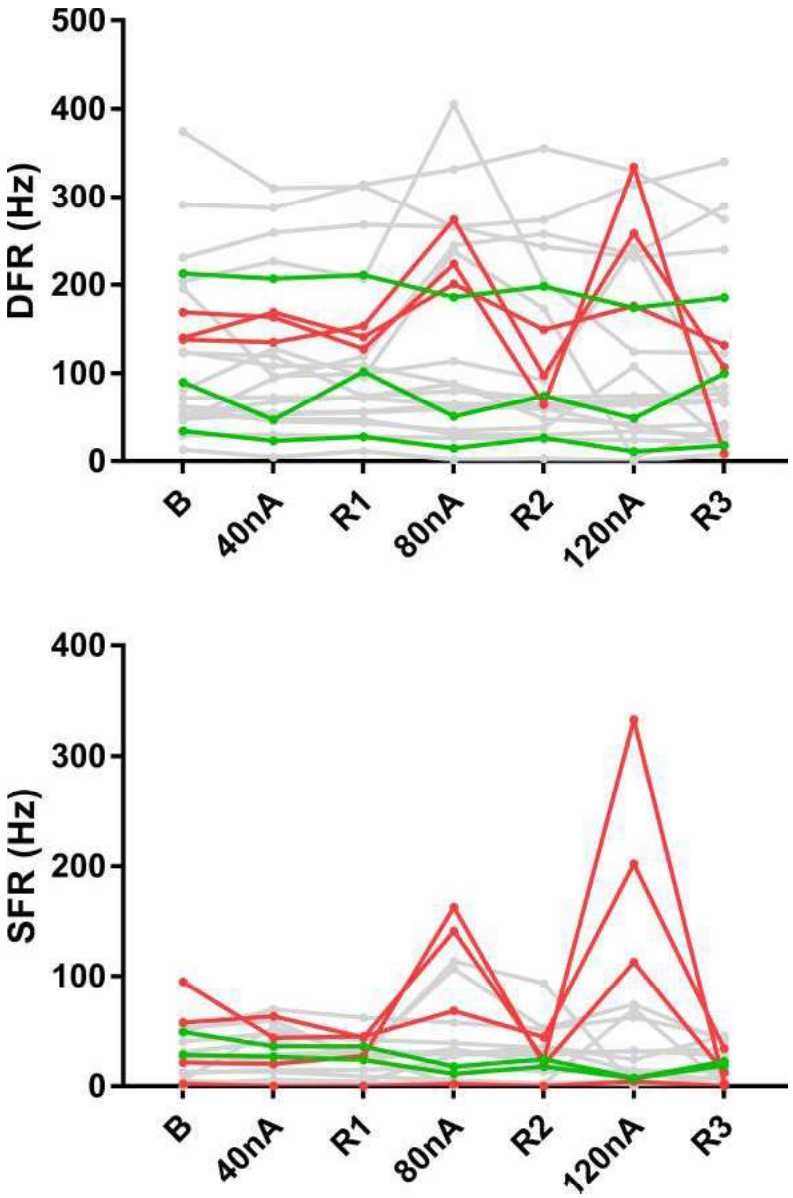


Fig. 3.8: Mean firing rates of 23 units during SNOG application. Changes of driven (top) and spontaneous (bottom) firing rates of VCN units elicited by SNOG application. Red highlights significant increases and green shows significant decreases.

In these experiments, it was expected that there would be a greater effect of NO donors on spontaneous activity, as due to the lower level of activity, there is a lower concentration of endogenous NO. It appears from my data that DFR's are NO-sensitive in a greater proportion of units, although NO has a larger effect on spontaneous rates (Fig 3.6 & Fig 3.8).

3.4 Nitric oxide synthase inhibition

The NOS inhibitor L-NAME is stable in aqueous solution. Its activation requires hydrolysis to L-NNA, its active compound. This is partially selective toward nNOS, with inhibitor potency (K_i) values of 15 nM, 39 nM and 4400 nM for nNOS, eNOS, and iNOS respectively, demonstrating the selectivity toward nNOS (Furfine et al., 1993). Inhibiting NOS locally using iontophoretic L-NAME ejection allowed characterisation of the effect of endogenous NO in the guinea pig VCN.

Due to the slower time-course of effect of L-NAME in comparison to NO donors it was applied for 20 minutes once during an hour, at a current of 80 nA. Larger bin sizes than those used for NO donors were used, as less temporal acuity was needed.

Measurements of spike rate over a period of one hour were used to identify the effect of L-NAME on VCN neurons. As before, a pure tone pulse-train was used (200 ms tone, 1000ms repeat rate) and driven and spontaneous data were analysed separately. Fig 3.9 shows changes in driven and spontaneous firing rates for a single VCN neuron during L-NAME application, with a correlated change in FSL; as driven firing rate increases, FSL decreases.

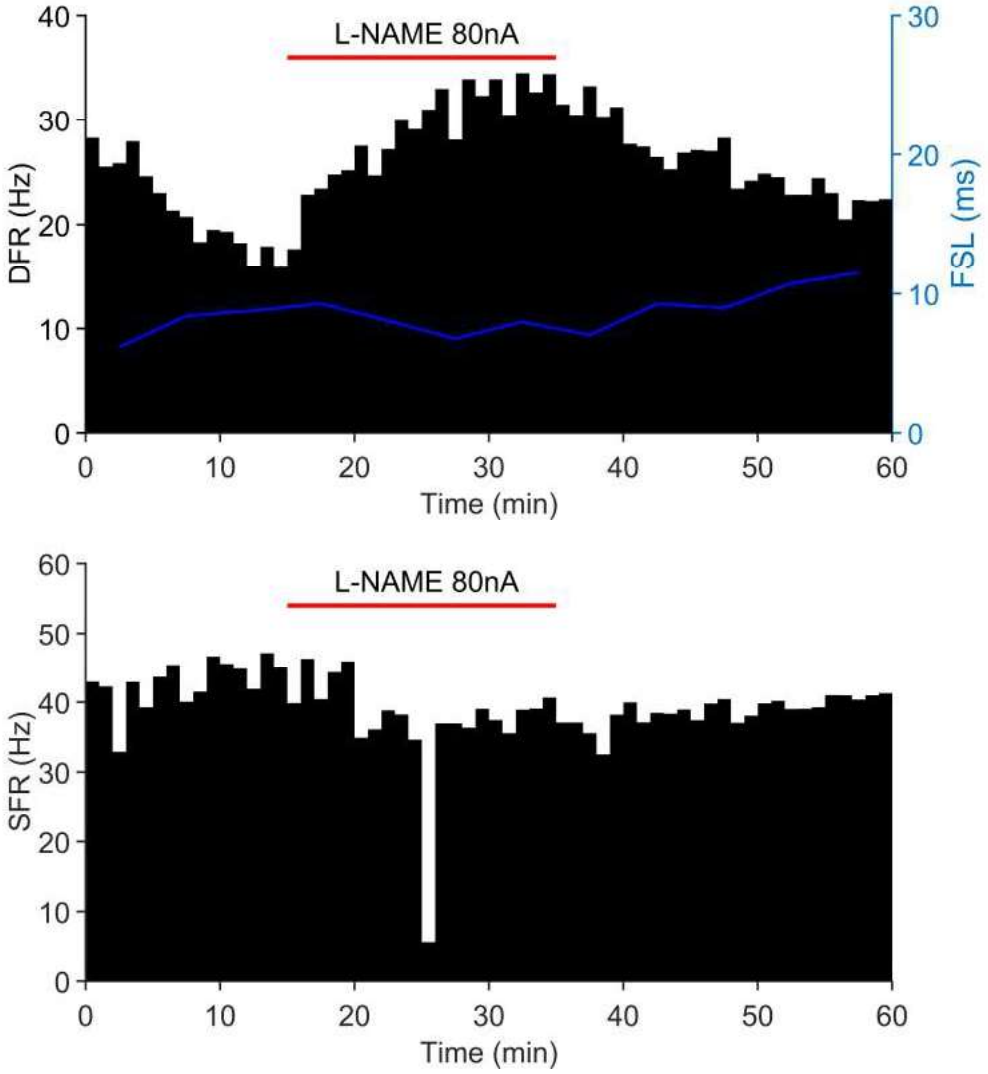


Fig. 3.9: The DFR and SFR spike-rate histograms of single VCN unit, showing increased (top; Ch 12 kHz) and decreased (bottom; Un 10 kHz) firing rates in response to iontophoretic L-NAME application. Bin size 1 min, 80 nA L-NAME application is indicated by the red bar. For driven firing rate, first spike latency (FSL) was recorded over the hour (blue line).

Hour long recordings with L-NAME application were conducted in a total of 9 animals (8 male, 1 female), with a total of 22 recordings. These consisted of 7 PrLi, 7 Ch, 4 PhLo, 2 On and 2 Un. As with NO donors, NOS inhibition via L-NAME application had a variable effect, with the ability to cause significant increases and decreases in firing rates (Fig 3.9).

When analysing the driven rate, four units significantly increased (170.4%, s.d. 35.3) their activity in response to L-NAME application, with no

significant decreases observed. The cell types and CF's of these neurons were: UN 10 kHz, PrLi 2.6 kHz, Ch 6 kHz, Ch 12 kHz.

When analysing the spontaneous rate, four units responded to L-NAME application, with 2 showing a significant increase (178.9%, s.d. 47.7) from baseline during L-NAME ejection and 2 units significantly decreasing (66.6%, s.d. 16.7). The cell types and CF's of these responsive neurons were as follows: increases (UN 10 kHz, On 12 kHz) decreases (Ch 14.25 kHz, UN 9.5 kHz).

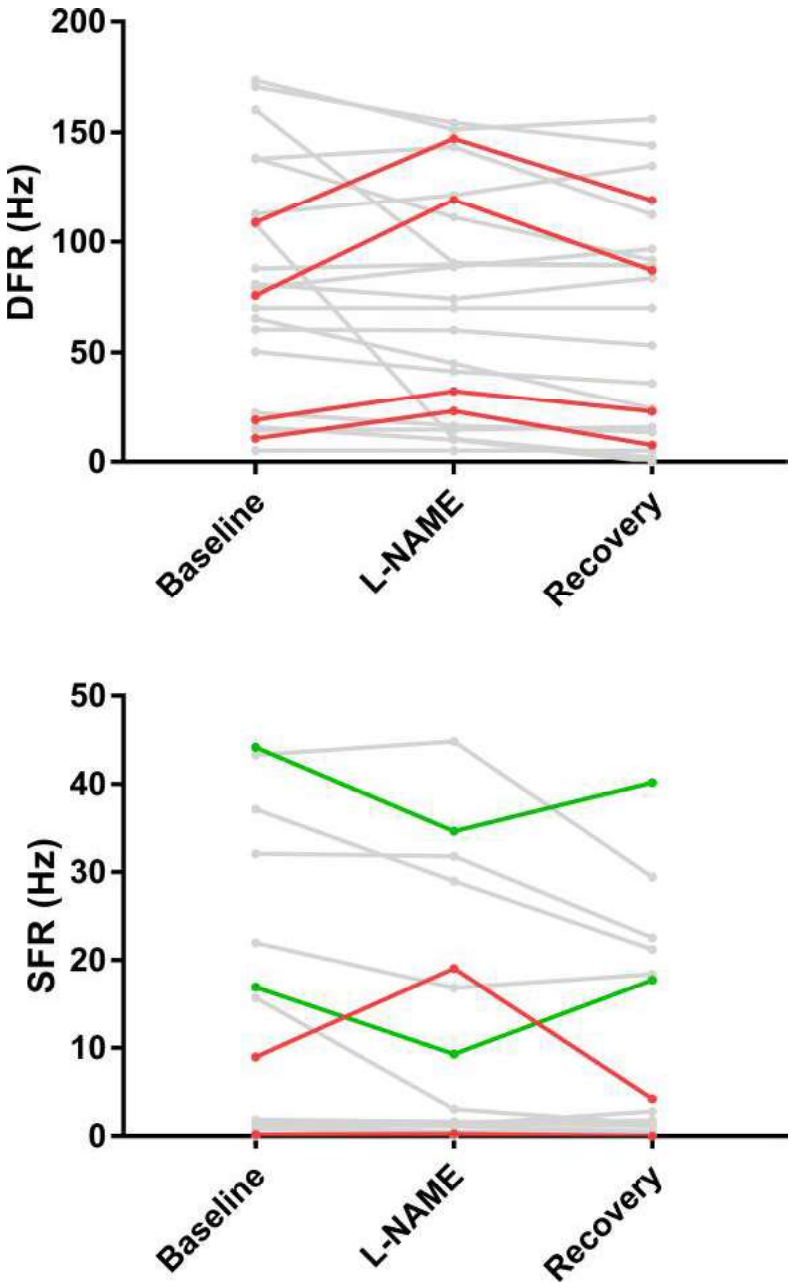


Fig. 3.10: Mean firing rates of 22 VCN units during each analysis period. Changes of driven (top) and spontaneous (bottom) firing rates are shown for the same set of units. Red and green lines highlight significant increases and decreases following L-NAME application, respectively.

3.4.1 PSTH comparisons

Comparisons of PSTHs before and during L-NAME application showed that when the DFR was affected by L-NAME, this modulation was throughout the 200 ms driven period (Fig 3.11). Large increases and decreases in spike probability are seen in the initial 20 ms of the driven period, likely due to

the slight decrease in first spike latency altering the timing of the chopping pattern.

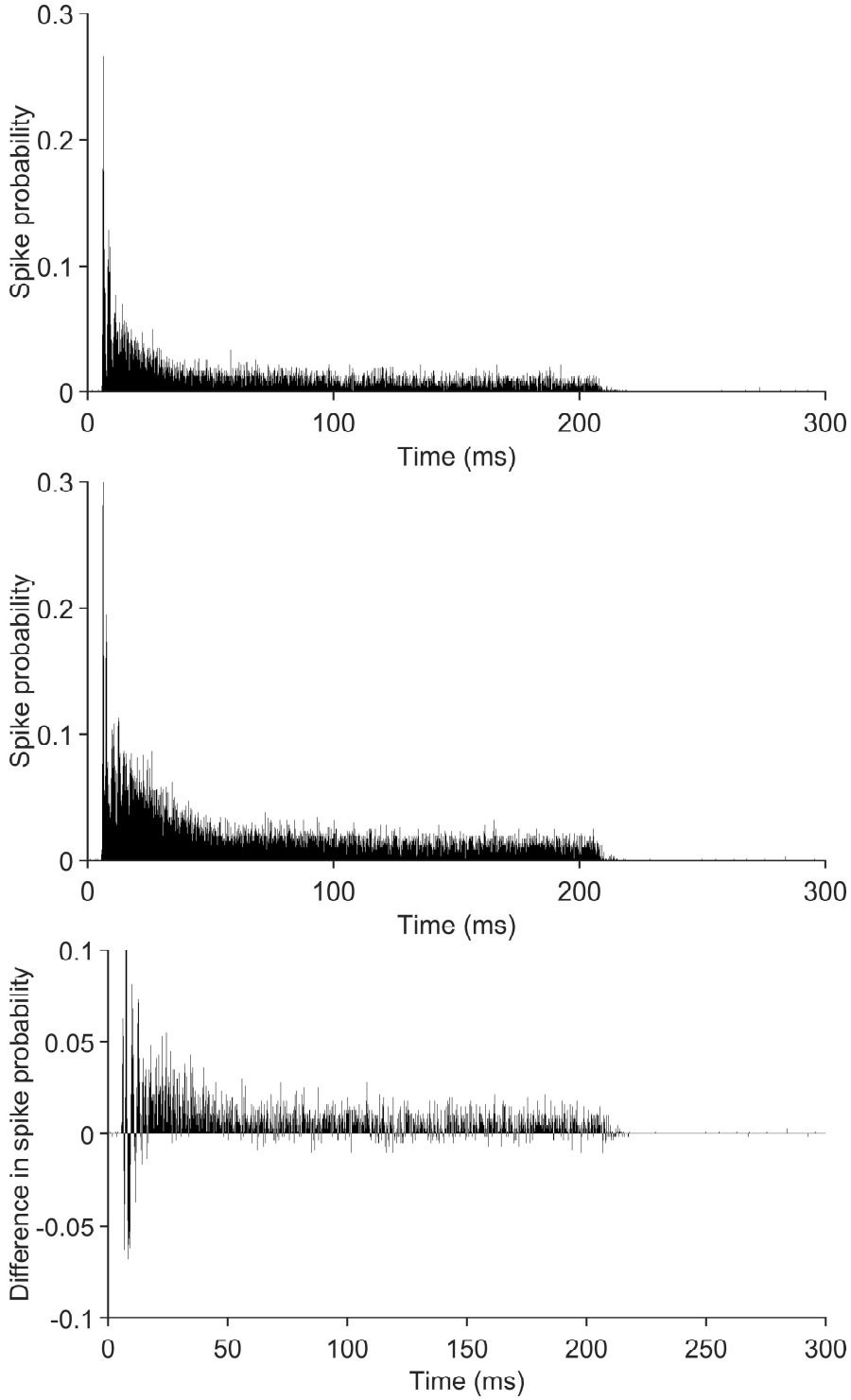


Fig. 3.11: Top: PSTH of the chopper unit from Fig 3.10 over the baseline period (10 minutes, sweeps 301-900; bin size 0.2 ms). Middle: The PSTH of the same unit during L-NAME application (10 minutes, sweeps 1501-2100; bin size 0.2 ms). Bottom: The change in this PSTH during L-NAME application (top - middle). A two-sample Kolmogorov-Smirnov used to compare between the distributions showed they were significantly different ($p < 0.01$).

3.4.2 D-NAME

D-NAME, the biologically inactive isomer of L-NAME, was used as a negative control for iontophoresis experiments using L-NAME (Fig 3.12). It would be expected that D-NAME would have no effect on firing rate of neurons, as it has no biological action. If an effect was seen, it would likely be due to pH changes, incorrect current balancing or pressure from drug ejection, all of which would be severe confounding variables.

Over a 100 minute period, 50 mM D-NAME and L-NAME were each applied at 80 nA for 20 mins. This procedure was carried out on 15 VCN neurons (6 Ch, 4 PrLi, 2 PhLo, 1 On and 2 Un) from three female animals. The majority of neurons (13/15) neither responded to D-NAME or L-NAME, however the remaining two neurons showed a significant increase in driven firing rate during L-NAME application alone. For example, the unit in Fig 3.12 shows no change during the initial D-NAME application, and only a minor increase following the second period of D-NAME ejection. This increase does not appear to be D-NAME related, as it decreases before the end of the ejection period, when D-NAME concentration would still be rising. These data suggest a true drug effect of L-NAME in this study.

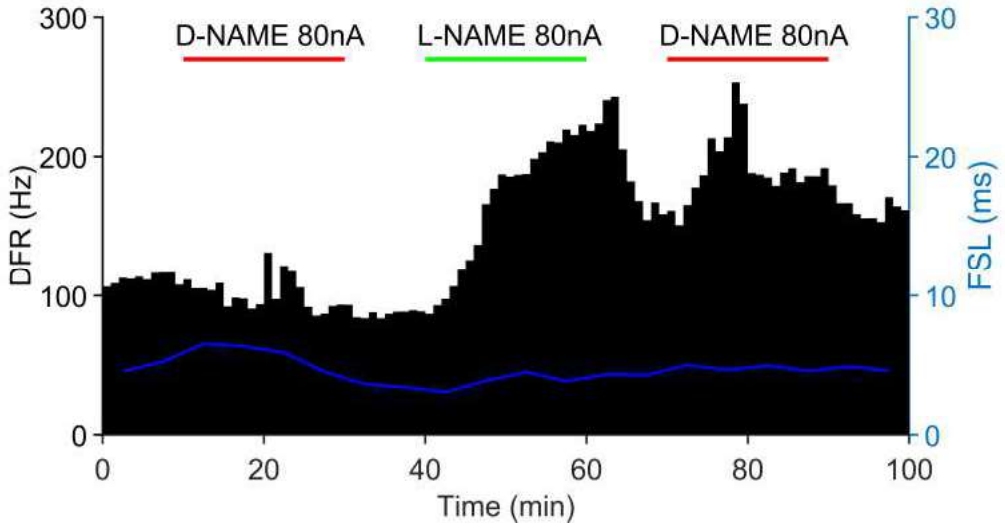


Fig. 3.12: A spike-rate histogram of driven activity of a VCN neuron over 100 mins showing no response to D-NAME (red bar), but an increase in driven firing rate during L-NAME application (green bar). Bin size 1 min. First spike latency (FSL) was also recorded (blue line).

3.5 NOS inhibition on NMDA evoked excitation

As differing effects of NOS inhibition were observed at different activity levels of the units, the effect of L-NAME on artificially induced excitation was tested. This involved application of a substance capable of evoking excitation, the amino acid derivative N-methyl-D-aspartate (NMDA), which mimics the action of glutamate at NMDA receptors. Using this compounds aids in determining between a pre or post-synaptic effect of NO, as it bypasses the presynaptic terminal. Therefore, any NO effect in this study must be postsynaptic.

When studying NO function, using NMDA has multiple advantages over glutamate. Glutamate acts at 3 ionotropic receptors, the α-amino-3-hydroxy-5-methyl-4-isoxazolepropionic acid (AMPA) receptor, NMDA receptor and the kainate receptor, whereas NMDA is specific for the NMDA receptor. Therefore, using NMDA reduces the types of receptors activated. The NMDA receptor when activated allows a calcium ion influx, resulting in depolarisation and NOS activation (Alderton et al., 2001). The NMDA receptor may not be activated by iontophoretically applied glutamate alone, as it will more readily bind to AMPA receptors (Purves et al., 2012).

During these experiments, the same auditory stimuli were used as before, a 200 ms tone every 100 ms. Data is therefore again classed as driven or spontaneous, with NMDA applied during these conditions. NMDA was applied before, during and after a period of L-NAME ejection. When the effect NMDA-mediated excitation was assessed, increases in spontaneous firing rate in response to NMDA application were observed (Fig 3.13).

The effect of L-NAME on NMDA-mediated excitation, was characterised in 3 male and 4 female animals. This produced 32 recordings, with cell types of: 9 Ch, 8 PrLi, 7 PhLo, 4 On and 4 Un. NMDA evoked an increase in SFR in 15/32 (47%) of units (6 Ch, 1 PrLi, 5 PhLo and 3 On) with no apparent correlation to cell type or SFR, other than perhaps a low proportion of PrLi units responding.

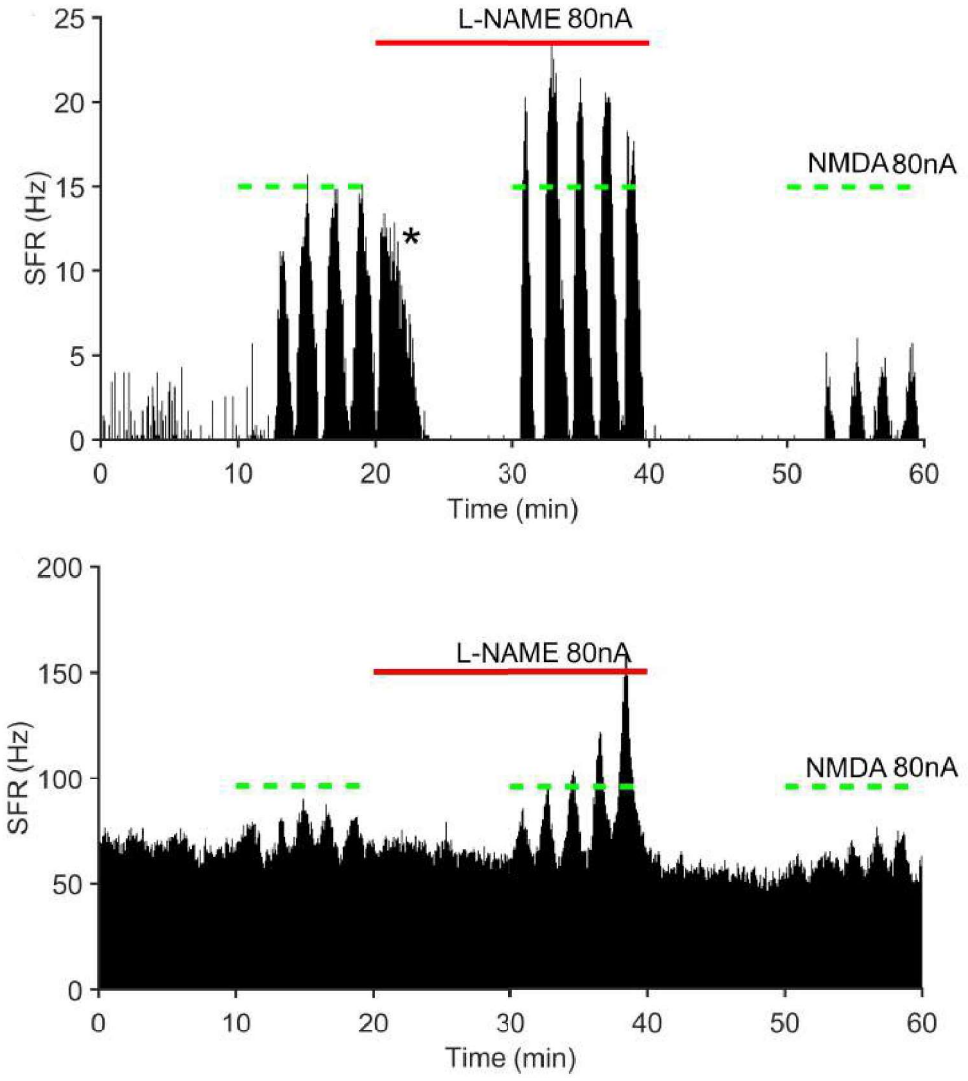


Fig. 3.13: Spike rate histograms of two VCN units with both displaying an increase in SFR during 1 min bursts of NMDA application (green bars). NMDA-evoked increases to low (top) and high (bottom) spontaneous rates is possible. Enhancement of this NMDA-evoked excitation occurred during the 20 minute L-NAME application (red bars). Bin size = 10 s.

A large effect of NOS inhibition was seen on spontaneous data, with 6/15 (40%) units showing significant enhancement of NMDA-evoked increases following L-NAME application (Fig 3.14). In 3 units, the application of L-NAME immediately following NMDA bursts induced SFR increases (shown by the * in Fig 3.13). This suggests that NO is contributing to the reduction in firing rate following NMDA application, as when its production is halted by L-NAME the firing rate returns to higher levels.

Of the 15 units that were NMDA-sensitive, L-NAME application enhanced NMDA excitation during the driven period in 3 (20%) units and reduced excitation in 1 (7%) (Fig 3.14). This driven data has the complication of two simultaneous forms of excitation; auditory input from the peripheral nerve and exogenous NMDA application.

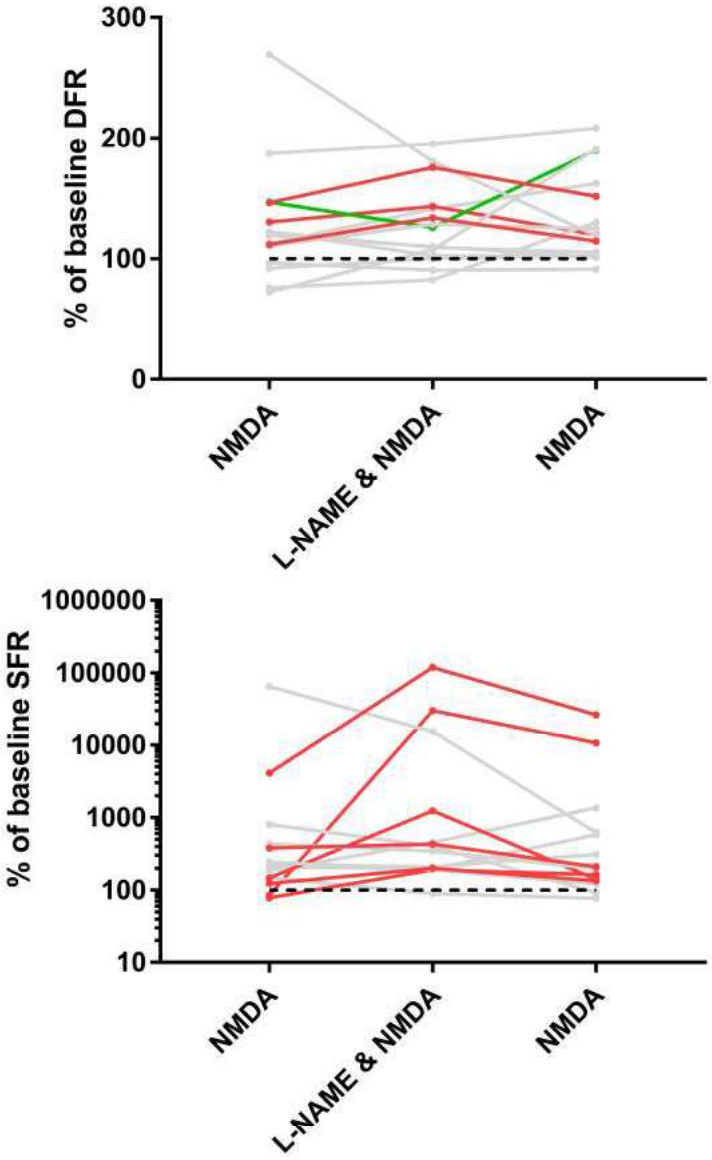


Fig. 3.14: The percentage of baseline driven and spontaneous firing rates evoked by NMDA bursts before, during and after L-NAME application. Log% was used for SFR increases due to the very low baseline SFR's in some units. Significant increases and decreases are highlighted by red and green lines, respectively. Black dotted line marks 100% (no change).

That L-NAME increases excitation corroborates data in the previous section, where NOS inhibition increased firing rate when the unit was auditory driven and therefore in a higher activity state.

3.6 No NO modulation of phase locking

Most of my analysis so far has been purely on spike numbers. However, I observed in *Section 3.4* that the timing of the first spike could be affected by the presence of L-NAME. Therefore, I sought to look for a more generalised effect on the precision or phase of spike timing by analysing the timing of spikes in the units that showed phase-locked activity at their CF.

The strength and timing of phase locking in phase-locked units was analysed for each of the three analysis periods, with comparisons made between the distributions using two-sample Kolmogorov-Smirnov tests between pairs. If phase locking during drug application was significantly different from baseline and recovery, and baseline and recovery were not significantly different, the phase locking of the unit was judged to have been altered.

Phase-locking was studied for all units with a CF below 5 kHz, for L-NAME, SNOG and SIN-1. Phase-locking was shown in 6, 3 and 6 units respectively, with none showing significantly altered phase locking due to drug application.

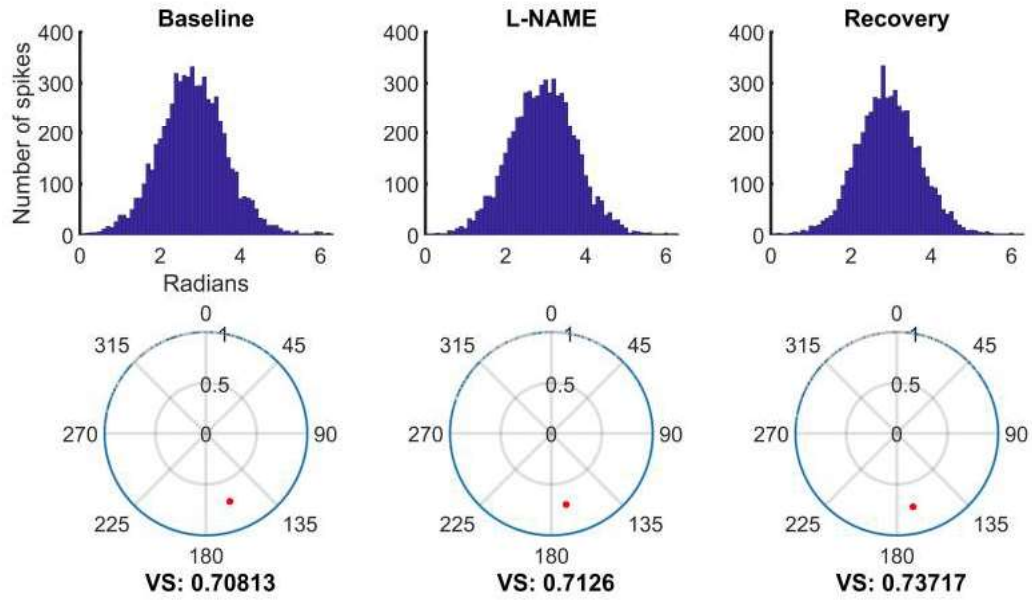


Fig. 3.15: Phase locking analysis (as described in *Section 2.5*) of a 400 Hz unit during the 3 analysis periods: Baseline, 80nA L-NAME and Recovery (columns left to right). Top: Vector histograms for spikes during each of the three analysis periods. Bottom: polar plot showing individual spikes as blue dots around the edge. Vector strength (length along radius) and characteristic phase (degrees) are indicated by the red circle. No changes in vector strength or timing are observed between the three analysis periods.

3.7 NO modulation of spike shapes

NO-mediated changes to firing rate may be due to changes in post-synaptic excitability. To determine if the effects observed had a post-synaptic element, the shape of the extracellular spike recorded was analysed for all data. The mean spike shape for each sweep (1 second) was calculated, with the peak to peak size and width at half amplitude recorded and plotted over the recording period.

For statistical analysis, data was binned as before, 1 minute bins for L-NAME and 10 second bins for NO donors. Again, comparisons between analysis periods were made using a Kruskal-Wallis test with Dunn's multiple comparison test.

As previously mentioned, in control experiments no significant changes to spike size or shape occurred in response to an 80 nA ejection current applied to a micropipette containing citrate-buffered saline of equal concentration and pH as the drug solutions. No significant changes to spike size or width occurred due to L-NAME or SNOG application. However, SIN-1 increased the spike width in 2 chopper units. These were both units which showed increased driven firing rates, suggesting that there is likely a correlation between the effect of nitric oxide on spike shape and excitability.

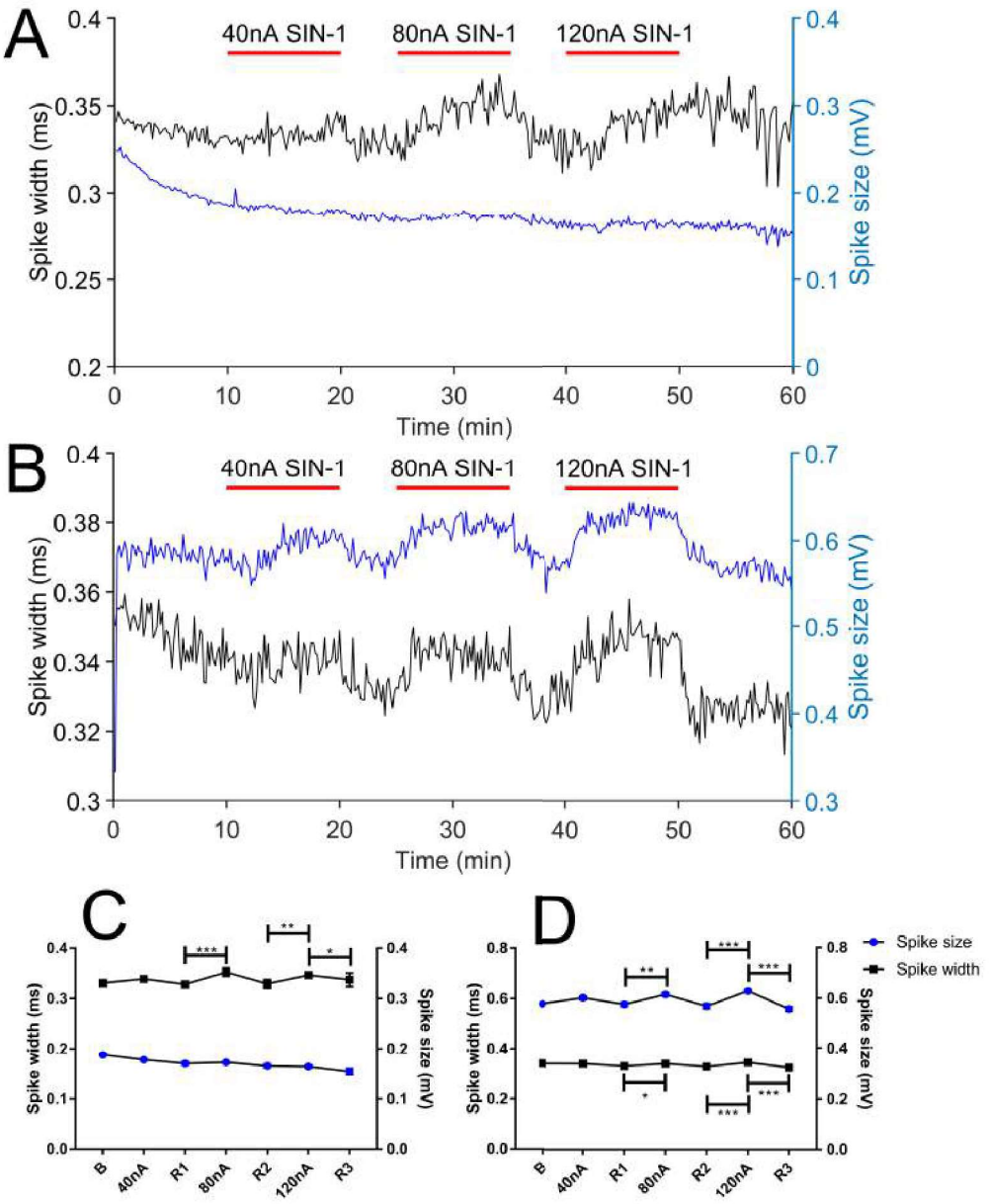


Fig. 3.16: A&B: Spike size (blue lines) and spike width (black lines) of two VCN units over 1 hour, during 3 periods of increasing strength of SIN-1 application. C&D: Quantification of the increases observed in A&B respectively, with the data in analysis periods as described previously. D shows a significant increase in spike size and spike width during SIN-1 application, while C displays increased spike width with no alteration to spike size.

Inter-spike intervals (ISIs) were calculated for both units that showed altered spike width. Interspike-interval histograms (ISIHs) were produced for each unit for the first 20 ms of auditory activation, when chopping

occurred, before and during SIN-1 application. Both units showed a reduced median ISI (example in Fig 3.17). This was not anticipated, as a wider spike width would result in a longer refractory period, increasing the ISIs. That a reduced ISI was seen may be linked to the increased firing rates of these unit, as increased activation would reduce the delay between spikes.

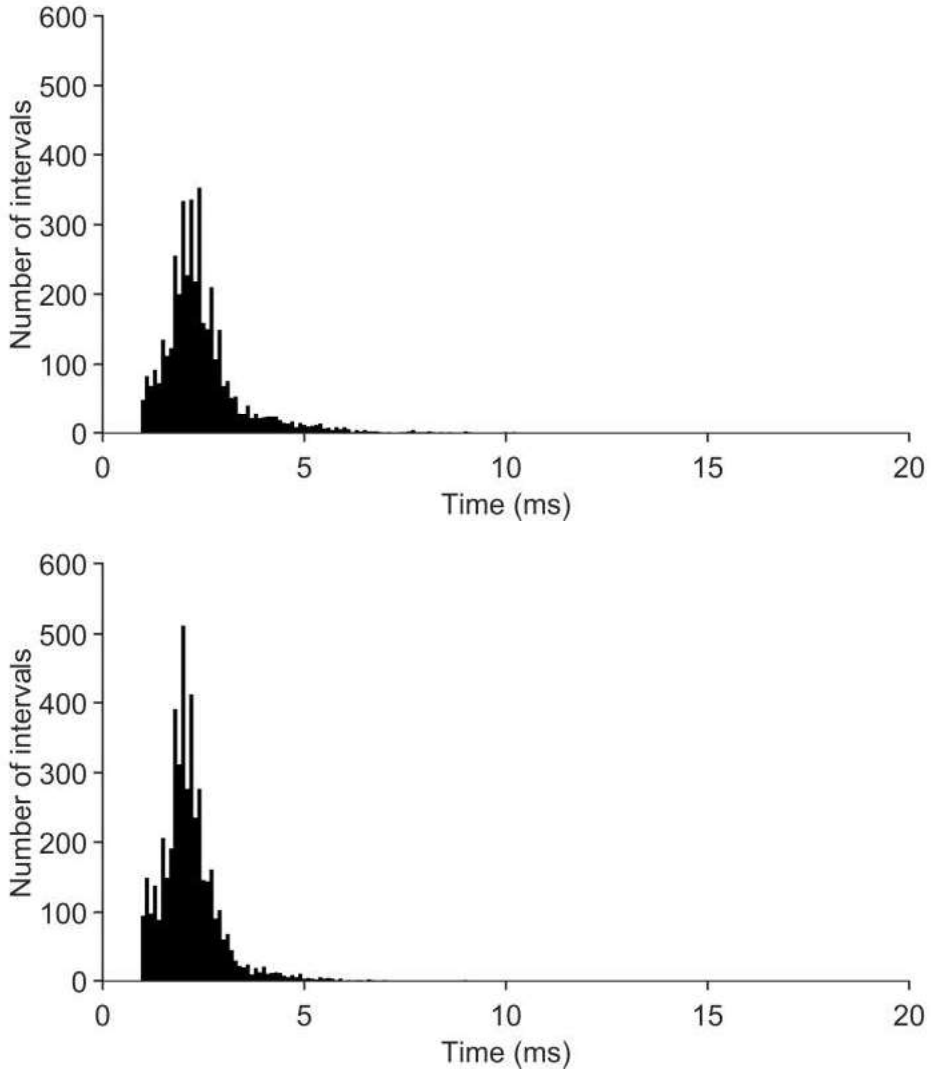


Fig. 3.17: Inter-spike interval histograms for one of the units in Fig 3.16, before (A) and during (B) SIN-1 application. A: median ISI = 2.2 ms. B: median ISI = 2.0 ms. A two-sample Kolmogorov-Smirnov showed the two distributions were significantly different ($p = 0.0436$)

3.8 A nonspecific effect of NO in the VCN

No associations between L-NAME, NMDA, SIN-1 or SNOG sensitivity and unit type were seen (Table 3.1). Effects observed during drug ejection are not cell-type specific, as the proportions of unit types responsive to each drug was similar to the proportion of unit types recorded overall, despite the comparatively low numbers of units responding to drugs.

Class	L-NAME		SIN-1		SNOG		NMDA	
	Applied	Responded	Applied	Responded	Applied	Responded	Applied	Responded
Ch	8	3	14	4	5	3	9	6
Pr	4	1	1	1	5	3	8	1
On	2	1	3	0	8	1	4	3
Ph	3	0	3	1	0	0	7	5
Un	5	2	4	0	5	2	4	0
Total	22	7	25	6	23	9	32	15

Table 3.1: A table of the number of units recorded from for each drug type, which cell types they were, and the numbers of each unit type found to be responsive to each drug.

Overall, 22/70 (31%) units that had NO-related drugs (L-NAME, SIN-1 or SNOG) applied showed altered firing rates, suggesting that around 31% of units in the VCN are modulated by NO.

CHAPTER 4

Changes in VCN nitric oxide function related to noise exposure and tinnitus

4.1 Introduction

The ventral cochlear nucleus is one of the first nuclei in the auditory pathway, receiving most of its input from the auditory nerve. Activity in the VCN could be mediated by neuromodulators which contribute to homeostatic plasticity, facilitating or suppressing strength of transmission to stabilise activity (Turrigiano, 1999). *Chapter 3* showed evidence for a functional role of nitric oxide within the VCN, with this chapter investigating any changes to this function following noise exposure and tinnitus development.

Radical changes in peripheral afferent input have been used to study NO in the auditory system. Cochleotomy, resulting in hugely decreased input, produces decreased spontaneous firing rates (Koerber et al., 1966) and increased NOS expression (Chen et al., 2004) in the VCN. Other less traumatic peripheral alterations such as acoustic over exposure (AOE) (Alvarado et al., 2016; Coomber et al., 2014) and salicylate administration (Zheng et al., 2006) also result in increases in cochlear nucleus NOS expression.

Unilateral AOE produces the majority of neural changes in the ipsilateral CN (Dong et al., 2009; Dong et al., 2010), due to the limited commissural fibres at the CN level of the auditory brainstem (Schofield & Cant, 1996). Increases occur, after AOE, in the relative amount of NOS in the side ipsilateral to the noise exposure compared to the contralateral side. and

this correlates with the behavioural evidence of tinnitus (Coomber et al., 2014). This suggests that NO production increases in the tinnitus VCN, however, how this relates to central gain is still not understood.

The action of NO is predominately via its action on cyclic guanosine monophosphate (cGMP) formation, which is regulated by phosphodiesterases (PDEs) (Rang et al., 2012). Drug trials with PDE5 inhibitors have been carried out to treat tinnitus in humans (Mazurek et al., 2009), or following blast exposure in rats (Mahmood et al., 2014), however these have had limited success.

NO has also been established as a potential therapeutic target in neuropathic pain, a condition often likened to tinnitus due to the similarities of increased central gain following peripheral damage (Cury et al., 2011).

The present study used the combination of in vivo extracellular recordings and microiontophoresis to first look for changes to VCN activity following noise exposure. Behavioural confirmation of tinnitus in these animals allowed correlation of such changes with tinnitus status. I then examined the change in physiological role of NO in the VCN following noise exposure and the development of behavioural evidence of tinnitus.

Synaptic plasticity producing gain changes in the auditory system is thought to underlie tinnitus (Noreña, 2011), with the role of NO in the control VCN observed in *Chapter 3* and the changes in NOS expression in tinnitus suggesting that NO may contribute to tinnitus generation.

As NO can increase or decrease neuronal excitability *Sections 1.5.1 & 1.5.2*, it is possible that the increase in NO concentration in the tinnitus VCN may have a range of effects in the VCN. Any change in the effect of NO in the VCN would have the potential to alter transmission, with a potential to contribute to the 'increased central gain' thought to be present in tinnitus animals. Alternatively, NO changes in the VCN may be an unrelated side effect of noise exposure or tinnitus; however, it is likely to have a functional role.

4.2 Methods

Methods are largely similar to those in *Section 3.2*, with animals from *Chapter 3* used as controls in this chapter. All data collected using the iontophoresis methods are used in this chapter, composed of 131, hour-long recordings from 30 control animals, 79, hour-long recordings from 14 noise exposed but non-tinnitus animals and 77, hour-long recordings from 12 noise exposed with tinnitus animals. The control group is formed of the 120 units from *Chapter 3* plus the 8 pH controls and 3 current balance controls.

Statistical confirmations of firing rate changes are as before, with any other statistics described where necessary. When looking at the effect of iontophoretically applied drugs in this chapter, as before, no cell type specific effects were observed. Therefore, cell types are only referred to when necessary through this chapter.

4.3 ABR changes following acoustic over exposure and behavioural confirmation of tinnitus

AOE and auditory brainstem response (ABR) recordings were conducted as laid out in *Section 2.3*. ABR recordings were repeated at the end point (8 weeks post-AOE) of the experiment prior to non-recovery experiments to determine whether any threshold shifts induced by the AOE were temporary or permanent. These followed the same protocol as before, however they were carried out under urethane and Hypnorm anaesthetic as opposed to ketamine and xylazine.

A typical set of ABR recordings from an animal is shown in Fig 4.1. Low ABR thresholds are seen before AOE, followed by a complete loss of ABRs up to 70 dB SPL following AOE. 8 weeks post-AOE there is a partial recovery of ABR thresholds, confirming that temporary threshold shifts had been induced and that permanent threshold shifts remained. There is also a partial recovery of ABR amplitudes at suprathreshold levels.

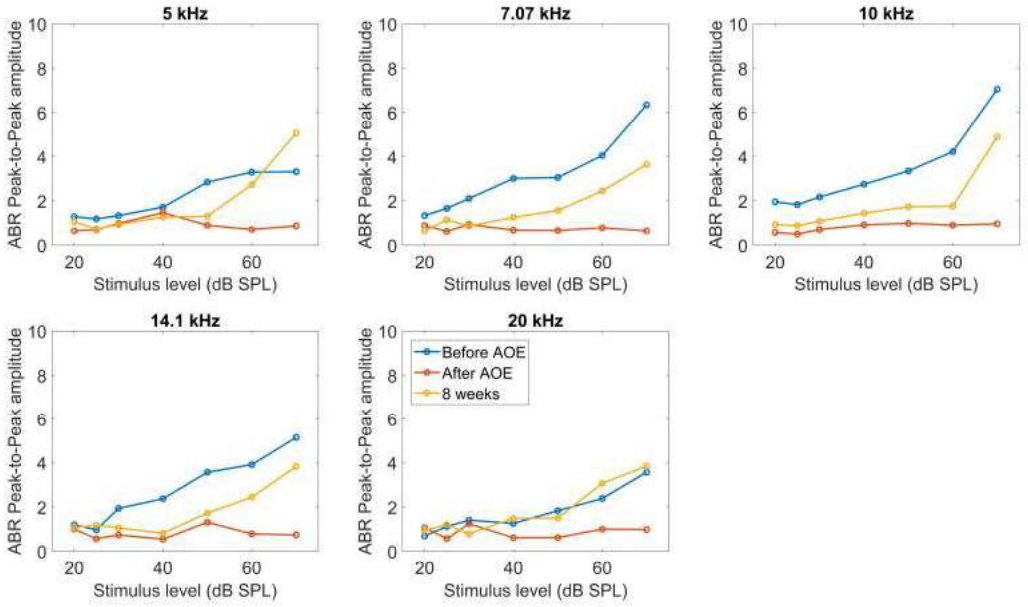


Fig. 4.1: Mean ABR amplitudes from one guinea pig at 5 different frequencies at 7 different sound levels, before, immediately after, and 8 weeks following AOE (number of repeats in each session = 63).

Tinnitus behavioural confirmation sessions were run as described in *Section 2.2*. Five behaviour sessions were run in weeks 7-9 post-AOE. The percentage of reduction in the five no gap and gap trials for baseline and 7-9 weeks was converted to a ratio of gap/no gap. Therefore in Fig 4.2, 1 represents no difference between the conditions and 0 is full inhibition of the startle by the gap. Occasionally if the animal was very active during one session, this was removed and a sixth session of baseline behaviour was recorded.

The baseline data were compared to the 7-9 weeks data using a 2-way ANOVA with Bonferroni's multiple comparison test. If a significant increase in the gap/no gap ratio was seen, the guinea pig was deemed to have tinnitus at this frequency.

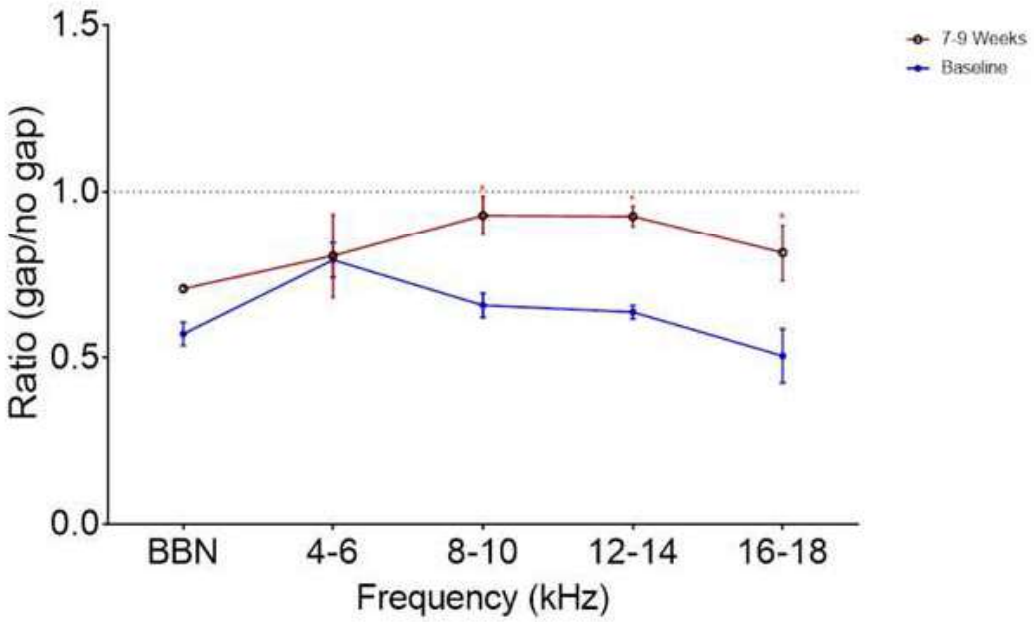


Fig. 4.2: The mean ± SEM ratio of gap/no gap startle amplitudes at each frequency and at different time points. Stars indicate significance p $<$0.05 (n = 5).

4.4 The effect of noise-exposure and tinnitus on VCN unit activity

The first hypothesis to address was that there are changes to VCN unit activity following noise-exposure and these changes correlate with behavioural evidence of tinnitus. The characteristic frequency of all neurons collected showed peaks at 0-4 kHz and 12-14 kHz, with no differences in driven or spontaneous rate through the frequency spectrum (Fig 4.3). Both sets of noise-exposed animals showed a decrease in the proportion of units in the 12-14 kHz section, with an increase in the 0-4 kHz area, with this change being more pronounced in the tinnitus group. A Friedman test showed there are significant differences between the three groups ($p = 0.019$), with the following Dunn's multiple comparison test showing that the significant difference exists between control and tinnitus ($p = 0.012$) but not between control and non-tinnitus ($p = 0.252$).

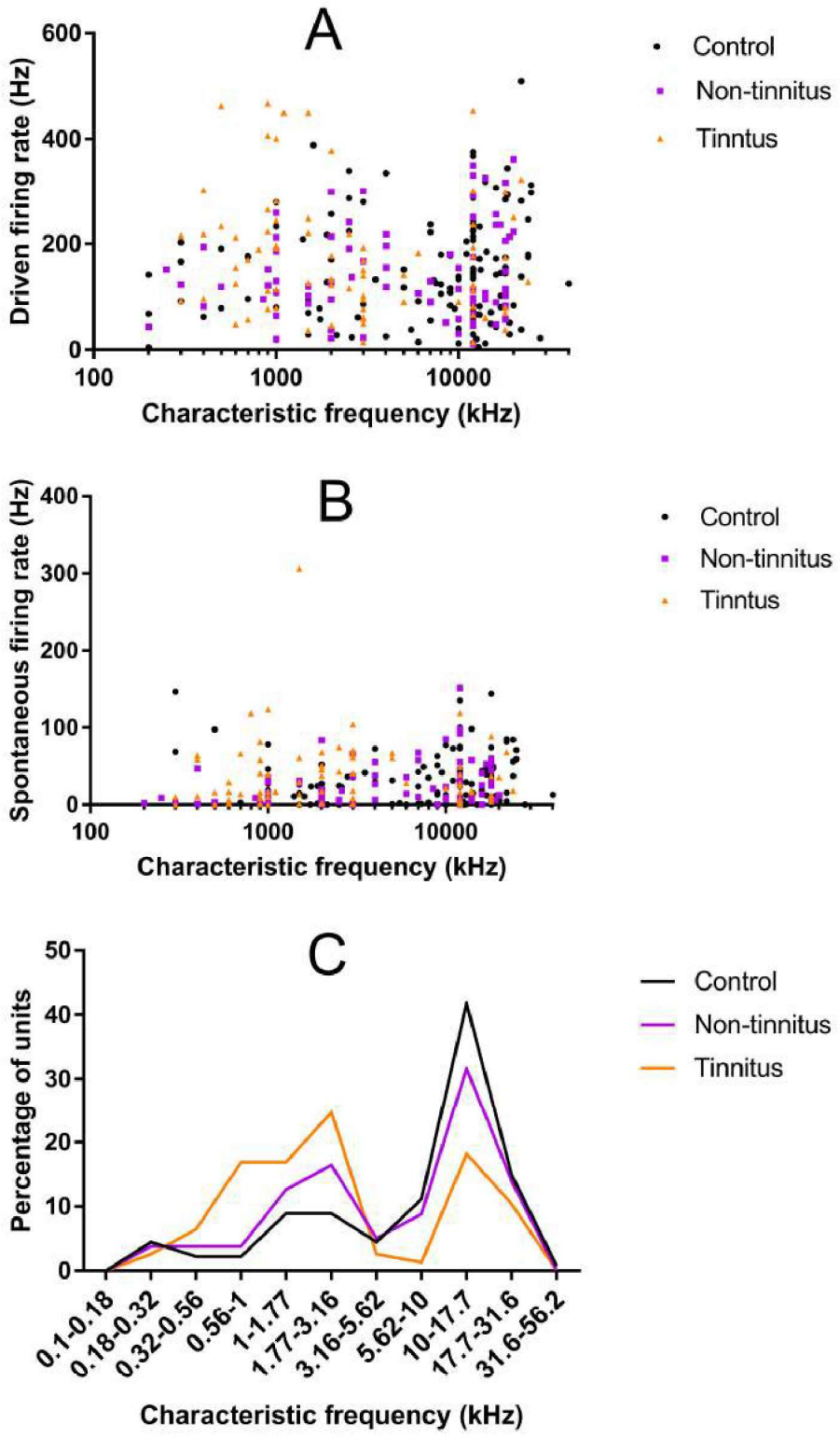


Fig. 4.3: A: Mean driven firing rate and CF of each unit for the first 10 minutes of recording. B: Mean spontaneous firing rate and CF of each unit for the first 10 minutes of recording. C: Proportion of units within each 0.25 octave frequency band, for each animal type. Control n = 131; non-tinnitus n = 79; tinnitus n = 77.

Fig 4.4 shows two example VCN chopper units, one from a control animal and one from a tinnitus animal. Increased activity can be seen in the driven period during the 200 ms tone. Following this, in the post-stimulus suppression (PSS) period, any spontaneous activity is reduced, for up to 100 ms (although often less than 50 ms). Following this, there is 700 ms of spontaneous activity recorded. This PSS period was observed in all units, hence it was analysed separately and not included in spontaneous data.

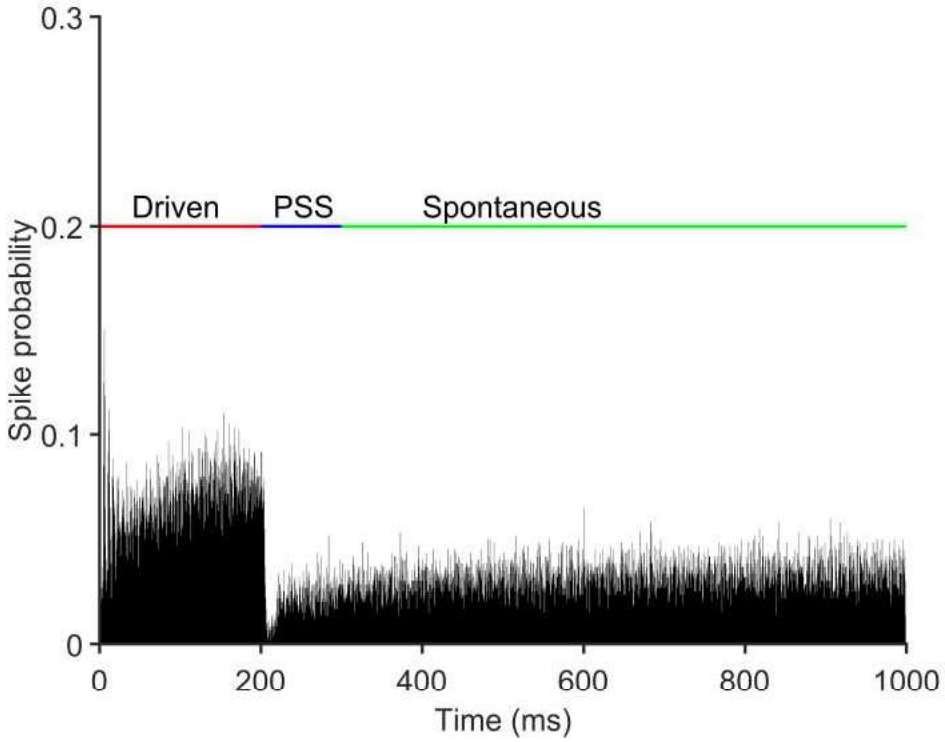


Fig. 4.4: PSTHs from a VCN chopper units from a tinnitus animal. The red, blue and green bars indicate driven, post-stimulus suppression (PSS) and spontaneous analysis periods. Bin size = 0.2 ms.

The effect of noise exposure or tinnitus on firing rates in the VCN was then analysed. Multi-units were removed for these analyses, with 1, 2 and 1 units removed from control, non-tinnitus and tinnitus groups respectively. As seen in Fig 4.5, neurons from non-tinnitus animals had a significantly lower mean driven firing rates than tinnitus animals (Kruskal-Wallis with Dunn's multiple comparison test; $p = 0.034$). This result appeared to be due to a reduction from control values in non-tinnitus animals rather than an increase in tinnitus animals. Significantly higher mean spontaneous rates was also observed in the VCN of animals with behavioural evidence

of tinnitus compared to controls (Kruskal-Wallis with Dunn's multiple comparison test; p = 0.012), with this change also significantly different from non-tinnitus animals (Kruskal-Wallis with Dunn's multiple comparison test; p = 0.049). When these data were divided by cell type, no cell-type specific effects were seen.

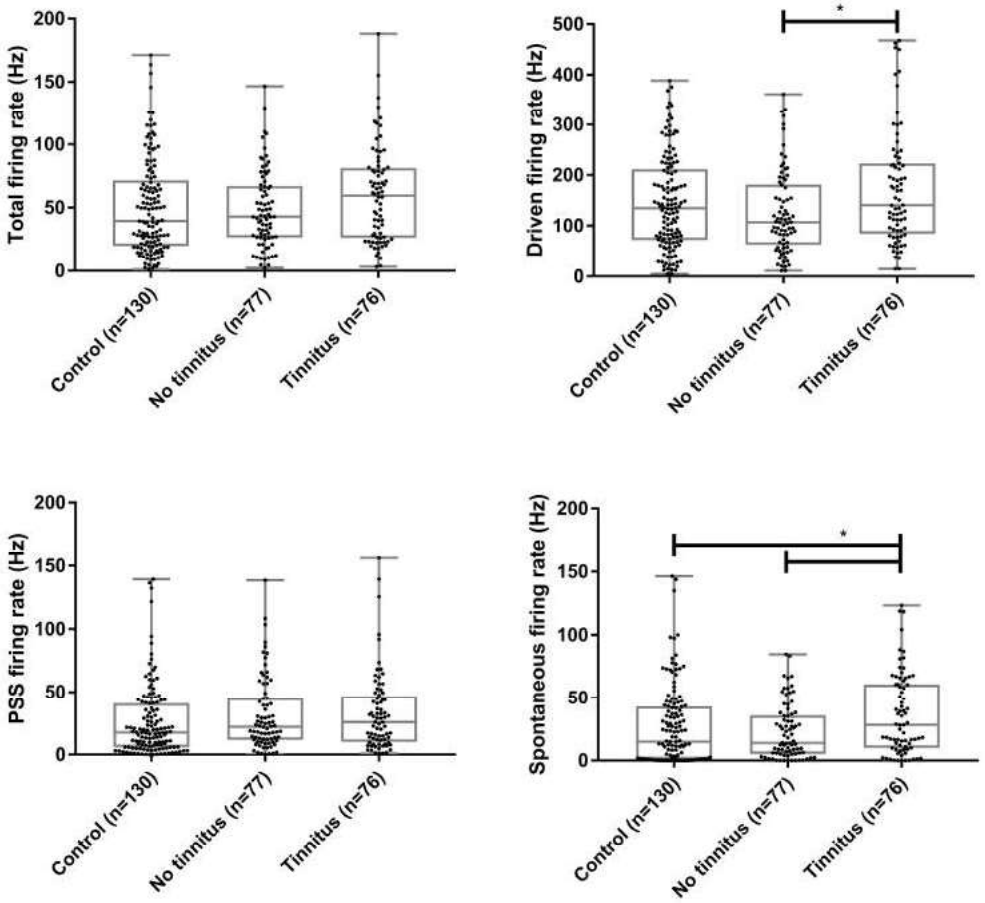


Fig. 4.5: Box and whisker plots of the effect of noise exposure and tinnitus on mean firing rates in the VCN. No effect of noise exposure or tinnitus is seen on total firing rates (0-1000 ms) or post stimulus suppression rate (PSS; 200-300 ms). However, driven firing rates (0-200 ms) in tinnitus animals are significantly higher than those in non-tinnitus animals. Also, units from animals with behavioural evidence of tinnitus showed significantly higher spontaneous firing rates, compared to controls and non-tinnitus animals.

First spike latency (FSL) is the delay between the beginning of an auditory stimulus and a neuronal spike. When taking all units combined, a larger FSL is observed in noise exposed animals that do not develop tinnitus. This

appears to be due to a combination of choppers and primary-like units (Fig 4.6). This greater FSL may be due to reduced excitability in the VCN requiring more input to reach threshold, or increased latency more peripheral to the cochlear nucleus.

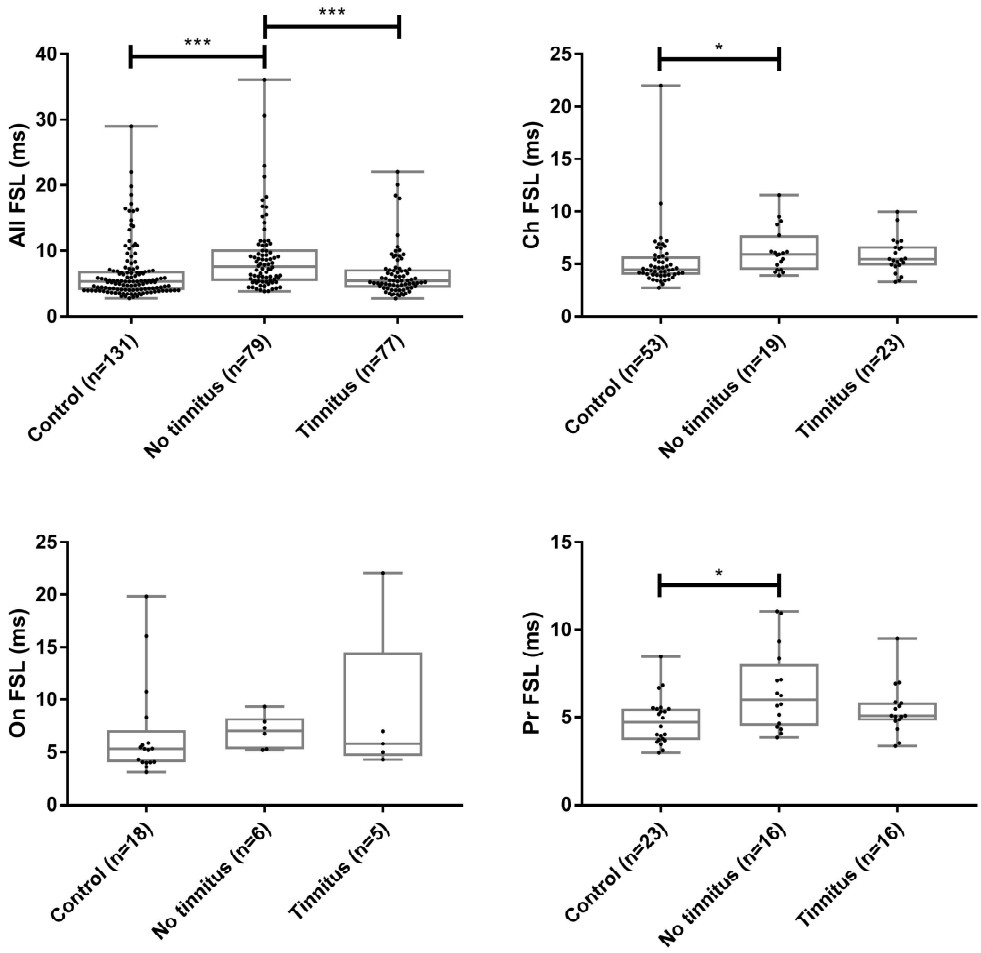


Fig. 4.6: Box and whisker plots of the effect of noise exposure and tinnitus on first spike latency (FSL) in the VCN. Clockwise from top left the data is separated by all units, choppers, primary-like and onset units.

These data show limited changes in the VCN following noise exposure, with only a small proportion of units increasing spontaneous firing rate in the tinnitus animals and a slight increase in FSL in non-tinnitus animals.

4.5 Iontophoresis of NO donor in noise-exposed animals.

The NO donor SIN-1 was applied to 25 units from 4 control animals, 24 from 3 non-tinnitus animals and 25 from 4 tinnitus animals. As shown in Fig 4.9, spontaneous and driven firing rates were significantly affected in each group.

One unexpected effect within these data was that 2 of the 4 tinnitus units that increased their driven firing rate simultaneously decreased their spontaneous firing rate during SIN-1 application. This within-unit rate-dependent effect was not observed in any other units from control, non-tinnitus or tinnitus animals with any iontophoretically applied drugs.

Fig 4.7 shows the PSTH of a tinnitus chopper neuron before and during SIN-1 application, and the difference in spike probability following SIN-1 application. Due to the length of the analysis period the chopping pattern cannot be seen. The effect observed demonstrates nitric oxide moving firing rates away from mean values in tinnitus animals, increasing excitability in high activity states and reducing it in low activity states Fig 4.8 shows the total, driven and spontaneous firing rates for this chopper unit, during the 7 analysis periods set out previously. Increases in driven firing rate occur with SIN-1 application, with decreases in spontaneous rate.

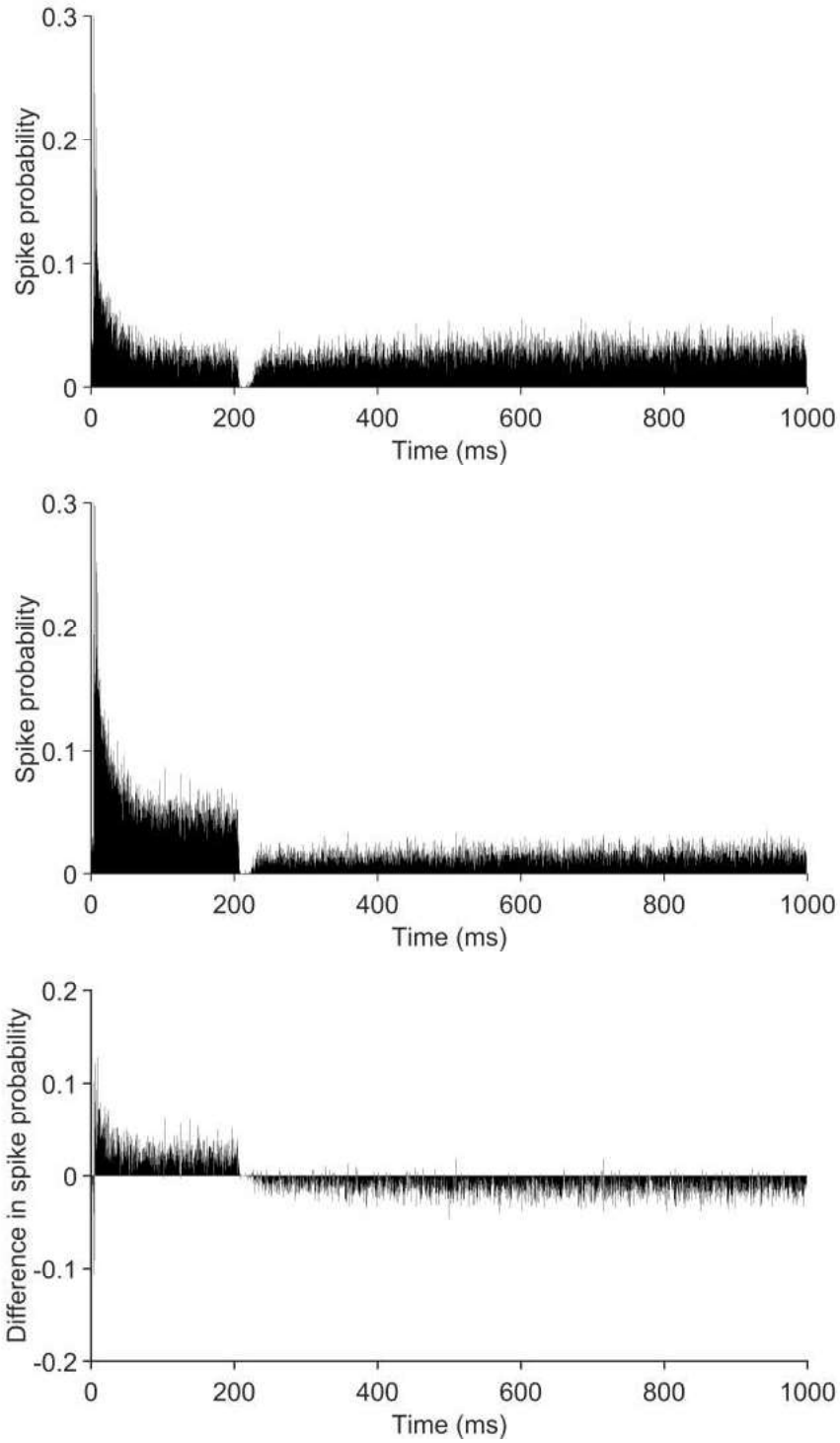


Fig. 4.7: Top: PSTH of a chopper unit from a tinnitus animal over the initial 5 minutes (sweeps 1-300). Middle: The PSTH of the same neuron following 120 nA SIN-1 application, resulting in increased driven rate and reduced spontaneous rate (sweeps 2701-3000). Bottom: The change of PSTH during 120 nA SIN-1 application. An increase in driven firing rate and decrease in spontaneous firing rate is observed. (bin sizes 0.5 ms). A two-sample Kolmogorov-Smirnov test confirmed the distributions are significantly different ($p < 0.01$)

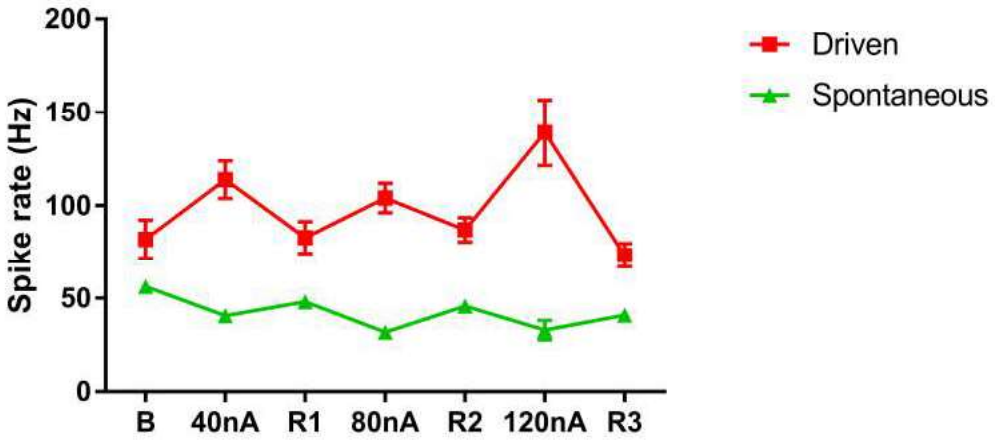


Fig. 4.8: The mean (+/- S.D.) spike rate for a VCN unit during each analysis period laid out in Fig 3.1. The criteria laid out in Section 3.2 confirmed significant increases and decreases in driven (red) and spontaneous (green) firing rates respectively during SIN-1 application (n = 12).

The control group showed increases in the driven activity in 5/25 units, with a decrease observed in the spontaneous activity in 1/25 unit, with no correlations with the initial firing rates (Fig 4.9). Following noise exposure, the proportion of units responding to SIN-1 application increased. Approximately half of units that responded to SIN-1 showed enhanced firing rates, with the other half displayed reduced firing rates. Fig 4.10 shows the proportion of units increasing and decreasing their firing rates in response to SIN-1 application for control (C), non-tinnitus (NT) and tinnitus (T) animals. Fisher's exact tests of the whole 3x3 tables showed no significant differences for driven activity ($p = 0.474$) but significant differences in the spontaneous data ($p = 0.006$). Further Fisher's exact tests showed this difference was due to significant differences between control and non-tinnitus ($p = 0.004$) and control and tinnitus ($p = 0.013$), with no significant difference between tinnitus and non-tinnitus ($p = 0.384$)

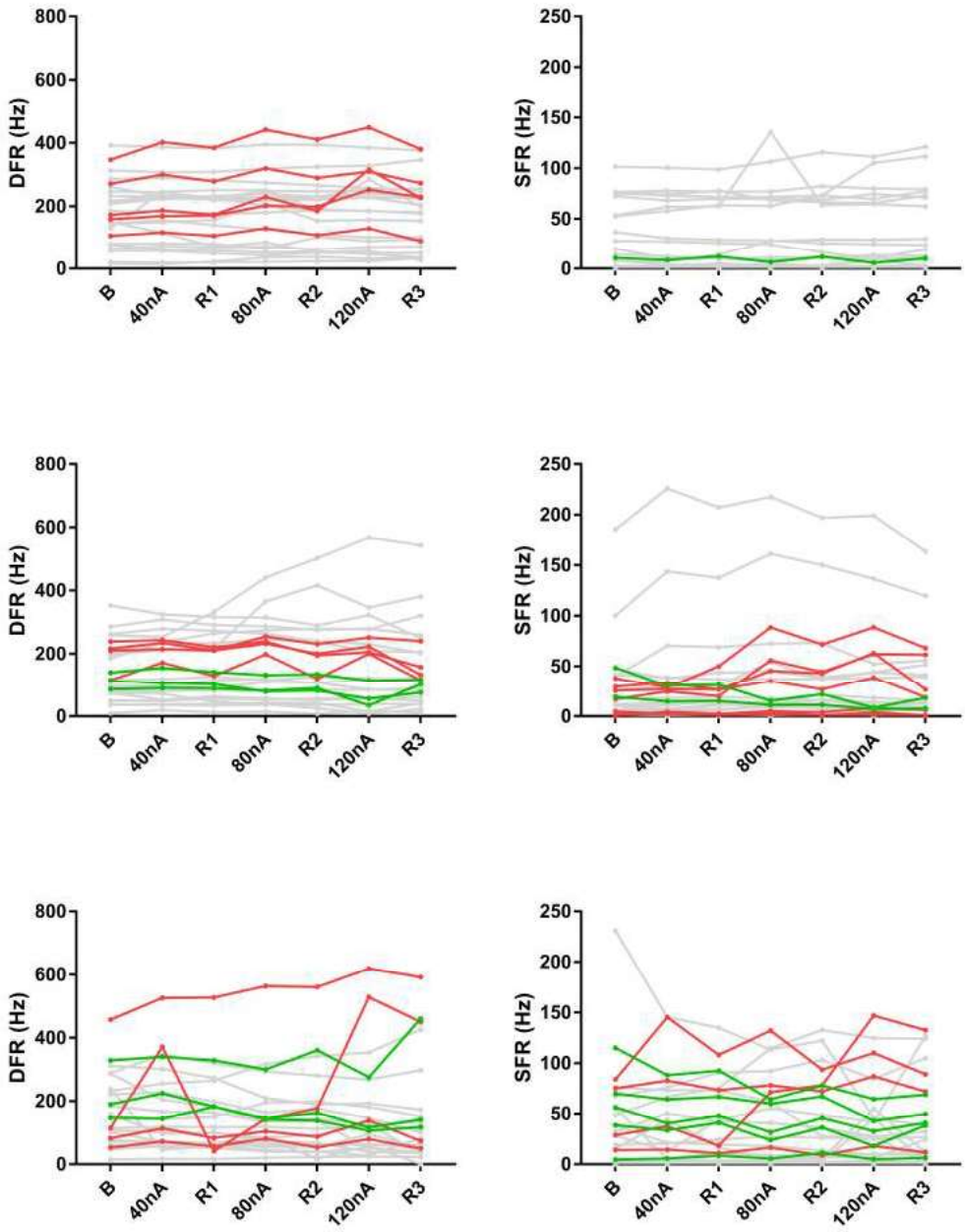


Fig. 4.9: The mean spike rates for each VCN unit during each analysis period laid out in Fig 3.1. Changes of driven (left) and spontaneous (right) firing rates following SIN-1 application, for control, non-tinnitus and tinnitus animals (top, middle and bottom rows, respectively). Red and green lines highlight significant increases and decreases, respectively, with grey lines showing all other units.

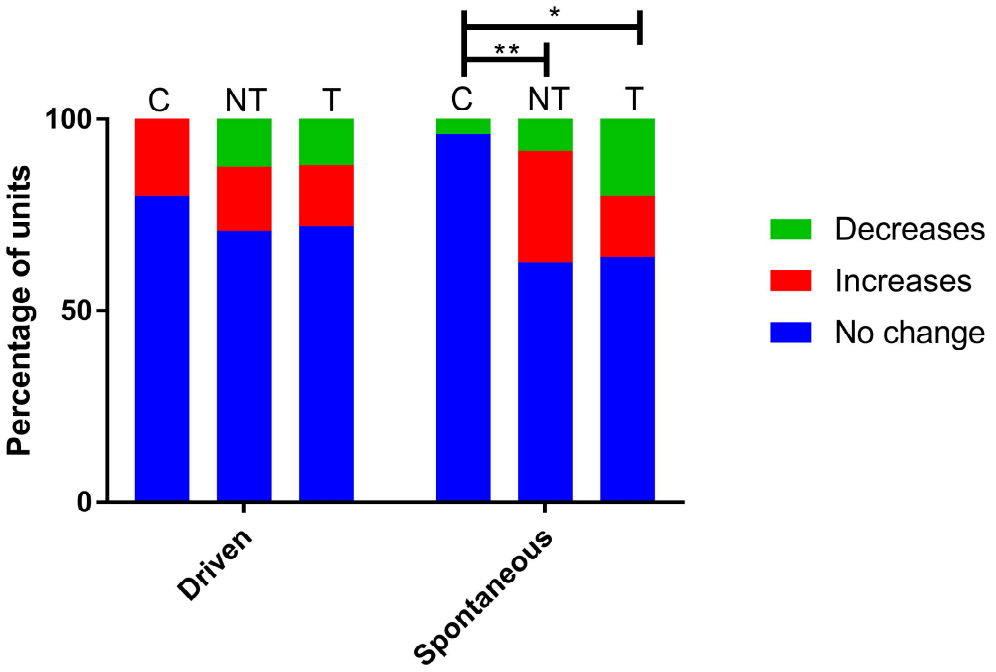


Fig. 4.10: The proportion of VCN units significantly increasing and decreasing their firing rates during SIN-1 application, for driven and spontaneous periods and each animal class (C, NT and T).

4.6 Iontophoresis of NOS inhibitor in noise-exposed animals.

Measurements of spike rate over a period of one hour were used to identify the effect of L-NAME on VCN neurons in control, non-tinnitus and tinnitus animals (n = 9, 5 & 4, respectively). In control, non-tinnitus and tinnitus animals, 22, 22 and 19 units were recorded, respectively.

L-NAME application to VCN units from control animals resulted in increases in the driven firing rate (DFR) in 18%, with no decreases observed (Fig 4.11). When analysing the SFR, increases and decreases occurred, with 9% showing a significant increase from baseline during L-NAME ejection and 9% significantly decreasing (Fig 4.11). As L-NAME increases driven activity, this suggests that NO is endogenously decreasing excitability in the VCN during this higher-activity state. This effect of NO appears to be dependent of the activity state of the cell (driven or spontaneous). However, when looking at the total neuron population studied, the baseline firing rates of units do not determine the effect of L-NAME.

Changes in the effect of L-NAME were observed in noise exposed animals, with a higher proportion of units decreasing their spontaneous and driven firing rates, particularly in animals with behavioural evidence of tinnitus (Fig 4.12). The clearest effect of tinnitus is on driven activity, where a much greater proportion of units (37%) decrease their driven firing rate as a result of NOS inhibition. Reductions in firing rate during NOS inhibition suggest endogenous NO is increasing excitability, and this is occurring to a greater extent in tinnitus animals.

Fisher's exact tests on each 3x3 table showed significant differences in the driven data ($p < 0.001$) but not spontaneous ($p = 0.392$). Further Fisher's exact tests between groups of the driven data revealed significant difference between control and tinnitus ($p = 0.004$) and non-tinnitus and tinnitus ($p = 0.041$) but not control and non-tinnitus ($p = 1.000$).

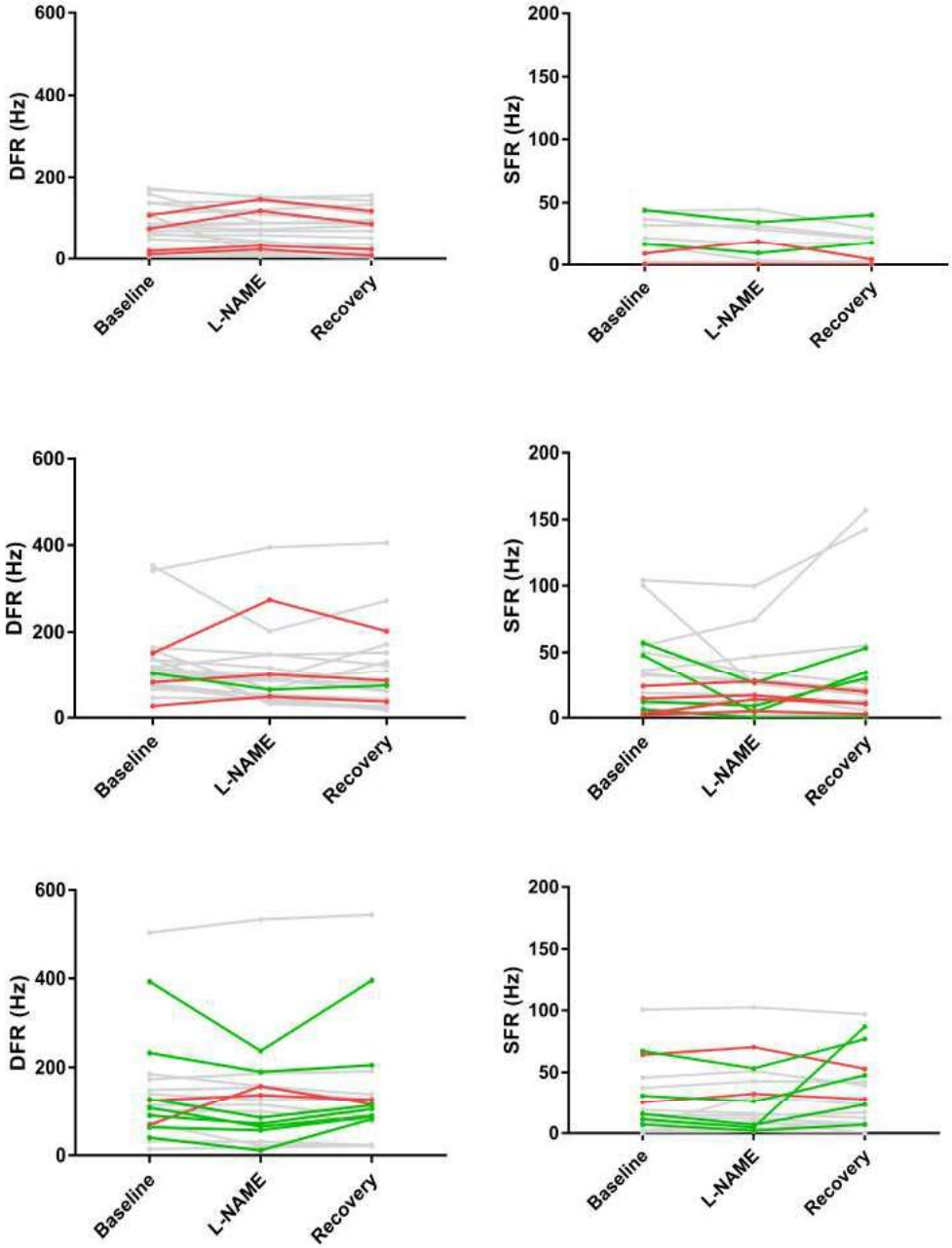


Fig. 4.11: The mean spike rates for each VCN unit during each analysis period laid out in Fig 3.1. Changes of driven (left) and spontaneous (right) firing rates following L-NAME application, for control, non-tinnitus and tinnitus animals (top, middle and bottom, respectively). Red and green lines highlight significant increases and decreases, respectively, with grey lines showing all other units.

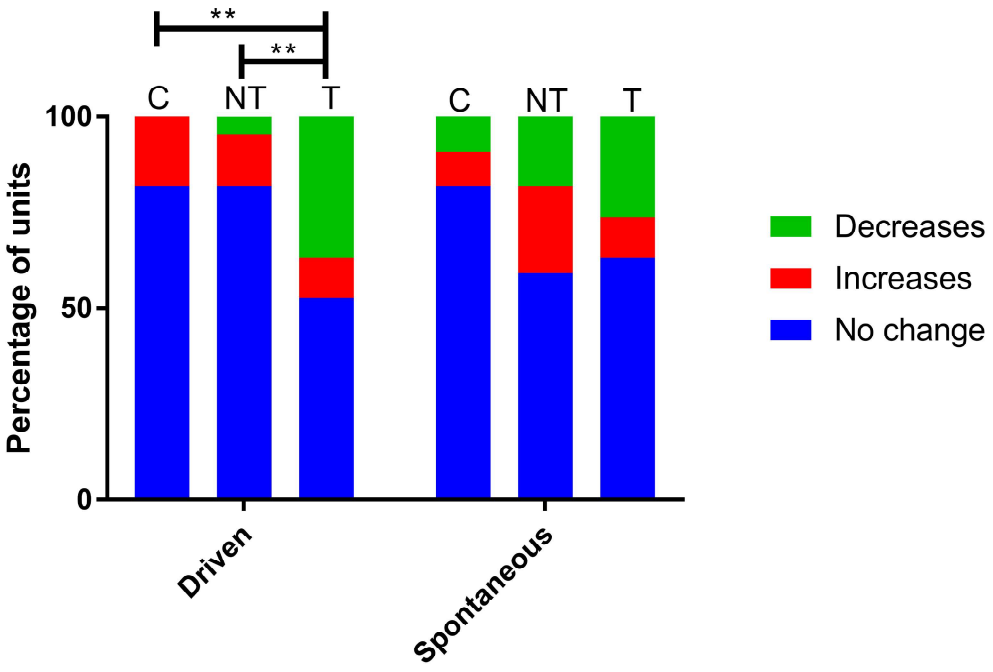


Fig. 4.12: The proportion of units significantly increasing and decreasing their spontaneous and driven firing rates in response to iontophoretic L-NAME application, for control (C), non-tinnitus (NT) and tinnitus (T) animals.

Correlations between the tinnitus behavioural measure (GPIAS) and the effect of L-NAME on firing were studied (Table 4.1) for all noise-exposed animals. A higher GPIAS percentage demonstrates a greater inhibition of the acoustic startle by the gap, suggesting the absence of tinnitus, with a low GPIAS percentage showing less effect of the gap and the presence of tinnitus. For driven and spontaneous data from each animal, the percentage of units decreasing firing rate during L-NAME application was subtracted from the percentage of units increasing firing rate to give the difference between increasing and decreasing.

Fig 4.13 plots the GPIAS percentage against the percent of increases minus the percent of decreases. The trendlines show that for driven data, the effect of L-NAME is reversed in tinnitus animals compared to non-tinnitus, with a positive correlation between GPIAS and the difference between increasing and decreasing ($R^2 = 0.4632$). An F-test confirms that this correlation is significantly different from zero ($F = 6.041$; $p = 0.0436$).

For spontaneous data there is a no correlation between GPIAS and the difference between increasing and decreasing (R2 = 0.1643). An F-test

confirms that this correlation is not significantly different from zero ($F = 1.376$; $p = 0.1643$).

Animal		Driven				Spontaneous			
T/NT	GPIAS	n units	Increase	Decrease	%i-%d	n units	Increase	Decrease	%i-%d
NT	37.4	4	0	0	0	4	0	4	-100
NT	23.8	4	1	0	25	4	1	0	25
NT	18.6	5	1	0	20	5	2	0	40
NT	23.8	3	1	0	33	3	1	0	33
NT	19.8	6	0	1	-17	6	1	0	17
T	13.8	3	0	1	-33	3	0	0	0
T	13.8	7	2	3	-14	7	1	2	-14
T	0.2	2	0	1	-50	2	1	1	0
T	11.4	7	0	2	-29	7	1	2	-14

Table 4.1: How the effect of L-NAME on the firing rate of units is related to GPIAS. For each animal, the tinnitus status is given and the mean GPIAS. The number of units recorded from (n units), number increasing and decreasing, and percentage of increasing minus decreasing (%i-%d) are shown, for driven and spontaneous analysis periods.

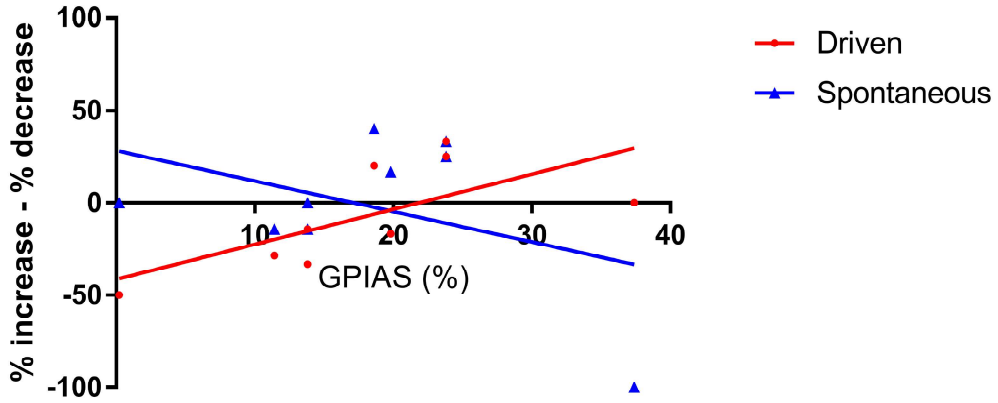


Fig. 4.13: Correlations between GPIAS percentage and the difference in the percentage of units increasing or decreasing driven or spontaneous firing rate following L-NAME application for each animal (pair of driven and spontaneous data points at a certain GPIAS). Higher GPIAS percentage indicates a non-tinnitus animal, with lower GPIAS indicating a tinnitus animal.

These data show the changes in the effect of L-NAME on the driven rate in tinnitus animals in Fig 4.12 are correlated to tinnitus behaviour. This demonstrates that the NO-mediated increased excitability in the VCN during auditory input in tinnitus animals is related to strength of behavioural evidence of tinnitus.

4.7 NOS inhibition during NMDA-evoked excitation in noise-exposed animals.

The effect of L-NAME on NMDA-mediated excitation was characterised in 7 control animals, before testing in 5 non-tinnitus and 4 tinnitus animals. In control animals, NMDA evoked an increase in firing rate in 15/32 (47%) of units (Fig 4.14) with no correlation to cell type or firing rate. In both non-tinnitus and tinnitus animals, the proportion of units where NMDA increased the firing rate was 17/33 (52%).

Of the 15 control units that were NMDA-sensitive, L-NAME application enhanced NMDA excitation during the driven period in 3 (20%) units and reduced excitation in 1 (7%) (Fig 4.14). A greater effect of L-NAME was observed on firing rate increases, where 40% showed significant enhancement of NMDA-evoked firing rate increases following L-NAME application (Fig 4.15). In the healthy VCN, L-NAME increases NMDA-evoked excitation in a similar manner to auditory-driven activation, further suggesting that NO reduces activity in high-excitation states.

Despite Fisher's exact tests showing no significant differences in either the driven data ($p = 0.213$) or the spontaneous data ($p = 0.290$), noise exposure resulted in a greater proportion of units decreasing activity during L-NAME application. This suggests the inhibitory effect of NO is reversed in a subsection of VCN units from noise exposed animals, hence increasing excitability. This effect is seen to a greater extent in spontaneous data, possibly due to the driven condition having the complication of two simultaneous forms of excitation; auditory nerve input and NMDA application. No correlations with tinnitus were observed in these data. One possible explanation for this is that the post-synaptic effect of NO may change following noise exposure, hence the chages in these data. However, in tinnitus animals, changes to NO function may be pre-synaptic effect, as any presynaptic effect would be bypassed in this experiment by the application of NMDA.

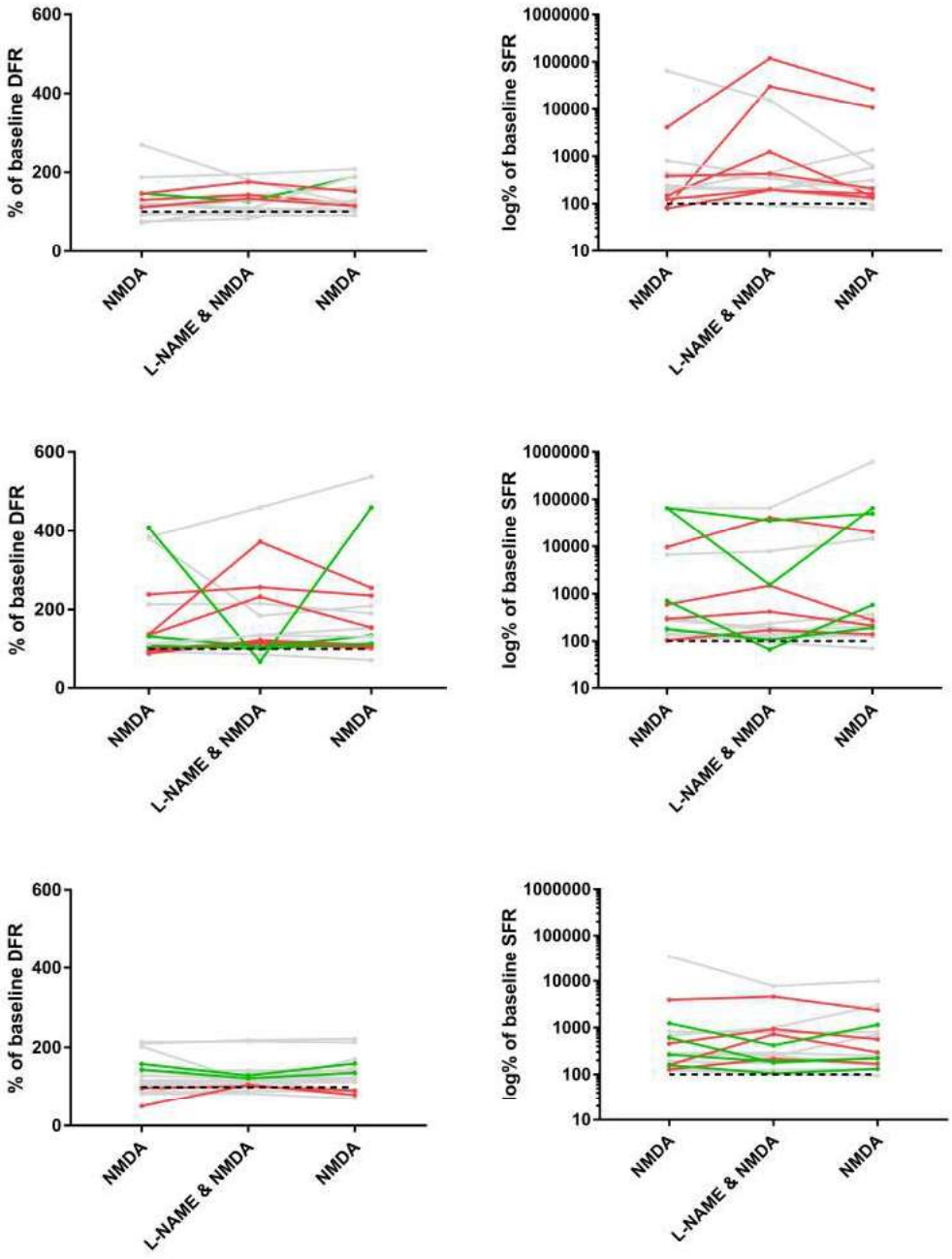


Fig. 4.14: Changes to firing rate evoked by NMDA application before, during and after L-NAME application. The percentage of baseline firing rate for driven (left) and spontaneous (right) firing rates, for control, non-tinnitus and tinnitus animals (top, middle and bottom, respectively).

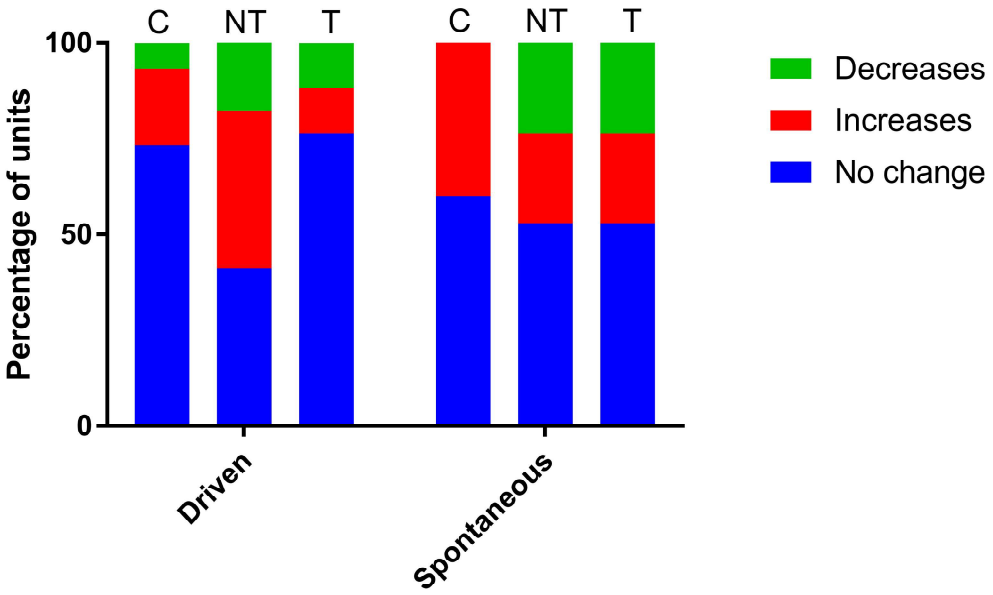


Fig. 4.15: The proportion of VCN units significantly increasing and decreasing their NMDA-evoked excitation during L-NAME application, for driven and spontaneous periods and each animal class.

CHAPTER 5

Preliminary testing of peripheral NOS inhibitor application

5.1 Introduction

This chapter builds upon the previous two chapters by assessing the possibility of applying NOS inhibitors peripheral to the cochlear nucleus to modulate endogenous NOS in the VCN. If peripherally applied NOS inhibitors show efficacy in the VCN this may suggest a route for developing the use of NO-modulating drugs to affect auditory processing in the clinical setting, possibly as future treatment for tinnitus.

Therefore, NOS inhibitors were applied indirectly to the cochlear nucleus, either via reverse microdialysis or systemic application (i.p.), and the effect of these drugs on either VCN activity or behavioural measures of tinnitus was studied. Reverse dialysis allows application of drug directly to the extracellular space, giving a semi-local effect, whereas systemic injection supplied the drug to the entire body.

Due to the different experimental designs, different NOS inhibitors were used for reverse microdialysis or systemic injection. These were nitro-L-arginine methyl ester hydrochloride (L-NAME) and 7-Nitroindazole (7-NI), respectively.

Both 7-NI and L-NAME cross the blood brain barrier (Brouillet et al., 1995; Bush & Pollack, 2001), suggesting either as a potential way to modulate VCN NOS by systemic application. 7-NI is non-selective between nNOS and eNOS in vitro, with IC50 (half maximal inhibitory concentration) values for rat nNOS, bovine eNOS and rat iNOS of 0.71, 0.78 and 5.8 μM

respectively (Babbedge et al., 1993; Bland-Ward et al., 1994). However, 7-NI produces anti-nociceptive effects with no effect on blood pressure (Moore et al., 1993), suggesting that in vivo the majority of the effect is at nNOS. My experiments also required a specific neuronal effect, with limited cardiovascular side-effects, therefore 7-NI was used for systemic administration in these experiments.

L-NAME was chosen for microdialysis due to the effects seen in iontophoresis experiments. L-NAME is also stable in aqueous solution, suiting it to the methodology used in microdialysis. Its activation requires hydrolysis to L-NG-Nitroarginine (L-NNA), the active compound. This is partially selective toward nNOS, with Ki (binding affinity) values of 15, 39 and 4400 nM for nNOS, eNOS, and iNOS respectively (Furfine et al., 1993).

The effect of systemically applied 7-NI on GPIAS was then studied. This was intended to assess any changes to tinnitus perception in guinea pigs following global NOS inhibition, further suggesting any clinical application of NOS inhibitors in tinnitus.

5.2 Global nNOS inhibition decreases VCN activity

Bilateral multielectrode assemblies were used to record from both VCNs simultaneously. For these experiments, methods were as explained in *Section 2.4*. During recording, the nNOS inhibitor 7-NI was administered i.p.; 7-NI is highly lipophilic so peanut oil was used as the solvent. Previously, i.p. 7-NI administration has been shown to result in increased hippocampal 7-NI within 1 hour in male Sprague-Dawley rats, followed by decreased NO production within 2 hours (Bush & Pollack, 2001). However, in our pilot data we observed a more rapid effect of 7-NI, within 5 minutes. Our experiment therefore consisted of an hour long recording, with vehicle injection at 15 mins, 10 mg/kg 7-NI at 30 mins and 50 mg/kg 7-NI at 45 mins. The experiment was run twice on each animal, with at least two hours between recording periods to allow breakdown of the 7-NI. Bilateral recordings with 4 electrodes on each side were conducted twice on 6 animals (4 male, 2 female), producing a total of 96 separate recording sites. Of these 96 recording sites 63 (66%) had LFPs and 37 (39%) had single units, as it was not always possible to get single units or LFPs on each electrode simultaneously. These 37 units consisted of 17 choppers, 10 primary-like, 4 phase-locked, 2 onset and 4 unclassified. An example PSTH and mean LFP waveform are shown in Fig 5.1. The PSTH shows that this is a classic primary-like VCN neuron, which produces a biphasic LFP at the onset of the stimulus, and a reversed biphasic response at the stimulus offset.

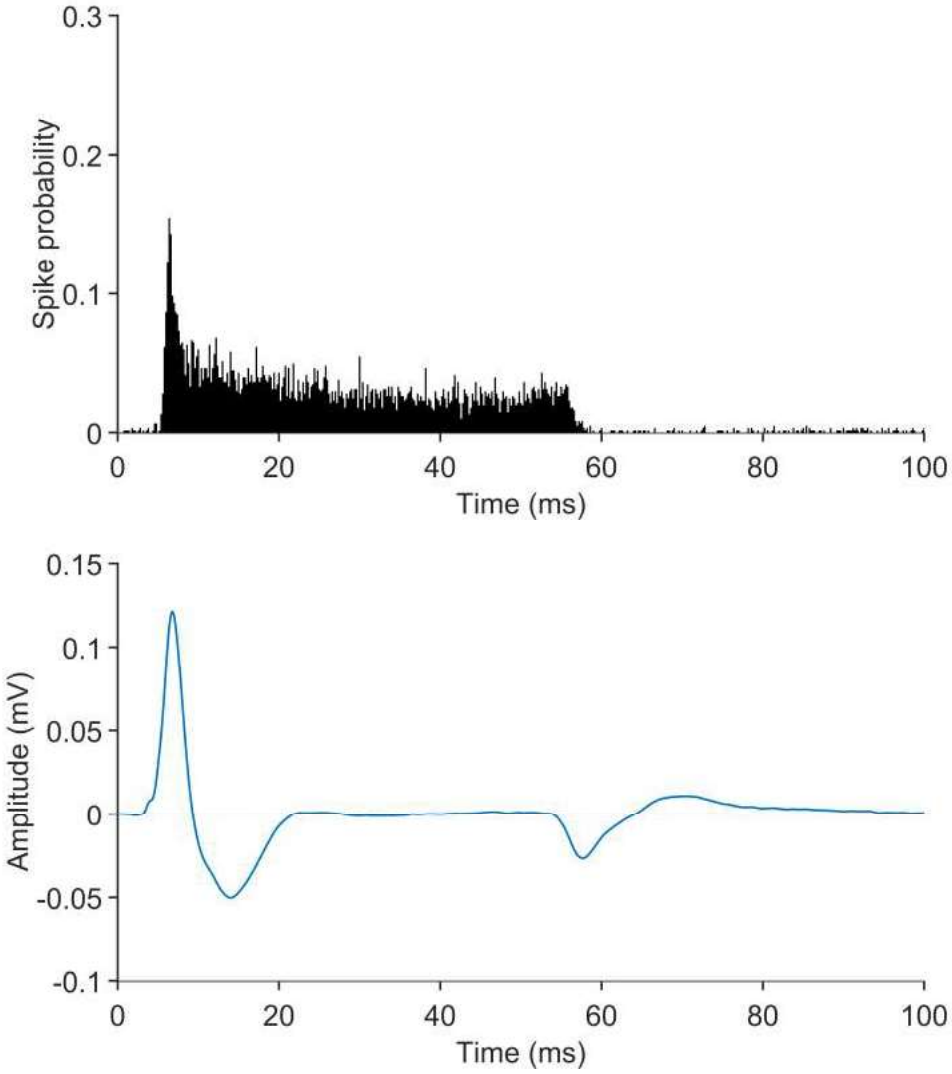


Fig. 5.1: The PSTH (top) and mean LFP waveform (bottom) of a primary-like VCN unit in response to 50 ms BBN bursts at 90dB (300 repeats; 1 minute). Both are recorded from the same electrode simultaneously but with different filters applied, as explained in *Section 2.5.4*.

Spike rate for the driven period (0-50 s) and LFP amplitude over the hour-long recording period were then analysed, during systemic 7-NI administration. LFP amplitude was measured by the peak-to-peak of the mean waveform over each minute (300 sweeps), between 0 and 30 ms.

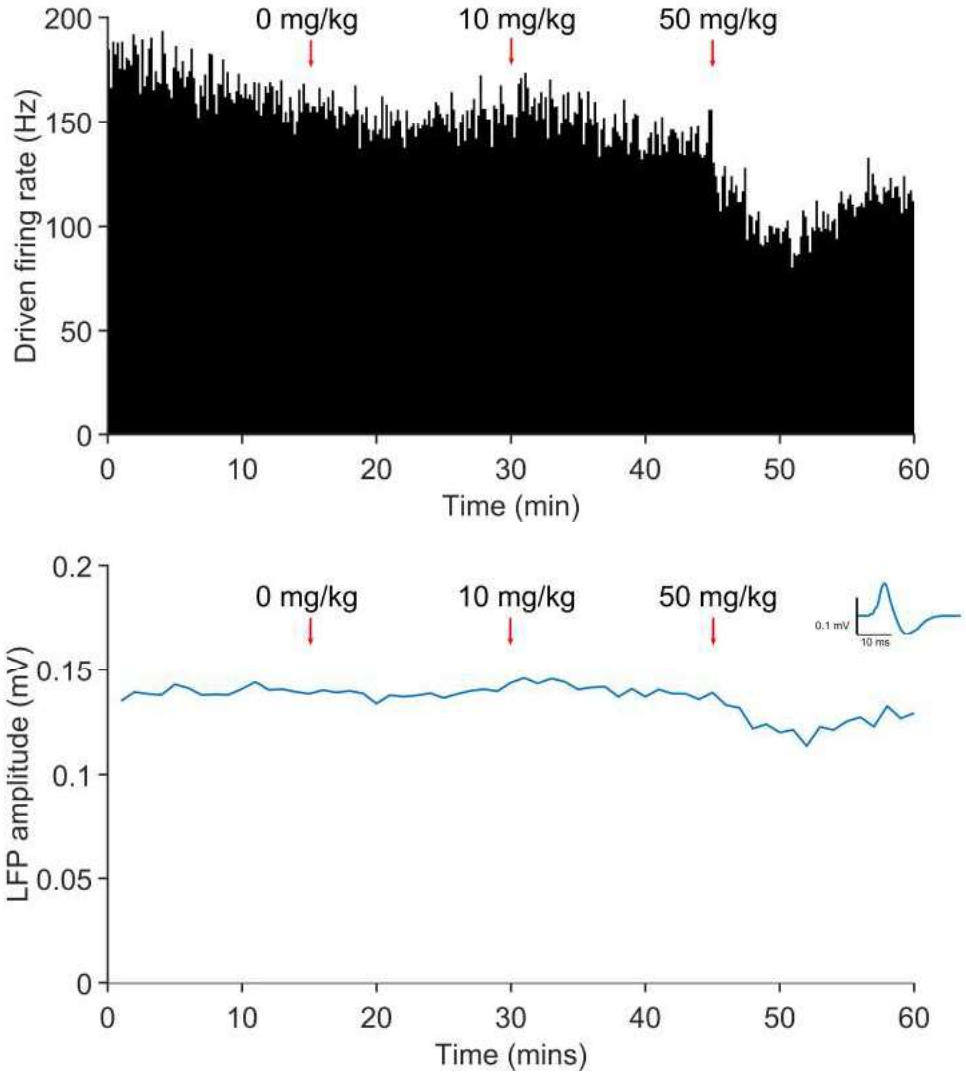


Fig. 5.2: Representative changes in activity of the unit in Fig 5.1 during systemic 7-NI administration. Top: A spike rate histogram of the single-unit driven firing rate (bin size = 10 s). Bottom: LFP amplitude (peak-to-peak) over the recording period. A decrease in spike rate and LFP amplitude is observed after 7-NI administration.

Overall, 3/37 (8%) units showed decreased firing rates in response to 50 mg/kg 7-NI administration, with LFP recordings from these 3 electrodes also showing reduced amplitudes. The three units to respond were 2 primary-likes and 1 chopper. No LFP amplitude changes were seen without single unit firing rate changes. LFP amplitude correlated well with single-unit activity, but was much more variable, possibly due to it being affected by neural activity from surrounding neurons. Therefore, single-unit activity was used for the following studies.

5.3 NOS inhibition in the cochlear nucleus increases VCN activity

Microdialysis allowed application of drugs to the area medial to the VCN, from where they would diffuse and have effect within the VCN. For the microdialysis experiments, methods were as explained in *Section 2.5.5* with BBN stimuli at a range of levels. 300 μM L-NAME was applied for 45 minutes during a 2 hour recording. Reverse microdialysis of the NOS inhibitor L-NAME was tested in 5 male animals, producing a total of 15 recording periods. There was therefore a total of 60 separate recording sites, as 4 tungsten electrodes were used simultaneously. Of these 60 recording sites, single units were recorded at 37 positions (62%). These 37 units consisted of 19 choppers, 13 primary-like, 1 phase-locked, 1 onset and 3 unclassified. The auditory stimuli were a 50 ms BBN burst every 200 ms at 10 different levels (30-120 dB SPL, 10 dB steps) randomly interleaved, creating a total sweep length of 2 s. This allowed plotting of the spike rate over time for each sound level, and production of a rate level function before, during and after drug application (10-30, 70-90 and 100-120 mins respectively). Spontaneous data was not recorded, however the 30 dB condition never produced any visible response, so was assumed to be spontaneous activity (Fig 5.3).

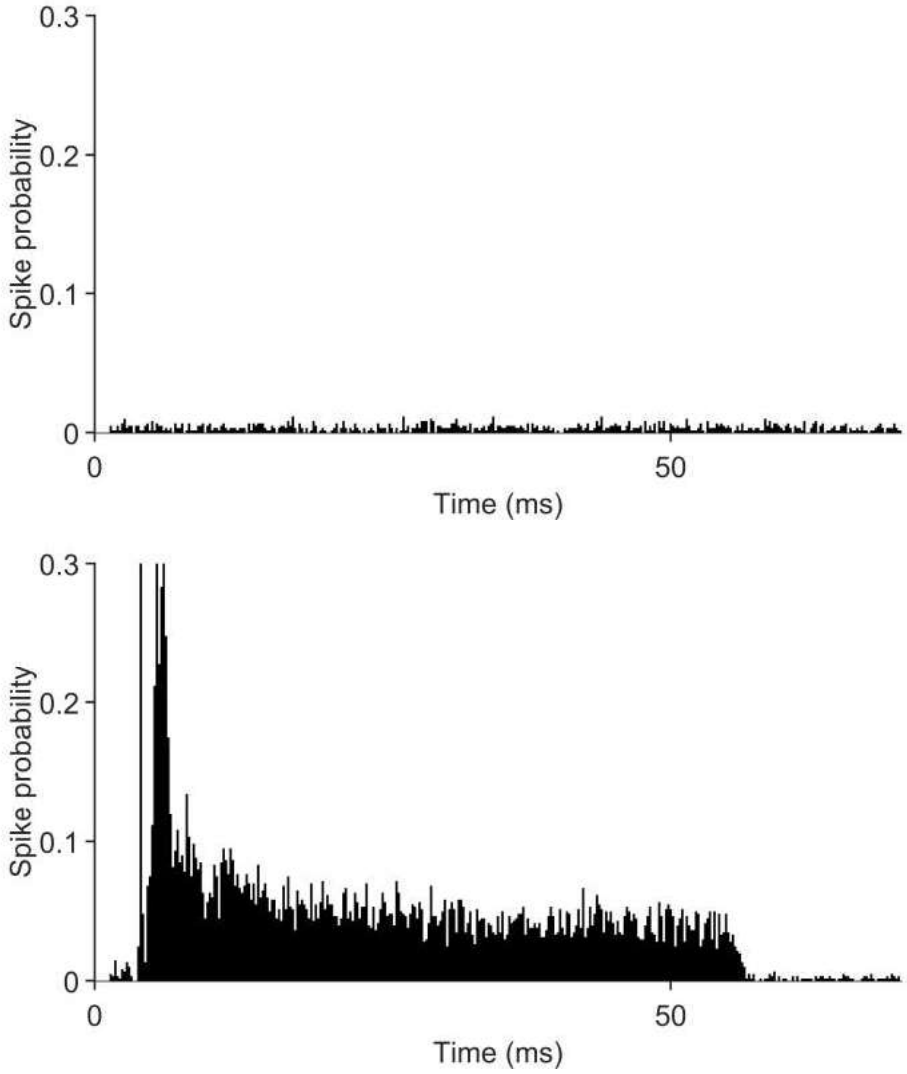


Fig. 5.3: PSTHs of a VCN unit in response to a 50 ms BBN of either 30 dB (top) or 120 dB (bottom). 300 repeats over 10 minutes. Responses in the 30 dB condition was assumed to be spontaneous data.

Analysis of the spike rate for each sound level over the 2 hour recording period showed increases in firing rate during L-NAME reverse microdialysis (Fig 5.4). Analysis of the rate-level function for this unit showed that increases in firing rate occurred at all sound levels (Fig 5.5).

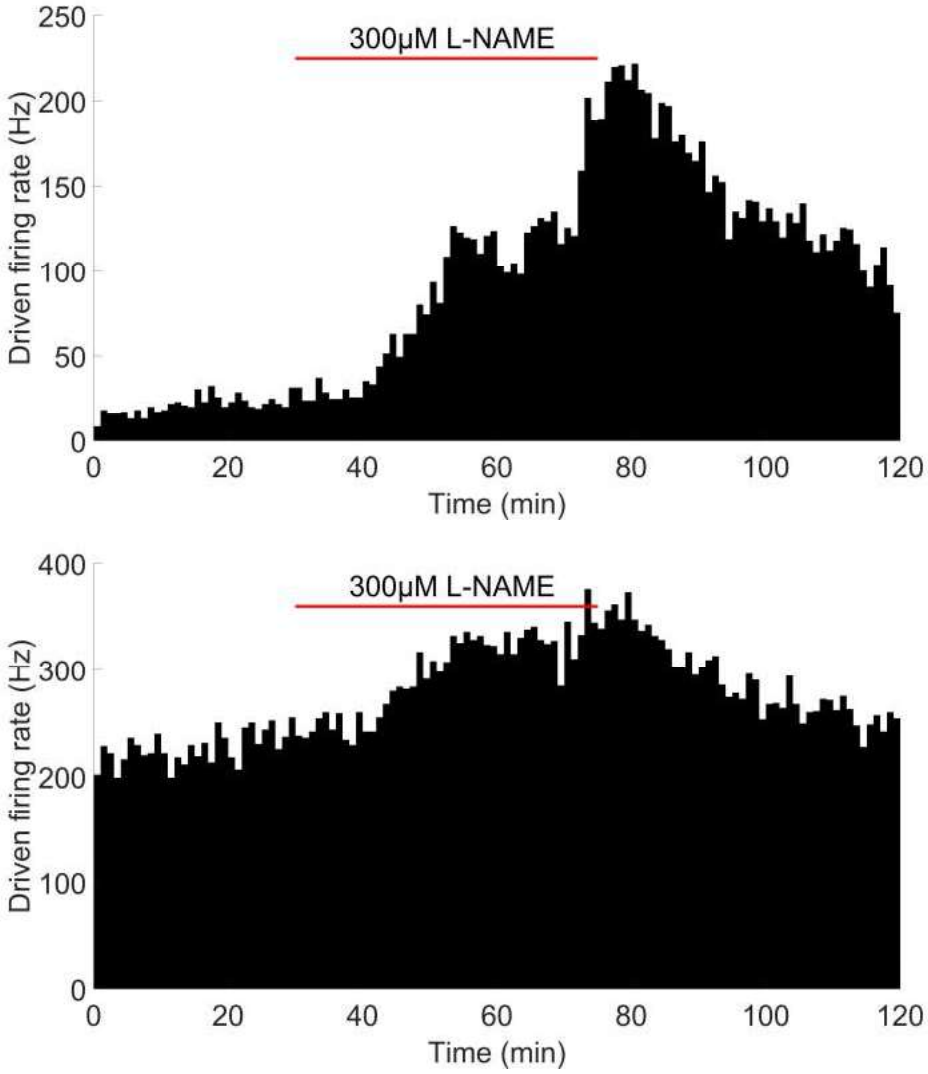


Fig. 5.4: Spike rate histograms over 2 hours for the unit from Fig 5.3, for the two extremes of sound level: 30 dB and 120 dB (top and bottom respectively). The 45 minute period of 300 μM L-NAME reverse microdialysis is indicated by the red bar.

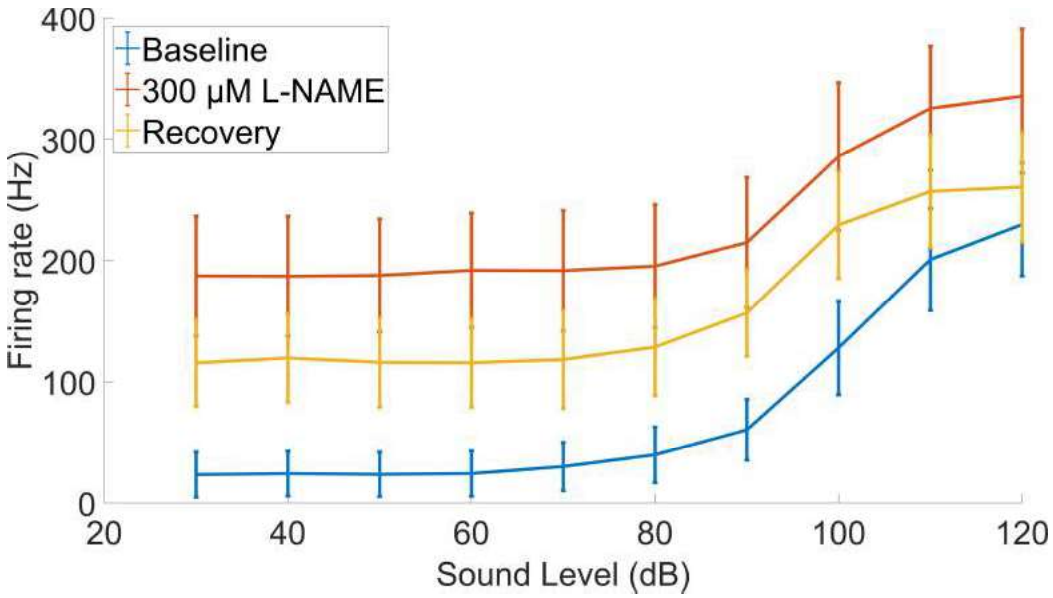


Fig. 5.5: Rate level functions for the unit in Fig 5.3 and Fig 5.4 for each analysis period (baseline, L-NAME and recovery). This shows the mean +/- s.d. firing rate at each sound level for each analysis period.

Overall, 2/37 units (5%) showed an increase in firing rate during reverse microdialysis of L-NAME, and in both cases, this was observed throughout the range of sound levels. These two units consisted of 1 primary-like and 1 chopper unit.

5.4 Global nNOS inhibition improves GPIAS of some animals with impaired GPIAS

Some guinea pigs did not show GPIAS before noise exposure. These guinea pigs with impaired GPIAS were not noise exposed, and the effect of 7-NI on their GPIAS was tested. On two consecutive days, a 30 mg/kg dose of 7-NI was administered i.p., with behavioural testing between 30-60 minutes post-injection.

Approximately 20% of healthy animals did not show significant GPIAS, despite having a pinna reflex. It was therefore hypothesised that these animals may have tinnitus. The effect of global nNOS inhibition on the GPIAS of these animals was tested, by administration of 7-NI followed by tinnitus behavioural testing.

Fig 5.6 shows the GPIAS of two animals during the baseline recording period and after 7-NI injection. For these two animals, 7-NI increased their GPIAS at a certain frequency, suggesting that nNOS inhibition increases gap salience, suggesting it is reducing the tinnitus percept.

The baseline data was compared to the 7-NI data using a 2-way ANOVAs with Bonferroni's multiple comparison test. If a significant decrease in the gap/no gap ratio was seen, the 7-NI was deemed to have improved the tinnitus at this frequency.

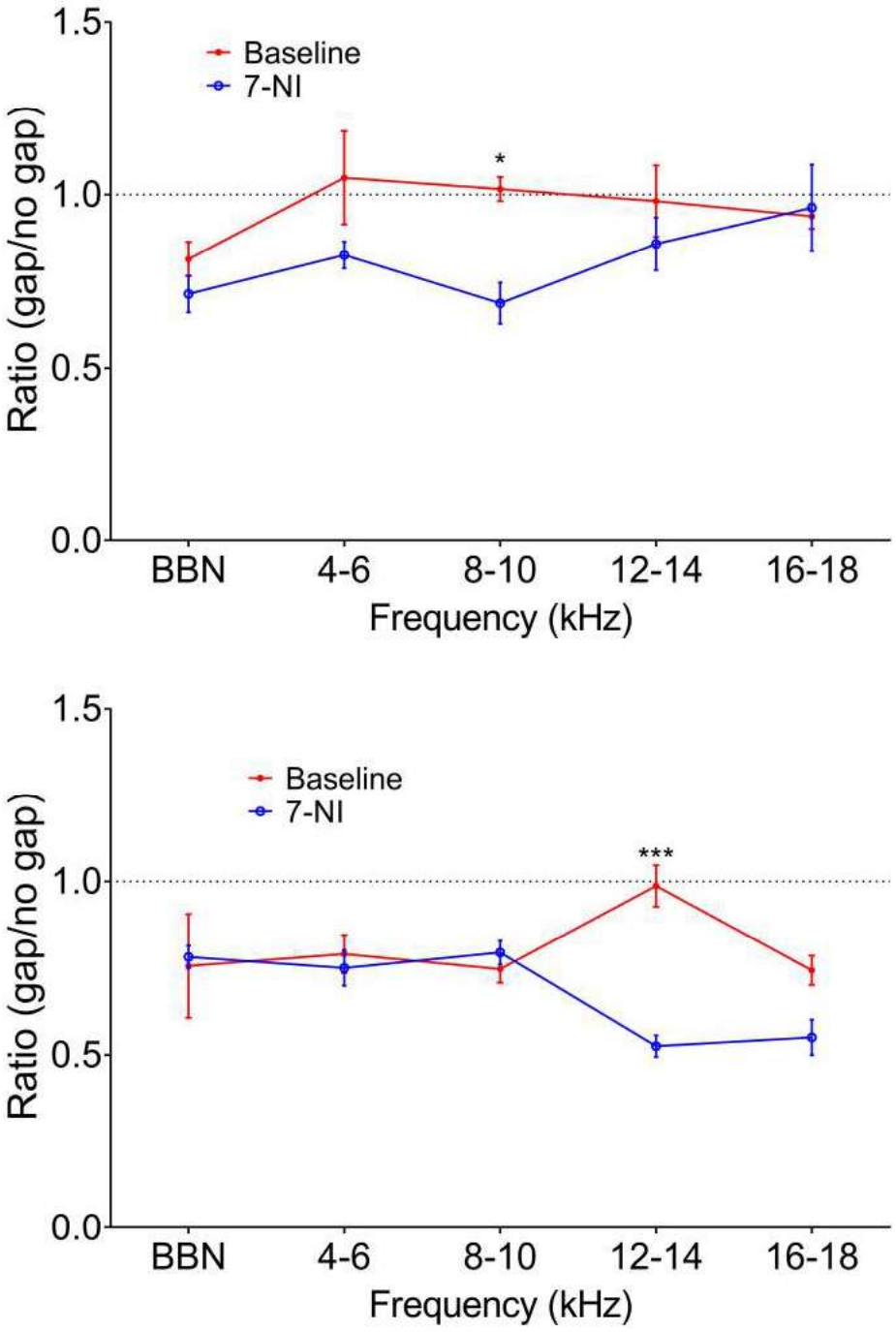


Fig. 5.6: The ratio of gap/no gap startle amplitudes at each frequency for baseline and after 7-NI, for two animals with impaired GPIAS. Plotted is mean +/- SEM, with stars indicating significance. Each demonstrate significantly improved GPIAS and one test frequency.

The effect of 7-NI on GPIAS was tested on 10 animals (6 female, 4 male), with two showing significant increases in GPIAS at one frequency. The remaining 8 animals showed no changes in GPIAS. Fig 5.7 shows the mean

ratio of gap/no gap startles across the 10 animals. The baseline GPIAS is impaired, as the gap/no gap ratio is close to 1 in the baseline condition, and there is no significant change to this following 7-NI injection.

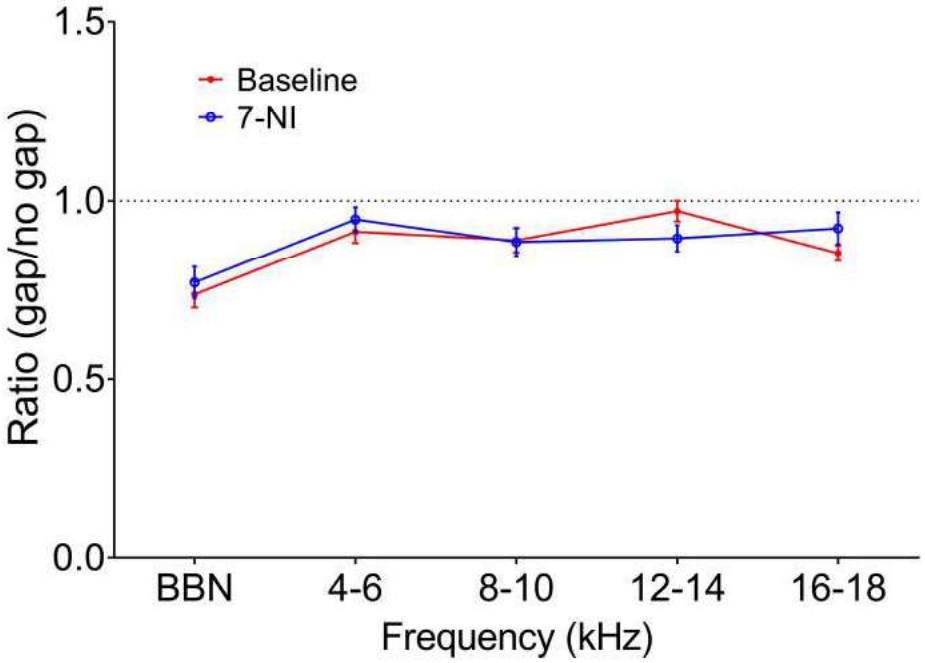


Fig. 5.7: Mean +/- SEM gap/no gap startle ratio for 10 guinea pigs with impaired GPIAS. 7-NI does not improve the GPIAS of animals when looking at the population level.

CHAPTER 6

General discussion

6.1 Nitric oxide function in the cochlear nucleus

My first results chapter focussed on the function of nitric oxide in the VCN of healthy guinea pigs. This section will review the results obtained and conclude the effect that nitrergic modulation has on VCN neural activity.

6.1.1 Exogenous NO application

Application of the NO donor SIN-1 resulted in 5/25 (20%) neurons increasing their DFR, with just 4% showing a decrease in SFR during SIN-1 application. That SIN-1 had an effect in a greater proportion of units during auditory driving demonstrates that sensitivity to NO is increased in higher-activity states. The fact that the NO increased DFR but decreased SFR shows that NO can have the opposite effects depending on the activation level of the neuron.

The differing action of NO during auditory-driven and spontaneous states must be due to the difference in firing rates. During auditory input the firing rate is higher - likely increasing endogenous nitric oxide production. This is mediated by activation of NMDA receptors, which, when activated, allow post-synaptic Ca^{2+} influx, resulting in activation of NOS (Alderton et al., 2001). Increased NO levels above those seen normally may result in other effects of NO occurring, such as S-nitrosylation, that occurs at higher concentrations of NO (Ahern et al., 2002).

In the present experiments, a greater effect of NO donors on spontaneous activity was expected, due to the lower level of activity likely producing

a lower concentration of endogenous NO. It was therefore hypothesised that there would be a greater potential for action due to the reduced endogenous effect. This was not observed, suggesting an increased sensitivity to NO at higher activity levels.

There are slight differences between SIN-1 and SNOG and how they liberate NO, which may underlie their difference in action in these experiments. The release of NO from SIN-1 occurs in two steps, the first of which can involve formation of SNOG, which then goes on to further release NO (Schrammel et al., 1998). This may have resulted in a slower, more gradual release of NO from SIN-1 compared to SNOG. The NO release from the donor molecules was assumed but never tested in my experiments.

6.1.2 NOS inhibition overview

Blocking of NO production by NOS inhibition with L-NAME produced a significant increase or decrease in either SFR or DFR in 7/22 (32%) units, demonstrating that endogenous NO controls firing rates in the VCN. That NO has an endogenous role in the VCN was hypothesised as NOS is localised in this area (Coomber et al., 2014), found in all cell types (Coomber et al., 2015), and is a neuromodulator (Steinert et al., 2008). That only a proportion of cells respond to NOS inhibition also may be due to the localisation of NOS, as it is present in only a sub-population of all cell types in the VCN (Coomber et al., 2015). Sensitivity to NO was found in a variety of cell types and did not appear to be cell type specific. This indicates that NO has a role of modulating neuronal excitability of a sub-population of each cell type in the guinea pig VCN.

It also appears from Fig 3.10 that L-NAME exerts differing effects on driven and spontaneous firing rates. Driven and spontaneous activity was therefore analysed separately, with driven data also compared to data collected during exogenous neuronal activation with NMDA application.

6.1.3 NOS inhibition during low-activity states

In the VCN, iontophoretic L-NAME application affects spontaneous rate with a ≈50:50 increase to decrease ratio (Fig 3.10). This variable effect on spontaneous activity suggests that in these lower activity states NO is modulating units bidirectionally to maintain ”correct” activity levels and therefore maintain firing rates within the dynamic range of each neuron. In

other systems, NO has been shown to increase and decrease spontaneous rates (Clasadonte et al., 2008; Kim et al., 2004a; Podda et al., 2004), so the variable effect seen here is not unexpected. However, this observation is based on the data from 4 cells, so may require further experimentation to determine a reliable effect.

6.1.4 NOS inhibition during high-activity states

During a higher activity state, with greater input from the auditory nerve, iontophoretic L-NAME application increases spike rate in a subgroup of units (18%) (Fig 3.10). Increases in this auditory-driven firing rate following NOS inhibition suggest that during these higher activity states NO reduces excitability.

Use of NMDA to stimulate units showed NMDA-evoked excitation in 47% of units, and with 40% of these units, NOS inhibition enhanced the excitation induced by NMDA on spontaneous activity (Fig 3.14). This corroborates data involving auditory input, by confirming an inhibitory effect of NO during a high excitation state, in this case NMDA-evoked excitation as opposed to auditory nerve input.

Current flow through NMDA channels is voltage dependent, with depolarisation of the cell required to remove the magnesium block. Then, activation of the NMDA receptor by endogenous glutamate or exogenous NMDA, in the presence of glycine, allows a postsynaptic calcium ion influx, resulting in depolarisation and excitation (Purves et al., 2012). Since Ca^{2+} is an activator of NOS, this would result in a tight signalling pathway between the two with higher activity increasing NO production (Alderton et al., 2001). Due to this signalling pathway between NMDA and NOS, the two molecules can be found bound at the postsynaptic density by PSD95, allowing Ca^{2+} influxes to immediately activate NOS (Sattler et al., 1999). These increases in firing rate following NOS inhibition suggest that during higher activity states, when NO concentration is higher due to NMDA activation, it is endogenously reducing excitability.

Due to the link between excitation and increased NO, it appears that in a subgroup of neurons in the VCN, increased NO production during greater activation is producing a regulatory effect on excitation, as has been seen previously in the striatum and substantia gelatinosa (Galati et al., 2008; Park et al., 2014). This plasticity appears to be activity dependent, not over

the neuron population studied, but for each individual neuron compared to its activity history. NO is therefore producing activity-dependent inhibitory modulation which controls excitation. This is a homeostatic plasticity effect which is maintaining stability, potentially to prevent runaway LTP (Watt & Desai, 2010).

6.1.5 Potential mechanisms of NO action

The contribution of NO to synaptic plasticity is well documented (Hardingham et al., 2013). The concentration of NO is likely to be altered by activity levels, and differences in NO function with concentration also occur, with NO capable of increasing or decreasing NMDA receptor currents at different concentrations (Chen et al., 2017; Neitz et al., 2014). The many functions of NO result in bidirectional modulation that appears to be unit-specific, with depolarisation resulting from low NO levels and hyperpolarisation resulting from increased NO levels (Park et al., 2014). This contributes to maintaining the balance of excitation and inhibition, in order to maintain correct neural coding (Le Roux et al., 2009).

As the half-life of NO in the brain is generally thought to be in the region of 10-1000 ms (Reviewed by Santos et al., 2012), it was possible for the NO-mediated inhibition observed in this study to be either a short-term (produced and showing an effect during each stimulus) or tonic effect (building up over the course of multiple stimuli). PSTH comparisons before and during L-NAME application showed that changes in rate were throughout the length of the 200 ms stimulus, suggesting tonic activity of NO over seconds to minutes (Fig 3.11).

As the results were mirrored using exogenous NMDA for excitation, the inhibitory effect of NO in the VCN must be at least partially post-synaptic, either altering the synaptic strength or excitability. Also, a greater proportion of units were affected by L-NAME during NMDA evoked excitation than auditory driving, likely due to the higher rates of excitation produced by NMDA than the auditory input at only 20 dB above threshold, suggesting that the effect of NO is greater at higher activity levels.

NO acts either directly or indirectly at many ion channels, such as cyclic nucleotide gated channels (CNGC), hyperpolarisation-activated cyclic nucleotide gated (HCN) channels, Na^+ and K^+ ion channels (Ahern et al., 2002; Jonas & Kaczmarek, 1996; Kopp-Scheinpflug et al., 2015; Light et

al., 1990). These interactions combine to give nitric oxide the property of controlling excitation (Artinian et al., 2010; Pehl & Schmid, 1997; Steinert et al., 2011), however from my experiments it was not possible to specify which mechanisms NO was acting by. One possible mechanism is via modulation of K^+ channels, considering that potassium channels regulate the excitability of VCN neurons (Cao et al., 2007; Rothman & Manis, 2003).

Other data that suggests that K^+ channels may alter excitability in the VCN comes from the MNTB. Here, slice work has shown that, at the calyx of Held, activity-dependent release of NO acts postsynaptically to alter excitability and synaptic strength (Steinert et al., 2008). Postsynaptic excitability has also been shown to be modulated by glutamatergic synaptic activity, via a NO-dependent mechanism which switches action potential repolarisation from predominantly Kv3, to Kv2 potassium channels (Steinert et al., 2011). This mechanism is capable of adjusting neurons between high and low activity states.

The NO mediated plasticity observed in my experiments was elicited by non-traumatic stimuli, and may therefore contribute to plastic effects previously observed in the VCN over a longer time course (Rees et al., 1985), contributing to central gain control.

6.1.6 Implications

Despite NO's role of controlling excitability in the VCN, the mechanisms mediating the effect are still unclear due to the many possible pathways that NO can influence simultaneously. The activity-dependent homeostatic modulation observed in this study suggests that pathologies such as age-related hearing loss or ototoxic damage, which alter auditory nerve input to the VCN, may affect cochlear nucleus NO production and function. Due to the upregulation in NOS expression in the VCN following a variety of pathological models, higher levels of NO would be present. This increased level of NO likely affects activity in the VCN in these pathological states, but whether this is in a compensatory or pathological manner is yet to be determined. Either outcome would provide an interesting avenue of research for pharmacological treatment of auditory disorders.

6.2 Nitric oxide changes following noise exposure and the development of tinnitus

My second results chapter repeated some of the experiments from *Chapter 3*, but in noise exposed animals, some of which showed behavioural evidence of tinnitus. This allowed comparison of NO function in healthy, noise exposed non-tinnitus and noise exposed tinnitus guinea pigs.

6.2.1 Noise exposure induced changes in the VCN

Noise exposure produces hyperactivity in VCN slices immediately after acoustic overexposure (AOE) (Gröschel et al., 2014). Changes have been also shown in the VCN *in vivo* following cochlear trauma, with hyperactivity occurring as a result of intense AOE or mechanical lesion (Vogler et al., 2011). A further study showed that this VCN hyperactivity was due to increased activity in primary-like and onset neurons (Robertston et al., 2013). They also showed that this hyperactivity increase occurs between 1 and 2 weeks post-AOE, and is preserved for up to 12 weeks. These experiments used a 10 kHz pure tone at 124 dB SPL for 2 hours.

My noise exposure protocol produced threshold shifts which did not fully recover, with ABRs showing increased thresholds and decreased suprathreshold amplitudes. This indicates cochlear neuropathy occurred, which preferentially affects the low spontaneous rate, high threshold fibres of the auditory nerve (HT ANFs) (Furman et al., 2013). This can result in a ”hidden hearing loss”, in which damage to the cochlea results in a normal audiogram, but impaired suprathreshold hearing (Kujawa & Liberman, 2009).

I used louder noise exposure stimuli than used in hidden hearing loss experiments, at 110 dB SPL compared to the 106 dB SPL capable of causing cochlear neuropathy (Furman et al., 2013), although my noise exposure was for 1 hour as opposed to 2 hours used by Furman et al. Using this protocol, I observed threshold shifts alongside suprathreshold ABR amplitude decreases. Hearing loss is often accompanied by tinnitus, however the dependence of tinnitus on hearing loss in unknown. Classical studies measuring the audiogram showed hearing deficits in approximately 90% of tinnitus patients (Reed, 1960), however, more recently this idea has been challenged (Barnea et al., 1990). The hearing loss produced in

my experiments is not a hidden hearing loss, but an overt hearing loss, with still likely more synaptopathy occurring at HT ANF synapses.

In the present experiments, following noise-exposure the driven firing rates in the VCN of animals without tinnitus was significantly lower than the animals with tinnitus. This difference appeared to be a reduction from control levels in non-tinnitus animals rather than an increase from controls in tinnitus animals. This suggested that the noise exposure was sufficient to decrease driven firing rates, however in tinnitus a compensatory mechanism is returning the driven firing rates to mean values. A small decrease in spontaneous rates was also produced by the AOE (Fig 4.5). This is consistent with a cochlear synaptopathy which affects HT ANFs and LT ANFs, but with a greater effect at the HT ANFs, which are known to be more susceptible (Furman et al., 2013).

6.2.2 The changing nitric oxide function with AOE and tinnitus

In the healthy guinea pig VCN I showed that in a subgroup of neurons, during activation by auditory nerve input or NMDA application, the likely increased levels of nitric oxide produce a regulatory effect on excitation. This activity dependent inhibitory modulation acts to control excitation and return firing rates toward long term mean firing levels. The activity-dependent modulation observed suggests that pathologies such as hearing loss, which alter auditory nerve input to the VCN, may affect NO production and function.

Fig 4.10 demonstrated an increase in both the proportion of units increasing and decreasing their spontaneous firing rate in response to SIN-1 following noise exposure (0% to 22%, and 4% to 14% respectively). That noise exposure resulted in a greater proportion of units responding to NO demonstrated that noise exposure increases sensitivity to NO. A large increase in the capability of NO to increase excitation occurred in noise-exposed animals. During auditory input however, noise exposure and behavioural tinnitus confirmation do not alter the effect of SIN-1 on the driven firing rates.

Differing effects of NO during different activity levels in the tinnitus VCN were shown in Fig 4.8, displaying a within-unit activity-dependent effect. One possible mechanism for this activity-dependence is a synapse-specific

effect of NO. The VCN receives input from HT ANFs and LT ANFs. LT ANFs provide the spontaneous input to the VCN, therefore if NO reduced the strength of the synapses of these fibres onto VCN neurons it would reduce spontaneous activity. This would also reduce driven firing rate, however if synapses from HT ANFs were strengthened this could offset the reduction in driven firing rate and cause an increase. This is the first evidence for a synapse-specific effect of NO in the tinnitus VCN.

Due to the upregulation in NOS expression in the VCN of tinnitus animals (Coomber et al., 2014), greater levels of NO are possible, dependent on the availability of arginine and the concentration of intracellular Ca^{2+}. My data using a NOS inhibitor suggests that the increased level of NO affects activity in the VCN during tinnitus, producing an increased gain within the VCN. I showed that tinnitus is associated with a significantly greater proportion of neurons decreasing their driven firing rate in response to NOS inhibition (Fig 4.12), with this change correlating with the strength of behavioural evidence of tinnitus (Fig 4.13). Therefore, in tinnitus animals, it appears the increased NO produces a different function to that in control animals, increasing excitability during auditory input in a proportion of neurons. This could produce an increase in transmission with potential to contribute to the ”increased central gain” thought to be present in tinnitus animals (Auerbach et al., 2014; Noreña, 2011).

However, no increases to driven firing rates compared to the normal VCN were observed in the VCN in tinnitus animals (Fig 4.5), suggesting that this gain is returning firing rates to long term mean levels. This is therefore compensating either for a decreased driven rate in the auditory nerve or an alternative mechanism decreasing excitability in the VCN in tinnitus animals. The following subsection attempts to relate the excitability changes observed in the VCN to estimated auditory nerve input and VCN activity, to create a clear picture of the role of NO in the tinnitus VCN.

6.2.3 A maladaptive hearing loss compensation

The HT ANFs, which are preferentially affected, control the driven rate of VCN neurons at high sound levels, with the spontaneous rate set by the high spontaneous rate, low threshold auditory nerve fibres (LT ANFs) (Koerber et al., 1966). The present experiments showed significantly decreased driven rates in non-tinnitus animals compared to tinnitus animals, which appeared

to be due to a decrease from controls in non-tinnitus animals. This suggests that damage to the HT ANFs ocurred as a result of the noise exposure. Therefore, the NO-mediated increased gain observed during driven activity in tinnitus animals appears to be compensating for the reduced auditory input resulting from cochlear synaptopathy.

The LT ANFs which control spontaneous rates would not be expected to be as affected by the acoustic overexposure used (Furman et al., 2013), and only a marginal decrease in mean spontaneous rates were produced by noise exposure (26.96 to 22.93 Hz) (Fig 4.5). During tinnitus, an increase (from 9% to 26%) in the proportion of units decreasing their spontaneous firing rate during NOS inhibition was observed, demonstrating NO-mediated excitability increases in tinnitus animals. This may underlie the increase in spontaneous rate that was observed across my unit sample, with mean spontaneous firing rates in tinnitus animals of 36.56 Hz (Fig 4.5). These data therefore point to increased spontaneous rates within the VCN resulting from increased gain within the VCN, mediated by NO.

Therefore, it seems most likely that, in tinnitus animals, the reduced auditory input following noise exposure produces a compensatory increase in NO production. The increased levels of NO increase synaptic strength and return driven VCN activity toward, and above, the levels observed in control animals. This also has a partial effect on spontaneous firing rates, increasing them significantly (Fig 6.1). This maladaptive homeostatic plasticity possibly acts as the first step in a system of increased gain capable of producing tinnitus perception. That a greater gain effect was observed on driven activity, with activity in tinnitus animals higher than that of controls, points to a hyperacusis effect, which has a high co-morbidity with tinnitus (Roberts, 2018).

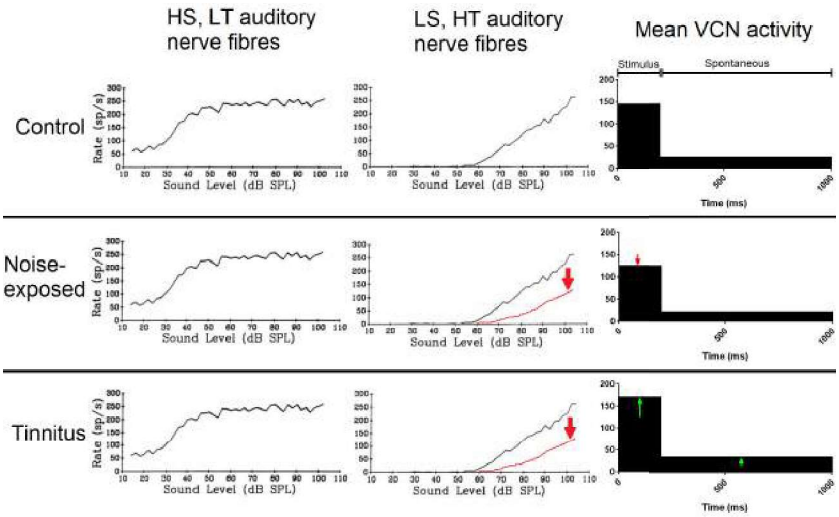


Fig. 6.1: How NO compensates for changes in auditory nerve activity following noise exposure. Centre and left columns display typical auditory nerve activity (Winter & Palmer, 1991). Cochlear neuropathy selectively affects low spontaneous rate, high threshold auditory nerve fibres (centre column, red arrows and lines). Right column shows mean VCN activity from my study. Reduced auditory nerve activity reduces driven activity in the VCN (centre right, red arrow). To compensate for reduced input, NO-mediated gain returns driven activity toward (and above) mean levels, while also pathologically increasing spontaneous activity (bottom right, green arrows). HS, LT = high spontaneous rate low threshold auditory nerve fibres; LS, HT = low spontaneous rate high threshold auditory nerve fibres.

Previously I showed evidence for a NO-mediated strengthening of synapses conveying driven activity and a simultaneous NO-mediated weakening of synapses transmitting spontaneous information. Here I am suggesting that in tinnitus animals, there is a population effect of increased gain at synapses from each type of auditory nerve fibre, returning auditory driven activity towards long term mean levels, while pathologically increasing spontaneous rates.

This supports the homeostatic plasticity mechanisms long suggested (Auerbach et al., 2014; Noreña, 2013; Schaette & Kempter, 2006; Schaette & Kempter, 2008; Schaette & McAlpine, 2011; Schaette & Kempter, 2012), whereby brainstem gain returns mean firing rates to long-term mean values, while simultaneously pathologically increasing spontaneous firing rates.

6.2.4 NO mechanisms in the tinnitus VCN

The results with auditory input were not matched with NMDA-evoked excitation, where NO-mediated excitability increases were seen in both noise-exposed groups (Fig 4.15). NMDA receptors have been shown in the VCN (Chen et al., 2004; Watanabe et al., 1994), and their presence is likely the main cause of Ca^{2+} influx, resulting in NOS activation. The differing results with auditory input and NMDA application may be due to differing pre and post-synaptic effects in tinnitus and non-tinnitus animals. Any pre-synaptic effect of NO would not affect firing rates when using exogenously applied NMDA, as we are directly applying the neurotransmitter and bypassing any presynaptic effect. Therefore, it seems from these data that noise exposure induces post-synaptic changes to NO function, increasing excitability. However, the pre-synaptic effects of NO only occur in tinnitus animals, increasing glutamate release.

Despite NOs role of controlling excitability in the VCN, and its changing role in tinnitus, the mechanisms mediating the effect are still unclear. Nitric oxide exerts its effect through many pathways simultaneously, and future experiments may elucidate this further. It appears from the SIN-1 data that noise exposure increases the sensitivity of the VCN to NO, however the L-NAME data showed that only in the tinnitus VCN is NO-mediated gain present. This may be due to the likely higher levels of NO in the tinnitus VCN (Coomber et al., 2014). The data using NMDA suggested that the effect is at least partially post-synaptic, so it appears that noise exposure is producing post-synaptic changes in the VCN, sensitising it to NO. NO is then increased in some animals, producing gain which contributes to a tinnitus percept.

6.3 Could nitric oxide-modulating drugs be used therapeutically?

Chapter 5 focussed on application of NO-modulating drugs outside of the cochlear nucleus, and the effect of these on processing within the cochlear nucleus and behavioural measures of tinnitus. NOS inhibitors applied either systemically or by microdialysis just medial to the cochlear nucleus both showed an effect within the cochlear nucleus. However, this was only in a low proportion of neurons, 3/37 (8%) and 2/37 (5%), respectively. Also, the opposite effects were observed with each application method, with systemic application producing decreased firing rates and microdialysis application increasing firing rates. Different NOS inhibitors were used in each to suit the methodology, however they have a very similar efficacy at each of the NOS isoforms, so the action would be likely to be similar. Therefore, I believe that differences between the two must be due to the area applied. When applied by microdialysis the vast majority of the drug action would be expected within the cochlear nucleus, however, when applied systemically it would act throughout the auditory system, from the cochlea, auditory nerve, cochlear nucleus and higher centres. The cochlea and auditory nerve are part of the peripheral nervous system, meaning the NOS inhibitor did not need to cross the blood brain barrier to act there. Therefore, a greater action of NO may be occurring in the cochlea and auditory nerve. The cochlea contains eNOS and nNOS (Fessenden & Schacht, 1998; Franz et al., 1996), making it a likely target for systemically applied NOS inhibitors.

Microdialysis of a NOS inhibitor onto the CN increased firing rates throughout the range of sound levels in 8% of units. This difference compared to local single-unit NOS inhibitor application may be due to inhibition of NOS over a larger area, or the difference in auditory stimuli used, with BBN used in these experiments compared to the pure tones used previously. The opposite was observed with systemic NOS inhibition, with my data showing reduced VCN activity. This may be due to other central effects, or possibly a reduction in cochlea activity.

Following on from this, the effect of systemic NOS inhibition on our behavioural measure of tinnitus (GPIAS) was assessed. In guinea pigs

with naturally impaired GPIAS I showed an improved GPIAS following NOS inhibition in 2/10 animals (20%).

Prepulse inhibition (PPI) is a phenomenon where a small stimulus placed before a larger stimulus reduces a physiological response to the larger stimulus. This occurs in response to auditory, somatosensory and visual stimuli. PPI is altered in synchrony with GPIAS in a rat salicylate model of tinnitus (Turner & Parrish, 2008), however, following noise exposure mice do not show changes in PPI, while they do show deficits in GPIAS (Turner et al., 2012).

NOS inhibition can improve PPI in rats with low PPI (Issy et al., 2011) and improve PPI of mice (Issy et al., 2014), with the research showing this is via modulation of the catecholamine system, affecting the sensorimotor gating system. This suggests that NO-mediated modulation of startle responses can occur.

Therefore, my data are not unequivocally a purely sensory effect, as changes observed after NOS inhibitor application may be due to changes in the modulation of the motor pathways of the acoustic startle reflex. However, previous data showing NO-mediated modulation of the acoustic startle did not measure GPIAS, which may have shown differences to PPI. In the future, conducting PPI and GPIAS tests in animals with impaired GPIAS/PPI could determine whether the impairment is due to sensorimotor gating disfunction or a possible tinnitus.

6.4 Are changes to firing rate in the VCN following noise exposure and tinnitus frequency specific?

Hyperactivity in the VCN has been shown not to correlate with cochlear compound action potential threshold changes after cochlea trauma, with hyperactivity occurring throughout the frequency spectrum (Robertston et al., 2013). In the IC, however, following cochlear trauma at a certain frequency band of the cochlea, hyperactivity correlates with this damaged frequency (Robertston et al., 2013). This neuronal hyperactivity in the IC has also been demonstrated to not be correlated with behavioural evidence of tinnitus, occurring throughout the frequency spectrum (Coomber et al., 2014). It is therefore unclear how IC hyperactivity relates to tinnitus, and even fewer studies relating VCN hyperactivity to tinnitus have been conducted. It is not known if hyperactivity in the VCN relates to tinnitus, with all previous studies of VCN hyperactivity focussing on cochlear trauma, with no comparisons to behavioural evidence of tinnitus having been made.

My data showed an increase in spontaneous firing rates in the VCN of tinnitus guinea pigs, but not in animals which were noise exposed but did not develop tinnitus. This hyperactivity was not frequency specific, with increases occurring throughout the frequency spectrum (Fig 4.3).

One other question to answer was whether the NO-mediated effect observed is frequency specific, potentially with a preference to the tinnitus frequency identified by the behavioural test used. NOS expression in the rostro-caudal direction in the VCN has a bimodal distribution, and changes with tinnitus occur at the peaks of this distribution (Coomber et al., 2015). Therefore, a frequency specific effect was possible.

Comparison of the frequency of NO-sensitive neurons in the VCN to the frequency at which tinnitus was determined was difficult due to the low sample size. The clearest change to NO function in tinnitus animals was that iontophoretic application of the NOS inhibitor L-NAME in tinnitus animals resulted in a greater proportion of neurons decreasing their driven firing rates. Therefore, this data was used to compare NO function to tinnitus frequency. No correlations were found, with NO-sensitive neurons having characteristic frequencies unrelated to the tinnitus frequency.

As has been shown previously, the methodology I used produces GPIAS deficits at a range of frequencies across the population (Coomber et al., 2014). This can be explained by either of the following 1) the tinnitus frequency produced is highly variable, not at or slightly above the noise exposure frequency used, as would be expected 2) the behavioural measure used to determine tinnitus is not accurate enough to correctly determine tinnitus frequency, and simply determines whether the animal has tinnitus or not.

6.5 Asymmetries in NOS function after noise exposure

One decision to make before starting my experiments was whether to study changes in NO function on the ipsi- or contralateral side to the noise exposure. Coomber et al. (2015) showed an asymmetry in NOS expression in noise-exposed guinea pigs which developed tinnitus. However, their method could not determine whether this was a result of increased NOS ispilateral or decreased NOS contralaterally, due to the variability in number of NOS-positive neurons between guinea pigs. The change is likely ipsilateral, as the peripheral changes are a single synapse from VCN neurons, meaning the peripheral changes would be likely to produce changes within the ipsilateral VCN. However, it would still have been interesting to use my experiments to determine where the change in NOS occurs, by comparing NO function on either side of tinnitus animals compared to controls. This would have been tested if the bilateral multi-electrode recordings paired with systemic NOS inhibitor application experiments had been extended to tinnitus animals, however the control experiments showed limited effect. Also, the long recordings using single channel iontophoresis electrodes required many animals to reach the required sample sizes, which, combined with technical limitations of the lab, meant the ipsilateral vs contralateral hypothesis was never tested.

6.6 Is tinnitus the result of enhanced excitation or reduced inhibition?

The mechanisms underlying central gain are still debated, with the question often posed of whether it is initiated by increased excitation or reduced inhibition.

Decreased inhibitory input has been observed in the dorsal cochlear nucleus of tinnitus mice, in correlation with hyperactivity (Middleton et al., 2011). At the level of the IC, decreased GABAergic transmission is also observed with deafness or tinnitus (Bledsoe et al., 1995; Wang et al., 2011). As high as the auditory cortex, acoustic overexposure induces reductions in inhibitory activity in the frequency band of hearing loss (Yang et al., 2011).

In the VCN, the majority of studies on neurochemical or physiological changes have utilised cochlea trauma or ablation, without looking at any correlations with tinnitus. This can however be useful to consider, as changes following cochlea trauma demonstrate the potential plastic changes which may also occur during tinnitus.

One transmitter system that modulates plasticity and has been identified in the cochlear nucleus is the acetylcholine (ACh) system. The guinea pig cochlear nucleus receives the majority of it's ACh input from the superior olivary complex, suggesting this may act as a feedback loop to control olivocochlear functions (Mellot et al., 2011). The majority of ACh input to the cochlear nucleus is to the DCN, with the remainder to chopper cells of the VCN (Robertson & Mulders, 2018). Noise exposure increases ACh receptor levels in the DCN (Kaltenbach & Zhang, 2006), while also increasing ACh synthesis in the AVCN and DCN (Jin et al., 2006). This is one demonstration of increased plasticity following noise exposure, however the contribution of this to tinnitus is unknown.

Measurement of the VCN postsynaptic density structure is one method for assessing levels of excitation. The postsynaptic density in the VCN is activity-dependent, capable of structural changes within 24 hours (Rees et al., 1985). Auditory deafferentation results in increases to the postsynaptic density of excitatory synapses within the VCN, with potential to increase excitation (Gulley et al., 1977; Redd et al., 2000). Reduced peripheral input, in the form of conductive hearing loss and cochleotomy, has been

shown to increase and redistribute AMPA and NMDA receptor levels in the VCN (Förster & Illing, 1998; Whiting et al., 2009). This increase is reversible, demonstrating the ability of the VCN to alter processing in response to peripheral input.

In the VCN, GAP-43 and NOS expression in neuronal growth cones increase following cochleotomy, demonstrating neural reorganisation (Chen et al., 2004). This synaptic reorganisation also occurs in the VCN after noise exposure, where degeneration of axons and terminals occurs in the first week and remains for 24 weeks (Kim et al., 2004b). Fitting with our time-frame for tinnitus, after 24 week Kim et al. showed axon growth and terminal formation, with excitatory synapses recovering to a greater extent than inhibitory synapses. Another group also showed reduced excitatory and inhibitory synapses following cochlear ablation, with a slow reduction in inhibitory synapses contrasted by a rapid decrease in excitatory synapses (Hildebrandt et al., 2011). This was followed by an increase in excitatory synapses, with no recovery to inhibitory inputs. It is currently unclear if the delayed increase in excitation or the sustained decrease is the pathological aspect, and any relationship to tinnitus development is currently unknown.

These experiments demonstrate that the excitatory pathways in the VCN are plastic, changing strength dependent on input from the periphery. To the best of my knowledge, no studies of tinnitus-correlated changes to the excitatory pathways within the VCN have been conducted. This would be an interesting future direction of study.

6.7 Methodology overview

This section will review the major techniques used throughout this thesis, and determine any changes that could have been made to improve the data collection process or quality of data collected.

6.7.1 Behavioural tinnitus confirmation

I used the gap prepulse inhibition of the acoustic startle (GPIAS) test to confirm tinnitus in guinea pigs. The test used, involving measurement of the Preyer reflex, has been shown to be a more robust measure than the whole body startle, showing less habituation through trials and a higher signal to noise ratio (Berger et al., 2013). Motion tracking of reflective markers glued to the pinna was used to measure the startle, with all data from this thesis recorded using a Vicon system. We have since replaced this dated and expensive system with one consisting of three Optitrack Flex 3 cameras. The replacement system has a lower sampling rate, of 100 Hz, but this is capable of reliable recording of the reflex, which has a duration of 50-100 ms. This has demonstrated a more cost-effective way of motion-tracking to record pinna reflexes.

The GPIAS test does however have some caveats. First, the need to control for hearing loss and hyperacusis, which can occur following noise exposure or administration of ototoxic drugs. Hearing loss can affect the test by reducing the detection of the background sound or the startle, whereas hyperacusis would be expected to increase startle amplitudes. Indeed, decreases in the startle intensity have been observed following noise exposure, potentially indicating hearing loss (Lobarinas et al., 2013) and increased acoustic startle responses following noise exposure have also been observed, consistent which a hyperacusis effect (Chen et al., 2013).

There is also the debate of what GPIAS is really testing. Initially it was hypothesised that tinnitus would 'fill the gap', however animal and human data has shown this likely to be a simplification of the neural mechanisms underlying GPIAS (reviewed by Galazyuk & Hébert, 2015). The mechanisms involved are therefore much more complicated that first thought, meaning the test must be carefully applied to truly show animals with tinnitus and avoid the pitfalls.

For these reasons, the GPIAS test needs to be carefully considered for tinnitus testing in animals, and should utilise cross-validation to confirm the effect. Previous methods have involved rewarding responses of the animal to silence, however this produces the effect that with training animals will learn to respond to silence. However, one recent study has cross-validated an operant conditioning task with GPIAS in tinnitus animals (Martel et al., 2018). Guinea pigs do not train well using positive reinforcement, so shocks were used if an animal did not respond to a sound, with tinnitus animals responding even when no sound is present. The 4 animals used by Martel et al. all showed significant evidence of tinnitus using both measures during salicylate treatment. Cross-validating of models is important to verify their reliability and that they are truly testing for tinnitus. One alternative that is proving increasing popular is a test involving stimulus classification (Jones & May, 2017). This is used to train animals to respond to tinnitus-like sounds, but not respond during alternative sounds. The variability between labs in tinnitus screening methods is currently an issue in tinnitus testing, but as further cross-validating of models is completed, their reliability is being proved. Until a truly accepted tinnitus screening method emerges, results from animal tinnitus studies must be regarded with a slight lack of confidence.

With all tinnitus behavioural screening there is the question of why only a proportion of animals develop tinnitus. This is useful in tinnitus testing, as they provide a negative control, with no changes expected from control animals, however the underlying cause of this needs to be understood. One possibility is that genetic factors increase susceptibility in some animals. Indeed, GPIAS differences have been found between different guinea pig colonies, suggesting a genetic factor (Leggett et al., 2018). If this is the case, knowledge of the genes involved and the relation to human tinnitus may be highly valuable.

6.7.2 Iontophoresis

Iontophoresis allows ejection of small amounts of drug accurately onto single units using electrical current, with the concentration of drug ejected being linearly proportional to the current applied (Hicks, 1984). It was developed in the mid-20th century for use in the neuromuscular junction, and by the 1960's was a widely used technique for assessing the action of drugs at synapses.

One issue with iontophoresis is the difficulty to confirm that drug ejection is onto the neuron isolated by the recording electrode. In my setup, this issue was minimised by gluing of the recording and ejection electrodes close to the tips, to reduce splitting of the tips upon tissue entry (Fig 2.5). Electrodes were examined on removal from the tissue between each track in order to determine if skew had occurred.

Data obtained from my proof of concept experiments demonstrated successful current balancing by our iontophoresis equipment for solutions of varied pH. Also, any current-evoked response would be almost instantaneous, unlike the slower changes we saw from some iontophoretic drug ejections (5-10 mins), further confirming true drug ejection.

All experiments using excitatory neurotransmitters (glutamate and NMDA) produced either increases in firing rate or, rarely, no change in firing rate. This indicates direct activation of the cell from which I was recording. Large stellate cells in the VCN innervate throughout the AVCN, and partially in the PVCN. These are inhibitory neurons, and therefore activating them with glutamate would have reduced the firing rate of surrounding cells to which they projected. No evidence of NMDA or glutamate induced inhibition was observed, suggesting that these inhibitory cells were never activated while recording was made from a different site. This is the best confirmation we achieved to demonstrate drug ejection and recording were occurring at the same unit. Even with drug application to a single neuron, multiple synapses are likely to be affected.

The diffusion distance of compounds in the interstitial space of the brain is variable (Syková & Nicholson, 2008), meaning the volume of tissue affected by my iontophoretically applied drugs was unknown. To test this, a set-up using iontophoresis electrodes with varied distances between the ejection and recording tips could be utilised. This would allow estimation of the distances that the different drugs used would diffuse. This was never tested, as a large number of animals would be required due to the recording lengths and effect rate of the drugs used in these experiments.

6.7.3 Reverse microdialysis

Microdialysis usually involves using a dialysis membrane to extract molecules from the interstitial space for measurement (Chefer et al., 2009; Höcht et al., 2005; Minton et al., 2009). A probe containing a dialysis

membrane is inserted into the tissue of interest, with fluid flowing past the external part of the membrane. Molecules diffuse across the dialysis membrane into this fluid, allowing quantification of a broad range of endogenous compounds. Reverse microdialysis, in comparison, involves using an identical setup but is used to apply drug by diffusion across a membrane (Höcht et al., 2007). This set-up has previously been used in the auditory system at the level of the IC (Orton & Rees, 2014).

I used a 4 tungsten electrode set-up glued to the microdialysis probe. This ensured distance between the probe and the recording electrodes remained constant at $\approx$ 1 mm. This provided a set distance between drug release and recording site. However, the inability to move the microdialysis probe independent of the recording elecrodes did limit the number of tracks that could be made before significant damage was caused to the cochlear nucleus. If the recording electrodes and microdialysis probe had been manipulated separately, the larger microdialysis probe could be left stationary while the smaller tungsten electrodes were moved between recording sites.

One issue with the iontophoresis experiments was the auditory stimuli used. Using the same tone repeated gave two different activity states, driven and spontaneous. This gave precise data, as 3600 recordings were made over the hour. Changes to these stimuli were made for microdialysis experiments to improve the speed and quality of data collected. 10 different sound levels were used to produce rate level functions, allowing assessment of changes to activity in response to different sound levels over time. This also removed the need to record 800 ms of spontaneous data, as the lowest sound level was sufficiently low to not produce driven activity and could therefore be assumed to be spontaneous. It was therefore possible to lower the simulus length to 50 ms and the repeat rate to 200 ms, resulting in 1800 recordings of each stimulus level over an hour-long period. This protocol was used in the microdialysis experiments following on from iontophoresis, and provided more information about the effects occurring at different sound levels.

Data collected from my reverse microdialysis experiments showed limited effect of drugs applied, with only 5% of units responding to NOS inhibitor application. The reasons for this are unclear, with possibilities being the different stimuli used compared to iontophoresis experiments, the different

area affected by the drug, the different auditory stimuli used, or the diffusion distance of the drug (Syková & Nicholson, 2008).

6.8 Conclusions

- These data show an endogenous role of NO in the VCN, modulating excitability in sub-populations of neurons.
- Animals with behavioural evidence of tinnitus display altered NO function, producing a compensatory increase in excitation following hearing loss.
- This increased excitation may be the source of increased spontaneous firing in the tinnitus VCN.
- The NO-mediated increase in transmission has the potential to contribute to the 'increased central gain' thought to be present in tinnitus.

6.9 Future directions

Clinical trials aiming to treat tinnitus with NO related drugs have so far been limited in number and efficacy. These studies have used phosphodiesterase type 5 (PDE5) inhibitors, which by reducing cGMP breakdown are amplifying any effect of NO. PDE2 is present in the cochlear nucleus (Stephenson et al., 2009) and parts of the auditory forebrain, and may be a more effective target for treating tinnitus. A PDE2 inhibitor has already been shown to have an anxiolytic effect (Masood et al., 2009) and so PDE2 inhibitors may have a dual action on the auditory and limbic systems, acting synergistically to treat tinnitus. However, my data suggest that PDE inhibition is the incorrect direction to alter the NO/cGMP pathway, as it increases cGMP concentration (Fig 1.11). Alternatives that decrease cGMP levels such as NOS inhibitors, sGC inhibitors and PDE activators may be more effective in treating tinnitus.

One molecule that may affect NO function in the VCN is asymmetric dimethylarginine (ADMA), an endogenous NOS inhibitor in the circulatory system (De Gennaro Colonna et al., 2009; Sibal et al., 2010). Levels of this inhibitor may alter the production of NO, meaning measurement of NOS protein levels is not an accurate way of assessing NO production.

Further understanding of auditory NO function and its role in tinnitus is required to aid the development of any potential treatments. This will likely come from physiological studies, of which I will suggest some possibilities. In my attempt to study the effect of NOS inhibitors applied to the entire cochlear nucleus, my data during microdialysis showed limited effects. One alternative method that may be used to deliver NO to the VCN involves the release of caged NO using pulses of light from an optic fibre. This photochemical NO release has been previously used *in vitro* (Murphy and Bliss, 1999), but to my knowledge has not yet been attempted *in vivo*. Methodology for chemically caging NO is currently under development (Burks et al., 2013), which may allow the use of this technique in the auditory system. This would allow widespread changes of NO levels in the VCN, as with microdialysis, but would also allow much more rapid alterations in NO concentration. NO release could be turned on and off rapidly, with the short half-life of NO ensuring that shortly after cessation of the light pulse, NO levels would quickly return to baseline. Data collection could then be much more rapid, with the possibility of

using multi-electrodes combined with release of caged NO to streamline experiments.

Changes to excitatory transmission in the VCN in tinnitus still needs to be understood. Changes to NMDA receptor localisation and to the post-synaptic density structure have been studied following cochlear trauma and ablation. However, no changes in tinnitus have been examined. Changes to NMDA receptor densities may occur in tinnitus, and any result would be easier to interpret than nitric oxide changes, as the role of NMDA activation is better understood than NO function. Therefore, I believe this is an area that could help further our knowledge of changes to the VCN in tinnitus.

References

Abraham, W. C. (2008). Metaplasticity: tuning synapses and networks for plasticity. *Nature reviews. Neuroscience*, **9**, 387–399.

Abraham, W. C., Logan, B., Greenwood, J. M., and Dragunow, M. (2002). Induction and experience-dependent consolidation of stable long-term potentiation lasting months in the hippocampus. *The Journal of Neuroscience*, **22**(21), 9626–9634.

Adjamian, P., Sereda, M., Zobay, O., Hall, D. A., and Palmer, A. R. (2012). Neuromagnetic indicators of tinnitus and tinnitus masking in patients with and without hearing loss. *JARO - Journal of the Association for Research in Otolaryngology*, **13**(5), 715–731.

Ahern, G. P., Klyachko, V. A., and Jackson, M. B. (2002). cGMP and S-nitrosylation: Two routes for modulation of neuronal excitability by NO. *Trends in Neurosciences*, **25**(10), 510–517.

Alderton, W. K., Cooper, C. E., and Knowles, R. G. (2001). Nitric oxide synthases: structure, function and inhibition. *Biochemical Journal*, **357**(3), 593.

Alvarado, J. C., Fuentes-Santamaría, V., Gabaldón-Ull, M. C., Jareño-Flores, T., Miller, J. M., and Juiz, J. M. (2016). Noise-Induced "Toughening" Effect in Wistar Rats: Enhanced Auditory Brainstem Responses Are Related to Calretinin and Nitric Oxide Synthase Upregulation. *Frontiers in Neuroanatomy*, **10**(March), 1–24.

Andreski, P., Chilcoat, H., and Breslau, N. (1998). Post-traumatic stress disorder and somatization symptoms: A prospective study. *Psychiatry Research*, **79**(2), 131–138.

Anisman, H., Kelly, O., Hayley, S., Borowski, T., Merali, Z., and McIntyre, D. C. (2000). Acoustic startle and fear-potentiated startle in rats selectively bred for fast and slow kindling rates: Relation to monoamine activity. *European Journal of Neuroscience*, **12**(12), 4405–4416.

Araújo, L. C., Magalhães, T. N., Souza, D. P. M., Yehia, H. C., and Loureiro, M. A. (2005). A Brief History of Auditory Models. *X Simpósio Brasileiro de Computacao Musical*, **1**(May), 1–6.

Arnott, R. H., Wallace, M. N., Shackleton, T. M., and Palmer, A. R. (2004). Onset Neurones in the Anteroventral Cochlear Nucleus Project to the Dorsal Cochlear Nucleus. *Journal of the Association for Research in Otolaryngology*, **5**(2), 153–170.

Artinian, L., Tornieri, K., Zhong, L., Baro, D., and Rehder, V. (2010). Cellular/Molecular Nitric Oxide Acts as a Volume Transmitter to Modulate Electrical Properties of Spontaneously Firing Neurons via Apamin-Sensitive Potassium Channels. *The Journal of Neuroscience*, **30**(5), 1699–1711.

Auerbach, B. D., Rodrigues, P. V., Salvi, R. J., Zhang, J., Shaikh, A. G., and Liu, B. (2014). Central gain control in tinnitus and hyperacusis. *Frontiers in Neurology*, **5**, 1–21.

Babbedge, R. C., Bland-Ward, P. A., Hart, S. L., and Moore, P. K. (1993). Inhibition of rat cerebellar nitric oxide synthase by 7- nitro indazole and related substituted indazoles. *Br.J.Pharmacol.*, **110**, 225–228.

Baguley, D., McFerran, D., and Hall, D. A. (2013). Tinnitus. *The Lancet*, **382**(9904), 1600–1607.

Baizer, J. S., Wong, K. M., Paolone, N. A., Weinstock, N., Salvi, R. J., Manohar, S., Witelson, S. F., Baker, J. F., Sherwood, C. C., and Hof, P. R. (2014). Laminar and neurochemical organisation of the dorsal cochlear nucleus of the human, monkey, cat, and rodents. *Anatomical record (Hoboken)*, **297**(10), 1865–1884.

Barnea, G., Attias, J., Gold, S., and Shahar, A. (1990). Tinnitus with Normal Hearing Sensitivity: Extended High-Frequency Audiometry and Auditory-Nerve Brain-Stem-Evoked Responses. *International Journal of Audiology*, **29**(1), 36–45.

Benowitz, L. I. and Routtenberg, A. (1987). A membrane phosphoprotein associated with neural development, axonal regeneration, phospholipid metabolism, and synaptic plasticity. *Trends in Neurosciences*, **10**(12), 527–532.

Berger, J. I., Coomber, B., Shackleton, T. M., Palmer, A. R., and Wallace, M. N. (2013). A novel behavioural approach to detecting tinnitus in the guinea pig. *Journal of Neuroscience Methods*, **213**(2), 188–195.

Blackburn, C. C. and Sachs, M. B. (1989). Classification of unit types in the anteroventral cochlear nucleus: PST histograms and regularity analysis. *Journal of neurophysiology*, **62**(6), 1303–1329.

Bland-Ward, P. A., Pitcher, A., Wallace, P., Gaffen, Z., Babbedge, R. C., and Moore, P. K. (1994). Isoform selectivity of indazole-based nitric oxide synthase inhibitors. *British Journal of Pharmacology-Proceedings Supplement*, **112**.

Bledsoe, S. C., Nagase, S., Miller, J. M., and Altschuler, R. A. (1995). Deafness-induced plasticity in the mature central auditory system. *Neuroreport*, **7**(1), 225–9.

Boettcher, F. A. and Salvi, R. J. (1993). Functional changes in the ventral cochlear nucleus following acute acoustic overstimulation. *Journal of the Acoustical Society of America*, **94**(4), 2123–34.

Brenman, J. E., Chao, D. S., Gee, S. H., McGee, A. W., Craven, S. E., Santillano, D. R., Wu, Z., Huang, F., Xia, H., Peters, M. F., Froehner, S. C., and Bredt, D. S. (1996). Interaction of nitric oxide synthase with the postsynaptic density protein PSD-95 and α1-syntrophin mediated by PDZ domains. *Cell*, **84**(5), 757–767.

Brouillet, E., Roeda, D., Valette, H., Fuseau, C., Guyot, M. C., and Crouzel, C. (1995). In vivo metabolites of Nomega-nitro-L-arginine methyl ester: Methanol and Nomega-nitro-L-arginine. *European Journal of Pharmacology: Environmental Toxicology and Pharmacology*, **293**, 487–490.

Bullock, D. C., Palmer, A. R., and Rees, A. (1988). Compact and easy-to-use tungsten-in-glass microelectrode manufacturing workstation. *Med. & Biol. Eng. & Comp.*, **26**, 669–672.

Burette, A., Petrusz, P., Schmidt, H. H., and Weinberg, R. J. (2001). Immunohistochemical localization of nitric oxide synthase and soluble guanylyl cyclase in the ventral cochlear nucleus of the rat. *The Journal of comparative neurology*, **431**(1), 1–10.

Burks, P. T., Garcia, J. V., Gonzalezirias, R., Tillman, J. T., Niu, M., Mikhailovsky, A. A., Zhang, J., Zhang, F., and Ford, P. C. (2013). Nitric oxide releasing materials triggered by near-infrared excitation through tissue filters. *Journal of the American Chemical Society*, **135**(48), 18145–18152.

Bush, M. A. and Pollack, G. M. (2001). Pharmacokinetics and Pharmacodynamics of 7-Nitroindazole, a Selective Nitric Oxide Synthase Inhibitor, in the Rat Hippocampus. *Pharmaceutical Research*, **18**(11), 1607–12.

Cai, S., Ma, W.-L. D., and Young, E. D. (2008). Encoding Intensity in Ventral Cochlear Nucleus Following Acoustic Trauma: Implications for Loudness Recruitment. *JARO - Journal of the Association for Research in Otolaryngology*, **10**, 5–22.

Cant, N. B. and Hyson, R. L. (1992). Projections from the lateral nucleus of the trapezoid body to the medial superior olivary nucleus in the gerbil. *Hearing Research*, **58**(1), 26–34.

Cao, X.-J., Shatadal, S., and Oertel, D. (2007). Voltage-Sensitive Conductances of Bushy Cells of the Mammalian Ventral Cochlear Nucleus. *Journal of Neurophysiology*, **97**, 3961–3975.

Casseday, J. H., Ehrlich, D., and Covey, E. (1994). Neural tuning for sound duration: Role of inhibitory mechanisms in the inferior colliculus. *Science*, **264**(5160), 847–850.

Chefer, V. I., Thompson, A. C., Zapata, A., and Shippenberg, T. S. (2009). Overview of Brain Microdialysis. *Curr Protoc Neurosci*, **7**(1), 1–35.

Chen, G., Lee, C., Sandridge, S. A., Butler, H. M., Manzoor, N. F., and Kaltenbach, J. A. (2013). Behavioral evidence for possible simultaneous induction of hyperacusis and tinnitus following intense sound exposure. *JARO - Journal of the Association for Research in Otolaryngology*, **14**(3), 413–424.

Chen, S. R., Jin, X. G., and Pan, H. L. (2017). Endogenous nitric oxide inhibits spinal NMDA receptor activity and pain hypersensitivity induced by nerve injury. *Neuropharmacology*, **125**, 156–165.

Chen, T. J., Huang, C. W., Wang, D. C., and Chen, S. S. (2004). Co-induction of growth-associated protein GAP-43 and neuronal nitric oxide synthase in the cochlear nucleus following cochleotomy. *Experimental Brain Research*, **158**(2), 151–162.

Cianfrone, G., Mazzei, F., Salviati, M., Turchetta, R., Orlando, M. P., Testugini, V., Carchiolo, L., Cianfrone, F., and Altissimi, G. (2015). Tinnitus Holistic Simplified Classification (THoSC): A new assessment for subjective tinnitus, with diagnostic and therapeutic implications. *Annals of Otology, Rhinology & Laryngology*, **124**(7), 550–560.

Clasadonte, J., Poulain, P., Beauvillain, J. C., and Prevot, V. (2008). Activation of neuronal nitric oxide release inhibits spontaneous firing in adult gonadotropin-releasing hormone neurons: A possible local synchronizing signal. *Endocrinology*, **149**(2), 587–596.

Clopton, B. M., Winfield, J. A., and Flammino, F. J. (1974). Tonotopic organization: review and analysis. *Brain Research*, **76**, 1–20.

Coomber, B., Berger, J. I., Kowalkowski, V. L., Shackleton, T. M., Palmer, A. R., and Wallace, M. N. (2014). Neural changes accompanying tinnitus following unilateral acoustic trauma in the guinea pig. *European Journal of Neuroscience*, **40**(2), 2427–2441.

Coomber, B., Kowalkowski, V. L., Berger, J. I., Palmer, A. R., and Wallace, M. N. (2015). Modulating Central Gain in Tinnitus: Changes in Nitric Oxide Synthase in the Ventral Cochlear Nucleus. *Frontiers in Neurology*, **6**, 1–12.

Coote, E. J. and Rees, A. (2008). The distribution of nitric oxide synthase in the inferior colliculus of guinea pig. *Neuroscience*, **154**(1), 218–225.

Cury, Y., Picolo, G., Gutierrez, V. P., and Ferreira, S. H. (2011). Pain and analgesia: The dual effect of nitric oxide in the nociceptive system. *Nitric Oxide - Biology and Chemistry*, **25**(3), 243–254.

Davis, M., Gendelman, D. S., Tischler, M. D., and Gendelman, P. M. (1982). A primary acoustic startle circuit: lesion and stimulation studies. *The Journal of Neuroscience*, **2**(6), 791–805.

De Gennaro Colonna, V., Bianchi, M., Pascale, V., Ferrario, P., Morelli, F., Pascale, W., Tomasoni, L., and Turiel, M. (2009). Asymmetric dimethylarginine (ADMA): an endogenous inhibitor of nitric oxide synthase and a novel cardiovascular risk molecule. *Medical science monitor : international medical journal of experimental and clinical research*, **15**(4), RA91–A101.

Dehmel, S., Eisinger, D., and Shore, S. E. (2012a). Gap prepulse inhibition and auditory brainstem-evoked potentials as objective measures for tinnitus in guinea pigs. *Frontiers in Systems Neuroscience*, **6**(42), doi: 10.3389/fnsys.2012.00042.

Dehmel, S., Pradhan, S., Koehler, S. D., Bledsoe, S. C., and Shore, S. E. (2012b). Noise over-exposure alters long-term somatosensory-auditory processing in the dorsal cochlear nucleus - possible basis for tinnitus-related hyperactivity? *J Neurosci.*, **32**(1), 1660–1671.

Dong, S., Mulders, W. H. A. M., Rodger, J., and Robertson, D. (2009). Changes in neuronal activity and gene expression in guinea-pig auditory brainstem after unilateral partial hearing loss. *Neuroscience*, **159**(3), 1164–1174.

Dong, S., Mulders, W. H. A. M., Rodger, J., Woo, S., and Robertson, D. (2010). Acoustic trauma evokes hyperactivity and changes in gene expression in guinea-pig auditory brainstem. *European Journal of Neuroscience*, **31**, 1616–1628.

Eggermont, J. J. (2015). Animal models of spontaneous activity in the healthy and impaired auditory system Auditory Nerve Firings. *Frontiers in Neural Circuits*, **9**(19), 1–11.

Eggermont, J. J. and Tass, P. A. (2015). Maladaptive Neural Synchrony in Tinnitus: Origin and Restoration. *Frontiers in Neurology*, **6**(29), 1–17.

Eliasson, M. J., Blackshaw, S., Schell, M. J., and Snyder, S. H. (1997). Neuronal nitric oxide synthase alternatively spliced forms: prominent functional localizations in the brain. *Proceedings of the National Academy of Sciences of the United States of America*, **94**(7), 3396–3401.

Fessenden, J. D., Altschuler, R. A., Seasholtz, A. F., and Schacht, J. (1999). Nitric oxide/cyclic guanosine monophosphate pathway in the peripheral and central auditory system of the rat. *Journal of Comparative Neurology*, **404**(1), 52–63.

Fessenden, J. D., Coling, D. E., and Schacht, J. (1994). Detection and characterization of nitric oxide synthase in the mammalian cochlea. *Brain research*, **668**, 9–15.

Fessenden, J. D. and Schacht, J. (1998). The nitric oxide/cyclic GMP pathway: A potential major regulator of cochlear physiology. *Hearing Research*, **118**(1-2), 168–176.

Folmer, R. L. and Griest, S. E. (2000). Tinnitus and insomnia. *American Journal of Otolaryngology*, **21**(5), 287–293.

Folmer, R. L., Griest, S. E., Meikle, M. B., and Martin, W. H. (1999). Tinnitus severity, loudness, and depression. *Otolaryngology - Head and Neck Surgery*, **121**(1), 48–51.

Förster, C. R. and Illing, R. B. (1998). Redistribution of NMDA receptors in the cochlear nucleus following cochleotomy. *NeuroReport*, **9**(15), 3531–3535.

Franz, P., Hauser-Kronberger, C., Böck, P., Quint, C., and Baumgartner, W. D. (1996). Localization of nitric oxide synthase I and III in the cochlea. *Acta otolaryngologica*, **116**(5), 726–31.

Friedman, J. T., Peiffer, A. M., Clark, M. G., Benasich, A. A., and Fitch, R. H. (2004). Age and experience-related improvements in gap detection in the rat. *Developmental Brain Research*, **152**(2), 83–91.

Furfine, E. S., Harmon, M. F., Paith, J. E., and Garvey, E. P. (1993). Selective inhibition of constitutive nitric oxide synthase by L-NG-nitroarginine. *Biochemistry*, **32**(33), 8512–7.

Furman, A. C., Kujawa, S. G., and Liberman, M. C. (2013). Noise-induced cochlear neuropathy is selective for fibers with low spontaneous rates. *Journal of Neurophysiology*, **110**(3), 577–586.

Gaese, B. H. and Ostwald, J. (2001). Anesthesia changes frequency tuning of neurons in the rat primary auditory cortex. *Journal of neurophysiology*, **86**(2), 1062–6.

Galati, S., D'Angelo, V., Scarnati, E., Stanzione, P., Martorana, A., Procopio, T., Sancesario, G., and Stefani, A. (2008). In vivo electrophysiology of dopamine-denervated striatum: Focus on the nitric oxide/cGMP signaling pathway. *Synapse*, **62**(6), 409–420.

Galazyuk, A. V. and Hébert, S. (2015). Gap-Prepulse Inhibition of the Acoustic Startle Reflex (GPIAS) for Tinnitus Assessment: Current Status and Future Directions. *Frontiers in neurology*, **6**, 88.

Gerken, G. M., Saunders, S. S., and Paul, R. E. (1984). Hypersensitivity to electrical stimulation of auditory nuclei follows hearing loss in cats. *Hearing Research*, **13**(3), 249–259.

Godfrey, D. A., Kiang, N. Y., and Norris, B. E. (1975). Single unit activity in the posteroventral cochlear nucleus of the cat. *The Journal of comparative neurology*, **162**(2), 247–268.

Goldberg, J. M. and Brown, P. B. (1969). Response of Binaural Neurons of Dog Superior Olivary Complex to Dichotic Tonal Stimuli: Some Physiological Mechanisms of Sound Localization. *American Physiological Society*, **32**(4), 613–636.

Gourévitch, B., Doisy, T., Avillac, M., and Edeline, J.-M. (2009). Follow-up of latency and threshold shifts of auditory brainstem responses after single and interrupted acoustic trauma in guinea pig. *Brain Research*, **1304**, 66–79.

Granger, A. J. and Nicoll, R. A. (2013). Expression mechanisms underlying long-term potentiation: a postsynaptic view, 10 years on. *Philosophical transactions of the Royal Society of London. Series B, Biological sciences*, **369**(1432), 721–726.

Groff, A. J. and Liberman, M. C. (2003). Modulation of Cochlear Afferent Response by the Lateral Olivocochlear System: Activation Via Electrical Stimulation of the Inferior Colliculus. *J Neurophysiol*, **90**, 3178–3200.

Gröschel, M., Ryll, J., Gotze, R., Ernst, A., and Basta, D. (2014). Acute and long-term effects of noise exposure on the neuronal spontaneous activity in cochlear nucleus and inferior colliculus brain slices. *BioMed research international*, **2014**, 909260.

Gu, J. W., Herrmann, B. S., Levine, R. A., and Melcher, J. R. (2012). Brainstem auditory evoked potentials suggest a role for the ventral cochlear nucleus in tinnitus. *JARO - Journal of the Association for Research in Otolaryngology*, **13**(6), 819–833.

Gulley, R. L., Wenthold, R. J., and Neises, G. R. (1977). Remodeling of neuronal membranes as an early response to deafferentation. A freeze-fracture study. *The Journal of Cell Biology*, **75**, 837–850.

Hardingham, N., Dachtler, J., and Fox, K. (2013). The role of nitric oxide in pre-synaptic plasticity and homeostasis. *Frontiers in Cellular Neuroscience*, **7**(October), 190.

Hayes, S. H., Radziwon, K. E., Stolzberg, D. J., and Salvi, R. J. (2014). Behavioral Models of Tinnitus and Hyperacusis in Animals. *Frontiers in Neurology*, **5**(September), 1–15.

Hicks, T. P. (1984). The history and development of microiontophoresis in experimental neurobiology. *Progress in neurobiology*, **22**(3), 185–240.

Hildebrandt, H., Hoffmann, N. A., and Illing, R.-B. (2011). Synaptic Reorganization in the Adult Rat's Ventral Cochlear Nucleus following Its Total Sensory Deafferentation. *PLoS ONE*, **6**(8), e23686.

Höcht, C., DiVerniero, C., Opezzo, J. A. W., and Taira, C. A. (2005). Applicability of microdialysis as a technique for pharmacokinetic- pharmacodynamic (PK-PD) modeling of antihypertensive beta-blockers. *Journal of Pharmacological and Toxicological Methods*, **52**(2), 244–250.

Höcht, C., Opezzo, J. A. W., and Taira, C. A. (2007). Applicability of reverse microdialysis in pharmacological and toxicological studies. *Journal of Pharmacological and Toxicological Methods*, **55**(1), 3–15.

House, J. W. and Brackmann, D. E. (1981). Tinnitus: surgical treatment. *CIBA Found. Symp.*, **85**, 201–216.

Huang, E. P. (1997). Synaptic plasticity: a role for nitric oxide in LTP. *Current biology*, **7**(3), R141–3.

Imig, T. J. and Morel, A. (1985). Tonotopic organization in ventral nucleus of medial geniculate body in the cat. *Journal of neurophysiology*, **53**(1), 309–340.

Issy, A. C., Lazzarini, M., Szawka, R. E., Carolino, R. O. G., Anselmo-Franci, J. A., and Del Bel, E. A. (2011). Nitric oxide synthase inhibitors improve prepulse inhibition responses of Wistar rats. *Behavioural Brain Research*, **217**(2), 416–423.

Issy, A. C., Pedrazzi, J. F. C., Yoneyama, B. H., and Del-Bel, E. A. (2014). Critical role of nitric oxide in the modulation of prepulse inhibition in Swiss mice. *Psychopharmacology*, **231**(4), 663–672.

Jaffrey, S. R., Erdjument-Bromage, H., Ferris, C. D., Tempst, P., and Snyder, S. H. (2001). Protein S-nitrosylation: a physiological signal for neuronal nitric oxide. *Nature cell biology*, **3**(2), 193–197.

Jastreboff, P. J. (1990). Phantom auditory perception (tinnitus): Mechanisms of generation and perception. *Neuroscience Research*, **8**(4), 221–254.

Jastreboff, P. J., Brennan, J. F., and Sasaki, C. T. (1988). An animal model for tinnitus. *The Laryngoscope*, **98**(3), 280–286.

Jastreboff, P. J., Hansen, R., Sasaki, P. G., and Sasaki, C. T. (1986). Differential Uptake of Salicylate in Serum, Cerebrospinal Fluid, and Perilymph. *Archives of Otolaryngology - Head and Neck Surgery*, **112**(10), 1050–1053.

Jin, Y.-M., Godfrey, D. A., Wang, J., and Kaltenbach, J. A. (2006). Effects of intense tone exposure on choline acetyltransferase activity in the hamster cochlear nucleus. *Hearing Research*, **216-217**(1-2), 168–175.

Jonas, E. A. and Kaczmarek, L. K. (1996). Regulation of potassium channels by protein kinases. *Current Opinion in Neurobiology*, **6**(3), 318–323.

Jones, A. and May, B. J. (2017). Improving the Reliability of Tinnitus Screening in Laboratory Animals. *JARO - Journal of the Association for Research in Otolaryngology*, **18**(1), 183–195.

Kaltenbach, J. A. (2011). Tinnitus: Models and mechanisms. *Hearing Research*, **276**, 52–60.

Kaltenbach, J. A. and Zhang, J. (2006). Intense sound-induced plasticity in the dorsal cochlear nucleus of rats: Evidence for cholinergic receptor upregulation. *Hearing Research*, **226**(1-2), 232–243.

Kim, H. W., Park, J.-S., Jeong, H.-S., Jang, M. J., Kim, B.-C., Kim, M.-K., Cho, K.-H., Kim, T. S., and Park, S. W. (2004a). Nitric oxide modulation of the spontaneous firing of rat medial vestibular nuclear neurons. *Journal of pharmacological sciences*, **96**(2), 224–8.

Kim, J. J., Gross, J., Morest, D. K., and Potashner, S. J. (2004b). Quantitative study of degeneration and new growth of axons and synaptic endings in the chinchilla cochlear nucleus after acoustic overstimulation. *Journal of Neuroscience Research*, **77**(6), 829–842.

Koerber, K. C., Pfeiffer, R. R., Warr, W. B., and Kiang, N. Y. S. (1966). Spontaneous spike discharges from single units in the cochlear nucleus after destruction of the cochlea. *Experimental Neurology*, **16**, 119–130.

Konishi, T., Hamrick, P. E., and Walsh, P. J. (1978). Ion Transport in Guinea Pig Cochlea:I. Potassium and Sodium Transport. *Acta Oto-Laryngologica*, **86**(1-6), 22–34.

Kopp-Scheinpflug, C., Pigott, B. M., and Forsythe, I. D. (2015). Nitric oxide selectively suppresses IHcurrents mediated by HCN1-containing channels. *Journal of Physiology*, **593**(7), 1685–1700.

Kraus, K. S., Ding, D., Jiang, H., Kermany, M. H., Mitra, S., and Salvi, R. J. (2013). Upregulation of GAP-43 in the chinchilla ventral cochlear nucleus after carboplatin-induced hearing loss: Correlations with inner hair cell loss and outer hair cell loss. *Hearing Research*, **302**, 74–82.

Kraus, K. S., Ding, D., Zhou, Y., and Salvi, R. J. (2009). Central auditory plasticity after carboplatin. *Hear Res*, **255**(1-2), 33–43.

Kraus, K. S. and Illing, R.-B. (2004). Superior olivary contributions to auditory system plasticity: Medial but not lateral olivocochlear neurons are the source of cochleotomy-induced GAP-43 expression in the ventral cochlear nucleus. *Journal of Comparative Neurology*, **475**, 374–390.

Kujawa, S. G. and Liberman, M. C. (2009). Adding insult to injury: cochlear nerve degeneration after "temporary" noise-induced hearing loss. *The Journal of Neuroscience*, **29**(45), 14077–14085.

Kuwada, S., Batra, R., and Stanford, T. R. (1989). Monaural and binaural response properties of neurons in the inferior colliculus of the rabbit: effects of sodium pentobarbital. *Journal of neurophysiology*, **61**(2), 269–82.

Landgrebe, M., Azevedo, A., Baguley, D., Bauer, C. A., Cacace, A., Coelho, C., Dornhoffer, J., Figueiredo, R. R., Flor, H., Hajak, G., van de Heyning, P., Hiller, W., Khedr, E., Kleinjung, T., Koller, M., Lainez, J. M., Londero, A., Martin, W. H., Mennemeier, M., Piccirillo, J., Ridder, D. D., Rupprecht, R., Searchfield, G., Vanneste, S., Zeman, F., and Langguth, B. (2012). Methodological aspects of clinical trials in tinnitus: A proposal for an international standard. *J Psychosom Res.*, **73**(2), 112–121.

Lange, M. D., Doengi, M., Lesting, J., Pape, H. C., and Jüngling, K. (2012). Heterosynaptic long-term potentiation at interneuron-principal neuron synapses in the amygdala requires nitric oxide signalling. *The Journal of physiology*, **590**(1), 131–43.

Langguth, B. and Elgoyhen, A. B. (2012). Current pharmacological treatments for tinnitus. *Expert opinion on pharmacotherapy*, **13**(17), 2495–2509.

Le Roux, N., Amar, M., Moreau, A. W., and Fossier, P. (2009). Roles of nitric oxide in the homeostatic control of the excitation-inhibition balance in rat visual cortical networks. *Neuroscience*, **163**(3), 942–951.

Leaver, A. M., Renier, L., Chevillet, M. A., Morgan, S., Kim, H. J., and Rauschecker, J. P. (2011). Dysregulation of Limbic and Auditory Networks in Tinnitus. *Neuron*, **69**(1), 33–43.

Lee, J.-J., Cho, Y.-W., Huh, Y., Cha, C. I., and Yeo, S. G. (2008). Effect of nitric oxide on auditory cortical neurons of aged rats. *Neuroscience letters*, **447**(1), 37–41.

Leggett, K., Mendis, V., and Mulders, W. H. A. M. (2018). Divergent Responses in the Gap Prepulse Inhibition of the Acoustic Startle Reflex in Two Different Guinea Pig Colonies. *The International Tinnitus Journal*, **22**(1).

Leitner, D. S., Hammond, G. R., Springer, C. P., Ingham, K. M., Mekilo, A. M., Bodison, P. R., Aranda, M. T., and Shawaryn, M. A. (1993). Parameters affecting gap detection in the rat. *Perception & Psychophysics*, **54**(3), 395–405.

Levine, R. A., Abel, M., and Cheng, H. (2003). CNS somatosensory-auditory interactions elicit or modulate tinnitus. *Experimental Brain Research*, **153**(4), 643–648.

Li, C. H., Wang, S. Z., Cai, Z. L., Liu, W. X., Xu, S. T., and Xiao, P. (2012). Effects of intrahippocampal l-NAME treatment on the behavioral long-term potentiation in dentate gyrus. *Neuroscience Letters*, **528**(2), 201–204.

Liberman, M. C. (1978). Auditory-nerve response from cats raised in a low-noise chamber. *The Journal of the Acoustical Society of America*, **63**, 442.

Light, D. B., Corbin, J. D., and Stanton, B. A. (1990). Dual ion-channel regulation by cyclic GMP and cyclic GMP-dependent protein kinase. *Letters to Nature*, **344**, 336–339.

Lobarinas, E., Hayes, S. H., and Allman, B. L. (2013). The Gap-Startle Paradigm for Tinnitus Screening in Animal Models: Limitations and Optimization. *Hearing Research*, **295**(1-2), 150–160.

Lonsbury-Martin, B. L. and Martin, G. K. (1981). Effects of moderately intense sound on auditory sensitivity in rhesus monkeys: behavioral and neural observations. *Journal of Neurophysiology*, **46**(3), 563–586.

Lundberg, J. O., Weitzberg, E., and Gladwin, M. T. (2008). The nitrateânitriteânitric oxide pathway in physiology and therapeutics. *Nature reviews. Drug discovery*, **7**(2), 156–167.

Luxon, L. (1993). Tinnitus: its causes, diagnosis, and treatment. *BMJ*, **306**(6891), 1490–1491.

Mahmood, G., Mei, Z., Hojjat, H., Pace, E., Kallakuri, S., and Zhang, J. S. (2014). Therapeutic effect of sildenafil on blast-induced tinnitus and auditory impairment. *Neuroscience*, **269**, 367–82.

Malenka, R. C. (1991). The role of postsynaptic calcium in the induction of long-term potentiation. *Molecular Neurobiology*, **5**(2-4), 289–295.

Masood, A., Huang, Y., Hajjhussein, H., Xiao, L., Li, H., Wang, W., Hamza, A., Zhan, C.-G., and O'Donnell, J. M. (2009). Anxiolytic effects of phosphodiesterase-2 inhibitors associated with increased cGMP signaling. *The Journal of pharmacology and experimental therapeutics*, **331**(2), 690–699.

Maurice, D. H., Ke, H., Ahmad, F., Wang, Y., Chung, J., and Manganiello, V. C. (2014). Advances in targeting cyclic nucleotide phosphodiesterases. *Nature reviews. Drug discovery*, **13**(4), 290–314.

Mazurek, B., Haupt, H., Szczepek, A. J., Sandmann, J., Gross, J., Klapp, B. F., Kiesewetter, H., Kalus, U., Stöver, T., and Caffier, P. P. (2009). Evaluation of vardenafil for the treatment of subjective tinnitus: a controlled pilot study. *Journal of negative results in biomedicine*, **8**(3).

McAlpine, D. and Palmer, A. R. (2002). Blocking GABAergic inhibition increases sensitivity to sound motion cues in the inferior colliculus. *The Journal of Neuroscience*, **22**(4), 1443–1453.

Mellott, J. G., Motts, S. D., and Schofield, B. R. (2011). Multiple origins of cholinergic innervation of the cochlear nucleus. *NSC*, **180**, 138–147.

Michelakis, E., Tymchak, W., and Archer, S. (2000). Sildenafil: From the bench to the bedside. *Cmaj*, **163**(9), 1171–1175.

Middleton, J. W., Kiritani, T., Pedersen, C., Turner, J. G., Shepherd, G. M. G., and Tzounopoulos, T. (2011). Mice with behavioral evidence of tinnitus exhibit dorsal cochlear nucleus hyperactivity because of decreased GABAergic inhibition. *Proceedings of the National Academy of Sciences of the United States of America*, **108**(18), 7601–6.

Middleton, J. W. and Tzounopoulos, T. (2012). Imaging the neural correlates of tinnitus: a comparison between animal models and human studies. *Frontiers in Systems Neuroscience*, **6**.

Minton, G. O., Young, A. H., McQuade, R., Fairchild, G., Ingram, C. D., and Gartside, S. E. (2009). Profound Changes in Dopaminergic Neurotransmission in the Prefrontal Cortex in Response to Flattening of the Diurnal Glucocorticoid Rhythm: Implications for Bipolar Disorder. *Neuropsychopharmacology*, **34**(10), 2265–2274.

Misurya, V. K. (1976). Tensor Tympani, a âTunerâ of Tensor Palati Muscle. *Acta Oto-Laryngologica*, **82**(1-6), 410–414.

Mongan, E., Kelly, P., Nies, K., Porter, W. W., and Paulus, H. E. (1973). Tinnitus as an Indication of Therapeutic Serum Salicylate Levels. *JAMA: The Journal of the American Medical Association*, **226**(2), 142–145.

Morest, D. K. (1968). The collateral system of the medial nucleus of the trapezoid body of the cat, its neuronal architecture and relation to the olivo-cochlear bundle. *Brain Research*, **9**(2), 288–311.

Müller, N., Lorenz, I., Langguth, B., and Weisz, N. (2013). rTMS induced tinnitus relief is related to an increase in auditory cortical alpha activity. *PloS one*, **8**(2).

Murphy, K. P. S. J. and Bliss, T. V. P. (1999). Photolytically released nitric oxide produces a delayed but persistent suppression of LTP in area CA1 of the rat hippocampal slice. *The Journal of Physiology*, **515**(2), 453–462.

Neitz, A., Mergia, E., Eysel, U. T., Koesling, D., and Mittmann, T. (2011). Presynaptic nitric oxide/cGMP facilitates glutamate release via hyperpolarization-activated cyclic nucleotide-gated channels in the hippocampus. *European Journal of Neuroscience*, **33**(9), 1611–1621.

Neitz, A., Mergia, E., Imbrosci, B., Petrasch-Parwez, E., Eysel, U. T., Koesling, D., and Mittmann, T. (2014). Postsynaptic NO/cGMP increases NMDA receptor currents via hyperpolarization-activated cyclic nucleotide-gated channels in the hippocampus. *Cerebral Cortex*, **24**(7), 1923–1936.

Noreña, A. J. (2011). An integrative model of tinnitus based on a central gain controlling neural sensitivity. *Neuroscience and Biobehavioral Reviews*, **35**, 1089–1109.

Noreña, A. J. and Farley, B. J. (2013). Tinnitus-related neural activity: Theories of generation, propagation, and centralization. *Hearing Research*, **295**, 161–171.

Oertel, D., Wright, S., Cao, X.-J., Ferragamo, M., and Bal, R. (2011). The Multiple Functions of T Stellate/Multipolar/Chopper Cells in the Ventral Cochlear Nucleus. *Hear Res*, **276**, 61–69.

Oertel, D., Wu, S. H., Garb, M. W., and Dizack, C. (1990). Morphology and physiology of cells in slice preparations of the posteroventral cochlear nucleus of mice. *Journal of Comparative Neurology*, **295**(1), 136–154.

Olthof-Bakker, B. M. J. (2017). *Nitric Oxide Signalling in the Inferior Colliculus*. PhD thesis, Newcastle University.

Ortmann, M., Mü, N., Schlee, W., and Weisz, N. (2011). Rapid increases of gamma power in the auditory cortex following noise trauma in humans. *European Journal ofNeuroscience*, **33**, 568–575.

Orton, L. D. and Rees, A. (2014). Intercollicular commissural connections refine the representation of sound frequency and level in the auditory midbrain. *Orton and Rees. eLife*, **3**, 3764.

Palmer, A. R. (1987). Physiology of the cochlear nerve and cochlear nucleus. [Review]. *Br Med Bull*, **43**(4), 838–855.

Palmer, A. R., Wallace, M. N., Arnott, R. H., and Shackleton, T. M. (2003). Morphology of physiologically characterised ventral cochlear nucleus stellate cells. *Experimental Brain Research*, **153**(4), 418–426.

Pan, B., Akyuz, N., Liu, X.-P., Sotomayor, M., Corey, D. P., Holt, J. R., Asai, Y., Nist-Lund, C., Kurima, K., Derfler, B. H., Gyö, B., Limapichat, W., Walujkar, S., and Wimalasena, L. N. (2018). TMC1 Forms the Pore of Mechanosensory Transduction Channels in Vertebrate Inner Ear Hair Cells In Brief Article TMC1 Forms the Pore of Mechanosensory Transduction Channels in Vertebrate Inner Ear Hair Cells. *Neuron*, **99**, 736–753.e6.

Pantev, C., Bertrand, O., Eulitz, C., Verkindt, C., Hampson, S., Schuierer, G., and Elbert, T. (1995). Specific tonotopic organizations of different areas of the human auditory cortex revealed by simultaneous magnetic and electric recordings. *Electroencephalography and Clinical Neurophysiology*, **94**(1), 26–40.

Park, A. R., Lee, H. I., Semjid, D., Kim, d. K., and Chun, S. W. (2014). Dual effect of exogenous nitric oxide on neuronal excitability in rat substantia gelatinosa neurons. *Neural Plasticity*, **2014**(0), 628531.

Pehl, U. and Schmid, H. A. (1997). Electrophysiological responses of neurons in the rat spinal cord to nitric oxide. Technical Report 2.

Petitpré, C., Wu, H., Sharma, A., Tokarska, A., Fontanet, P., Wang, Y., Helmbacher, F., Yackle, K., Silberberg, G., Hadjab, S., and Lallemend, F. (2018). Neuronal heterogeneity and stereotyped connectivity in the auditory afferent system. *Nature Communications*, **9**(3691).

Pickles, J. O. (2012). *An Introducion to the Physiology of Hearing (Forth Edition)*. Emerald.

Ping, J. and Schafe, G. E. (2010). The NO-cGMP-PKG signaling pathway coordinately regulates ERK and ERK-driven gene expression at pre- and postsynaptic sites following LTP-inducing stimulation of thalamo-amygdala synapses. *Neural Plasticity*, **2010**.

Podda, M. V., Marcocci, M. E., Oggiano, L., D'Ascenzo, M., Tolu, E., Palamara, A. T., Azzena, G. B., and Grassi, C. (2004). Nitric oxide increases the spontaneous firing rate of rat medial vestibular nucleus neurons in vitro via a cyclic GMP-mediated PKG-independent mechanism. *European Journal of Neuroscience*, **20**(8), 2124–2132.

Popelár, J., Syka, J., and Berndt, H. (1987). Effect of noise on auditory evoked responses in awake guina pigs. *Hearing Research*, **26**(3), 239–247.

Postorino, A., Vetri, T., Leggio, L., Serio, R., and Bonvissuto, F. (1998). Nitric oxide as a neuromodulator of sympathetic transmission in rat vas deferens. *Journal of Autonomic Pharmacology*, **18**, 21–29.

Pratt, H., Ben-David, Y., Peled, R., Podoshin, L., and Scharf, B. (1981). Auditory brain stem evoked potentials: Clinical promise of increasing stimulus rate. *Electroencephalography and Clinical Neurophysiology*, **51**(1), 80–90.

Purves, D., Augustine, G. J., Fitzpatrick, D., Hall, W. C., LaMantia, A., and White, L. E. (2012). *Neuroscience 5th Edition*. Sinauer.

Rang, H. P., Dale, M. M., Ritter, J. M., Flower, R. J., and Henderson, G. (2012). *Rang & Dale's Pharmacology 7th Edition*. Elsevier.

Rapisarda, C. and Bacchelli, B. (1977). The brain of the guinea pig in stereotaxic coordinates. *Arch Sci Biol (Bologna)*, **61**(1-4), 1–37.

Redd, E. E., Pongstaporn, T., and Ryugo, D. K. (2000). The effects of congenital deafness on auditory nerve synapses and globular bushy cells in cats. *Hearing Research*, **147**(1-2), 160–174.

Reed, G. F. (1960). An Audiometric Study of Two Hundred Cases of Subjective Tinnitus. *Archives of Otolaryngology - Head and Neck Surgery*, **71**(1), 84–94.

Rees, S., Güldner, F. H., and Aitkin, L. (1985). Activity dependent plasticity of postsynaptic density structure in the ventral cochlear nucleus of the rat. *Brain research*, **325**(1-2), 370–374.

Rhode, W. S., Linn Roth, G., and Recio, A. (2010). Response Properties of Cochlear Nucleus Neurons in Monkeys. *Hear. Res.*, **259**(1-2), 18–34.

Rhode, W. S. and Smith, P. H. (1986). Encoding timing and intensity in the ventral cochlear nucleus of the cat. *Journal of neurophysiology*, **56**(2), 261–286.

Roberts, L. E. (2018). Neural plasticity and its initiating conditions in tinnitus. *HNO*, **66**(3), 172–178.

Roberts, L. E., Eggermont, J. J., Caspary, D. M., Shore, S. E., Melcher, J. R., and Kaltenbach, J. A. (2010). Ringing ears: the neuroscience of tinnitus. *The Journal of Neuroscience*, **30**(45), 14972–14979.

Robertson, D., Bester, C., Vogler, D., and Mulders, W. H. A. M. (2013). Spontaneous hyperactivity in the auditory midbrain: Relationship to afferent input. *Hearing Research*, **295**, 124–129.

Robertson, D. and Mulders, W. H. A. M. (2018). Cholinergic responses of acoustically-characterized cochlear nucleus neurons: An in vivo iontophoretic study in Guinea pig. *Hearing Research*, **367**, 97–105.

Rodrigo, J., Springall, D. R., Uttenthal, O., Bentura, M. L., Abadia-Molina, F., Riveros-Moreno, V., Martinez-Murillo, R., Polak, J. M., and Moncada, S. (1994). Localization of nitric oxide synthase in the adult rat brain. *Philosophical Transactions of the Royal Society of London*, **345**, 175–221.

Rose, J. E., Galambos, R., and Hughes, J. (1959). Microelectrode studies of the cochlear nuclei of the cat. *Bulletin of the Johns Hopkins Hospital*, **104**(5), 211–51.

Rosenblum, K., Futter, M., Voss, K., Erent, M., Skehel, P. A., French, P., Obosi, L., Jones, M. W., and Bliss, T. V. P. (2002). The role of extracellular regulated kinases I/II in late-phase long-term potentiation. *The Journal of Neuroscience*, **22**(13), 5432–5441.

Rothman, J. S. and Manis, P. B. (2003). The Roles Potassium Currents Play in Regulating the Electrical Activity of Ventral Cochlear Nucleus Neurons. *Journal of Neurophysiology*, **89**, 3097–3113.

Ryugo, D. K., Montey, K. L., Wright, A. L., Bennett, M. L., and Pongstaporn, T. (2006). Postnatal development of a large auditory nerve terminal: The endbulb of Held in cats. *Hearing Research*, **216-217**, 100–115.

Salvi, R. J., Saunders, S. S., Gratton, M. A., Arehole, S., and Powers, N. (1990). Enhanced evoked response amplitudes in the inferior colliculus of the chinchilla following acoustic trauma. *Hearing Research*, **50**(1-2), 245–257.

Salvi, R. J., Wang, J., and Ding, D. (2000). Auditory plasticity and hyperactivity following cochlear damage. *Hearing Research*, **147**(1-2), 261–274.

Sammut, S., Threlfell, S., and West, A. R. (2010). Nitric oxide-soluble guanylyl cyclase signaling regulates corticostriatal transmission and short-term plasticity of striatal projection neurons recorded in vivo. *Neuropharmacology*, **58**(3), 624.

Samra, S. K., Lilly, D. J., Rush, N. L., and Kirsch, M. M. (1984). Fentanyl Anesthesia and Human Brain-stem auditory Evoked Potentials. *Anesthesiology*, **61**, 261–265.

Santos, R. M., Lourenço, C. F., Ledo, A., Barbosa, R. M., and Laranjinha, J. (2012). Nitric oxide inactivation mechanisms in the brain: Role in bioenergetics and neurodegeneration. *International Journal of Cell Biology*, **2012**.

Sattler, R., Cook, S. W. J., Schultz, C. A. P. S. C., Shields, G. C., Steitz, T. A., Macdonald, J. F., and Tymianski, M. (1999). Nitric Oxide Neurotoxicity by PSD-95 Protein Specific Coupling of NMDA Receptor Activation to Nitric Oxide Neurotoxicity by PSD-95 Protein. *Science*, **284**(1999), 1845–1849.

Schaette, R. and Kempter, R. (2006). Development of tinnitus-related neuronal hyperactivity through homeostatic plasticity after hearing loss: A computational model. *European Journal of Neuroscience*, **23**(11), 3124–3138.

Schaette, R. and Kempter, R. (2008). Development of hyperactivity after hearing loss in a computational model of the dorsal cochlear nucleus depends on neuron response type. *Hearing Research*, **240**(1-2), 57–72.

Schaette, R. and Kempter, R. (2012). Computational models of neurophysiological correlates of tinnitus. *Frontiers in Systems Neuroscience*, **6**(May), 1–10.

Schaette, R. and McAlpine, D. (2011). Tinnitus with a Normal Audiogram: Physiological Evidence for Hidden Hearing Loss and Computational Model. *Journal of Neuroscience*, **31**(38), 13452–13457.

Schofield, B. R. and Cant, N. B. (1996). Origins and targets of commissural connections between the cochlear nuclei in guinea pigs. *Journal of Comparative Neurology*, **375**(1), 128–146.

Schrammel, A., Pfeiffer, S., Schmidt, K., Koesling, D., and Mayer, B. (1998). Activation of soluble guanylyl cyclase by the nitrovasodilator 3-morpholinosydnonimine involves formation of S-nitrosoglutathione. *Molecular pharmacology*, **54**(1), 207–12.

Sedley, W., Teki, S., Kumar, S., Barnes, G. R., Bamiou, D.-E., and Griffiths, T. D. (2012). Single-subject oscillatory gamma responses in tinnitus. *Brain*, **135**, 3089–3100.

Sha, L., Miller, S. M., and Szurszewski, J. H. (1995). Nitric oxide is a neuromodulator in cat pancreatic ganglia: histochemical and electrophysiological study. *Neuroscience Letters*, **192**, 77–80.

Shargorodsky, J., Curhan, G. C., and Farwell, W. R. (2010). Prevalence and characteristics of tinnitus among US adults. *American Journal of Medicine*, **123**, 711–718.

Shiva, S. (2013). Nitrite: A physiological store of nitric oxide and modulator of mitochondrial function. *Redox Biology*, **1**(1), 40–44.

Sibal, L., Agarwal, S. C., Home, P. D., and Boger, R. H. (2010). The Role of Asymmetric Dimethylarginine (ADMA) in Endothelial Dysfunction and Cardiovascular Disease. *Current Cardiology Reviews*, **6**, 82–90.

Smith, P. H. and Rhode, W. S. (1987). Characterization of HRPâlabeled globular bushy cells in the cat anteroventral cochlear nucleus. *Journal of Comparative Neurology*, **266**(3), 360–375.

SoRelle, R. (1998). Nobel Prize Awarded to Scientists for Nitric Oxide Discoveries. *Circulation*, **98**, 2365–2366.

Spangler, K. M., Warr, W. B., and Henkel, C. K. (1985). The projections of principal cells of the medial nucleus of the trapezoid body in the cat. *Journal of Comparative Neurology*, **238**(3), 249–262.

Spoendlin, H. (1967). The innervation of the organ of corti. *J Laryngol Otol.*, **81**(7), 717–738.

Steinert, J. R., Kopp-Scheinpflug, C., Baker, C., Challiss, R. A. J., Mistry, R., Haustein, M. D., Griffin, S. J., Tong, H., Graham, B. P., and Forsythe, I. D. (2008). Nitric Oxide Is a Volume Transmitter Regulating Postsynaptic Excitability at a Glutamatergic Synapse. *Neuron*, **60**(4), 642–656.

Steinert, J. R., Robinson, S. W., Tong, H., Haustein, M. D., Kopp-Scheinpflug, C., and Forsythe, I. D. (2011). Nitric Oxide Is an Activity-Dependent Regulator of Target Neuron Intrinsic Excitability. *Neuron*, **71**(2), 291–305.

Stephenson, D. T., Coskran, T. M., Wilhelms, M. B., Adamowicz, W. O., O'Donnell, M. M., Muravnick, K. B., Menniti, F. S., Kleiman, R. J., and Morton, D. (2009). Immunohistochemical localization of phosphodiesterase 2A in multiple mammalian species. *The journal of histochemistry and cytochemistry : official journal of the Histochemistry Society*, **57**(10), 933–949.

Stolzberg, D., Salvi, R. J., and Allman, B. L. (2012). Salicylate toxicity model of tinnitus. *Frontiers in Systems Neuroscience*, **6**.

Syková, E. and Nicholson, C. (2008). Diffusion in brain extracellular space. *Physiological reviews*, **88**(4), 1277–1340.

Thiels, E., Kanterewicz, B. I., Norman, E. D., Trzaskos, J. M., and Klann, E. (2002). Long-term depression in the adult hippocampus in vivo involves activation of extracellular signal-regulated kinase and phosphorylation of Elk-1. *The Journal of Neuroscience*, **22**(6), 2054–2062.

Turner, J. G., Brozoski, T. J., Bauer, C. A., Parrish, J. L., Myers, K., Hughes, L. F., and Caspary, D. M. (2006). Gap detection deficits in rats with tinnitus: a potential novel screening tool. *Behavioral neuroscience*, **120**(1), 188–195.

Turner, J. G. and Parrish, J. (2008). Gap Detection Methods for Assessing Salicylate-Induced Tinnitus and Hyperacusis in Rats. *American Journal of Audiology*, **17**, S185–192.

Turrigiano, G. (1999). Homeostatic plasiticity in neuronal networks: the more things change, the more they stay the same. *Trends in Neuroscience*, **22**(5), 221–227.

Tyler, R. S. and Baker, L. J. (1983). Difficulties Experienced by Tinnitus Sufferers. *Journal of Speech and Hearing Disorders*, **48**, 150–154.

Tziridis, K., Ahlf, S., Jeschke, M., Happel, M. F. K., Ohl, F. W., and Schulze, H. (2015). Noise Trauma Induced Neural Plasticity Throughout the Auditory System of Mongolian Gerbils: Differences between Tinnitus Developing and Non-Developing Animals. *Frontiers in Neurology*, **6**.

Tzounopoulos, T. (2008). Mechanisms of synaptic plasticity in the dorsal cochlear nucleus: Plasticity-induced changes that could underlie tinnitus. *American Journal of Audiology*, **17**(2), 170–176.

Tzounopoulos, T., Kim, Y., Oertel, D., and Trussell, L. O. (2004). Cell-specific, spike timing-dependent plasticities in the dorsal cochlear nucleus. *Nature neuroscience*, **7**(7), 719–725.

van der Loo, E., Gais, S., Congedo, M., Vanneste, S., Plazier, M., Menovsky, T., Van de Heyning, P., and De Ridder, D. (2009). Tinnitus intensity dependent gamma oscillations of the contralateral auditory cortex. *PLoS ONE*, **4**(10), 1–5.

Vitureira, N. and Goda, Y. (2013). The interplay between hebbian and homeostatic synaptic plasticity. *Journal of Cell Biology*, **203**(2), 175–186.

Vogler, D. P., Robertson, D., and Mulders, W. H. A. M. (2011). Hyperactivity in the ventral cochlear nucleus after cochlear trauma. *The Journal of Neuroscience*, **31**(18), 6639–6645.

Voitenko, L. P. and Marlinsky, V. V. (1993). Stereotaxic atlas of the guinea pig brainstem. *Neurophysiology*, **25**(1), 43–67.

Von Der Behrens, W. (2014). Animal models of subjective tinnitus. *Neural Plasticity*, **2014**.

Wang, H., Brozoski, T. J., and Caspary, D. M. (2011). Inhibitory neurotransmission in animal models of tinnitus: Maladaptive plasticity. *Hearing Research*, **279**(1-2), 111–117.

Ward, P. H., Babin, R., Calcaterra, T. C., and Konrad, H. R. (1975). Operative Treatment of Surgical Lesions with Objective Tinnitus. *Annals of Otology, Rhinology & Laryngology*, **84**(4), 473–482.

Watanabe, M., Mishina, M., and Inoue, Y. (1994). Distinct distributions of five NMDA receptor channel subunit mRNAs in the brainstem. *The Journal of Comparative Neurology*, **343**(4), 520–531.

Watt, A. J. and Desai, N. S. (2010). Homeostatic plasticity and STDP: Keeping a neuron's cool in a fluctuating world. *Frontiers in Synaptic Neuroscience*, **2**(JUN), 1–16.

Weissman, B. A., Jones, C. L., Liu, Q., and Gross, S. S. (2002). Activation and inactivation of neuronal nitric oxide synthase: characterization of Ca(2+)-dependent [125I]Calmodulin binding. *European journal of pharmacology*, **435**(1), 9–18.

Weisz, N., Moratti, S., Meinzer, M., Dohrmann, K., and Elbert, T. (2005). Tinnitus perception and distress is related to abnormal spontaneous brain activity as measured by magnetoencephalography. *PLoS medicine*, **2**(6).

Whiting, B., Moiseff, A., and Rubio, M. E. (2009). Cochlear nucleus neurons redistribute synaptic AMPA and glycine receptors in response to monaural conductive hearing loss. *Neuroscience*, **163**(4), 1264–1276.

Winter, I. M. and Palmer, A. R. (1991). Intensity coding in low-frequency auditory-nerve fibers of the guinea pig. *The Journal of the Acoustical Society of America*, **90**(1958).

Wu, C., Martel, D. T., and Shore, S. E. (2015). Transcutaneous induction of stimulus-timing-dependent plasticity in dorsal cochlear nucleus. *Frontiers in Systems Neuroscience*, **9**(August), 1–10.

Wu, K. K. (2000). Aspirin and salicylate. *Circulation*, **102**, 2022–2023.

Wu, M. D., Kimura, M., Hiromichi, I., and Helfert, R. H. (2008). A classification of NOergic neurons in the inferior colliculus of rat according to co-existence with classical amino acid transmitters. *Okajimas Folia Anat.Jpn.*, **85**(1), 17–27.

Wu, S. H. and Oertel, D. (1984). Intracellular injection with horseradish peroxidase of physiologically characterized stellate and bushy cells in slices of mouse anteroventral cochlear nucleus. *The Journal of neuroscience : the official journal of the Society for Neuroscience*, **4**(6), 1577–1588.

Yang, S., Weiner, B. D., Zhang, L. S., Cho, S.-J., and Bao, S. (2011). Homeostatic plasticity drives tinnitus perception in an animal model. *Proceedings of the National Academy of Sciences*, **108**(36), 14974–14979.

Zhang, Y., Suga, N., and Yan, J. (1997). Corticofugal modulation of frequency processing in bat auditory system. *Nature*, **387**, 900–903.

Zhao, Y., Song, Q., Li, X., and Li, C. (2016). Neural Hyperactivity of the Central Auditory System in Response to Peripheral Damage. *Neural Plasticity*, **2016**.

Zheng, Y., Seung Lee, H., Smith, P. F., and Darlington, C. L. (2006). Neuronal nitric oxide synthase expression in the cochlear nucleus in a salicylate model of tinnitus. *Brain Research*, **1123**(1), 201–206.

Zucker, R. S. and Regehr, W. G. (2002). Short-term plasticity. *Annual Review of Physiology*, **64**(1), 355–405.

Zurita, P., Villa, A. E., de Ribaupierre, Y., de Ribaupierre, F., and Rouiller, E. M. (1994). Changes of single unit activity in the cat's auditory thalamus and cortex associated to different anesthetic conditions. *Neuroscience research*, **19**(3), 303–16.